AD-A136 424 WIDEBAND MONOLITHIC MICROWAVE AMPLIFIER STUDY(U) 1/1
WISCONSIN UNIV-MADISON DEPT OF ELECTRICAL AND COMPUTER
ENGINEERING J B BEYER ET AL. SEP 83 ECE-83-6
UNCLASSIFIED N00014-80-C-0923 F/G 9/5 NL

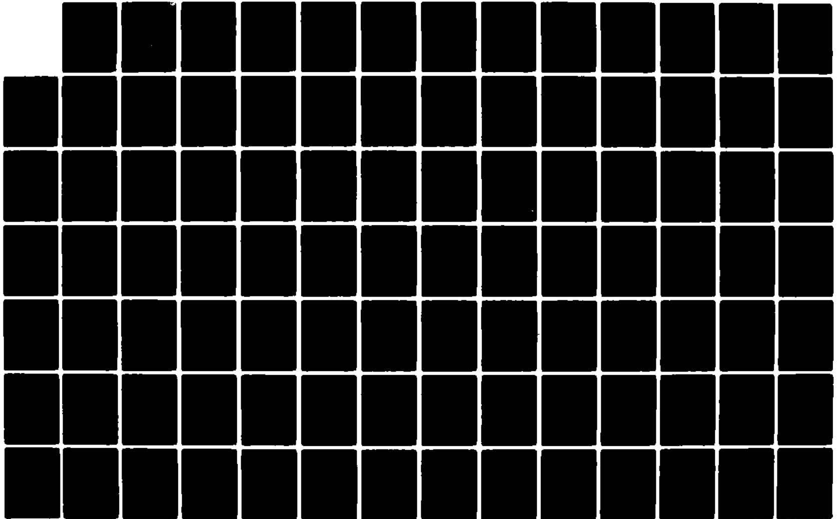

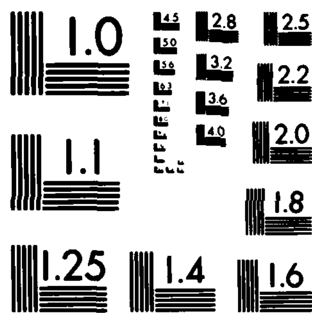

MICROCOPY RESOLUTION TEST CHART
NATIONAL BUREAU OF STANDARDS-1963-A

130

Electrical

Computer

Engineering

DEPARTMENT OF ELECTRICAL
AND COMPUTER ENGINEERING

UNIVERSITY OF WISCONSIN-MADISON

A136424

ECE-83-6 September 1983

Wideband Monolithic Microwave Amplifier Study

J. B. Beyer, S. N. Prasad, R. C. Becker
J. E. Nordman, G. K. Hohenwarter, Y. Chen

Contract N00014-80-C-0923
Contract Authority NR 243-033

Approved for Public Release;
distribution unlimited;

Reproduction of this document, in whole or in part, is permitted for any purpose of the U.S. Government.

DTIC FILE COPY

DTIC
DEC 8 1983
E

83

ENGINEERING EXPERIMENT STATION
MADISON, WISCONSIN 53706

SECURITY CLASSIFICATION OF THIS PAGE (When Data Entered)

REPORT DOCUMENTATION PAGE

READ INSTRUCTIONS BEFORE COMPLETING FORM

1. REPORT NUMBER	2. GOVT ACCESSION NO.	3. RECIPIENT'S CATALOG NUMBER
	AD-A136 424	

4. TITLE (and Subtitle)	5. TYPE OF REPORT & PERIOD COVERED
Wideband Monolithic Microwave Amplifier Study	Final Technical July 1980 - September 1983
	6. PERFORMING ORG. REPORT NUMBER
7. AUTHOR(s) J. B. Beyer, S. N. Prasad, J. E. Nordman, R. C. Becker, G. K. Hohenwarter, Y. Chen	8. CONTRACT OR GRANT NUMBER(s) N00014-80-C-0923
9. PERFORMING ORGANIZATION NAME AND ADDRESS Department of Electrical & Computer Engineering University of Wisconsin-Madison	10. PROGRAM ELEMENT, PROJECT, TASK AREA & WORK UNIT NUMBERS PE 61153N, RR021-02-03 NR 243-033
11. CONTROLLING OFFICE NAME AND ADDRESS Office of Naval Research, Code 414 800 North Quincy St. Arlington, VA 22217	12. REPORT DATE September 1983 13. NUMBER OF PAGES
14. MONITORING AGENCY NAME & ADDRESS(if different from Controlling Office)	15. SECURITY CLASS. (of this report) Unclassified 15a. DECLASSIFICATION/DOWNGRADING SCHEDULE

16. DISTRIBUTION STATEMENT (of this Report)

Approved for public release; Distribution unlimited.

17. DISTRIBUTION STATEMENT (of the abstract entered in Block 20, if different from Report)

18. SUPPLEMENTARY NOTES

19. KEY WORDS (Continue on reverse side if necessary and identify by block number)

Distributed Monolithic Microwave Amplifier

20. ABSTRACT (Continue on reverse side if necessary and identify by block number)

Work is continued on the analysis and design of GaAs FET distributed amplifiers. Design tradeoffs are established for type of device, number of devices, gain, impedance level and line cutoff frequency. The procedure for achieving the maximum gain-bandwidth product is detailed. Preliminary work on a broadband 0-360° phase shifter is reported. The design of an integral part of the phase shifter, a distributed paraphase amplifier from 2 - 20 GHz, is presented.

DD FORM 1 JAN 73 1473 EDITION OF 1 NOV 65 IS OBSOLETE
S/N 0102-LF-014-6601

SECURITY CLASSIFICATION OF THIS PAGE (When Data Entered)

TABLE OF CONTENTS

SECTION PAGE

I. INTRODUCTION....1

II. DISTRIBUTED AMPLIFIER ANALYSIS AND DESIGN

- 2.1 Gain and Optimum Number of Devices....4
- 2.2 Attenuation on Gate and Drain Lines....11
- 2.3 Normalized Frequency Response and Constant - Fractional Bandwidth Curves....15
- 2.4 Gain-Bandwidth Product....19
- 2.5 Amplifier Design....22
- 2.6 Synthesis of Inductors using Microstrip Transmission Lines....34
- 2.7 Image Parameter Terminations and Sources....41
- 2.8 Conclusion....48

III. DISTRIBUTED PARAPHASE AMPLIFIER

- 3.1 Introduction....49
- 3.2 Phase Shifter Principle....49
- 3.3 Distributed Paraphase Amplifier Design Consideration....49
- 3.4 Computer Simulation of Distributed Paraphase Amplifier....54
- 3.5 Analysis....57
- 3.6 Design Curves for the Distributed Paraphase Amplifier....62
- 3.7 Conclusion....73

IV. SUMMARY, CONCLUSION AND PRESENT EFFORTS....74

APPENDIX

- A. Equation for gate-to-source voltage....76
- B. Equations for phase shifts on gate and drain lines....78
- C. Image impedances of gate and drain lines....80
- D. Equations for gain unbalance, phase deviation and characteristic impedance....82

Accession For
NTIS GRA&I X
DTIC TAB
Unannounced
Justification
By
Distribution/
Availability Codes
Dist | Avail and/or Special
A-1

I. Introduction

This report covers work done during the period 1 July 1980 to 30 Sept. 1983. It is the final report on contract N00014-80-C-0923 and hence includes refinements of some of the work done during the previous two years of the program to investigate the concept of distributed amplifiers for use as broadband monolithic microwave amplifiers. During the final year of this project we have made some progress in unifying our ideas for design tradeoffs which will yield a desired gain and bandwidth for a given transistor type. Our results also place gain-bandwidth product bounds on distributed amplifiers utilizing a particular transistor type. Finally the theory developed in this report allows the specification of the required transistor to achieve a particular desired gain, bandwidth and impedance level. An overview of the bounds can easily be seen for the microwave region of the spectrum.

Because the microwave GaAs FET has finite input and output resistive losses the gain of a distributed amplifier constructed from such a transistor will be less than or at best equal to the MAG of the active device itself. The concept of achieving useful gain at frequencies where the active device gain is less than one, valid for the lossless case, is not valid for microwave amplifiers. In addition the concept that distributed amplifier bandwidth is limited only by the transmission line cutoff frequency is also invalid because of the inherent losses, and the amplifier's ultimate upper frequency will always be less than the device f_{max}. One should keep in mind, however, that the broadband low pass response through very high microwave frequencies is a distinct advantage of the configuration. This report will treat these limits in quantitative detail but a qualitative view can easily be obtained from the following simple example.

Figure 1.1 shows a block diagram of a microwave distributed amplifier with its input (gate) and output (drain) transmission lines and individual transistors each having resistive loss in both their input and output circuits. These loss elements result in attenuation to waves on each transmission line. The gate line attenuation is frequency dependent, so at

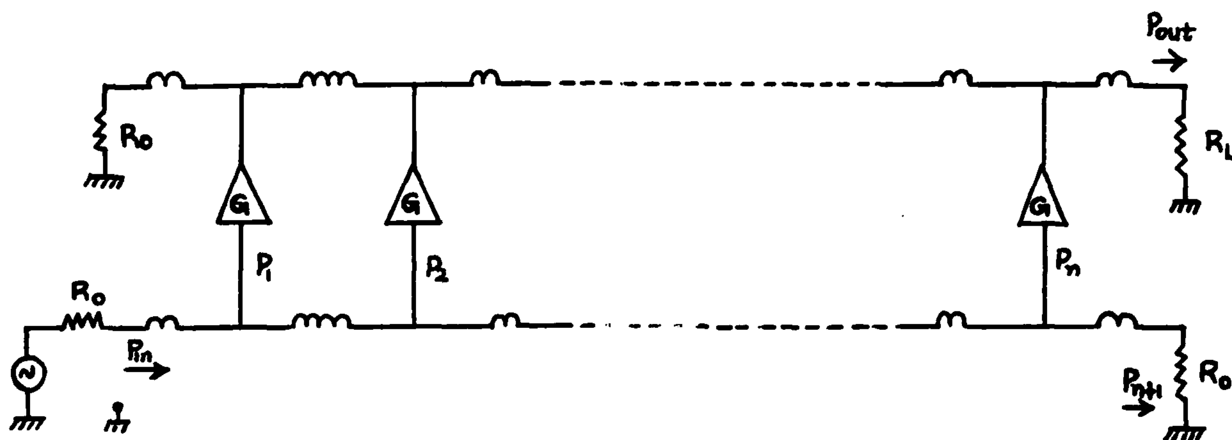

Figure 1.1. Microwave Distributed Amplifier

each frequency there will be an optimum number of active devices for a given amplifier. The optimum number results from the fact that gate line attenuation prevents downstream devices from receiving full excitation. Hence at any given frequency the optimum number is reached when the addition of a device beyond this number results in a net loss to the system because that device is insufficiently excited to overcome the loss its parasitic resistance adds to the drain line.

Using the same reasoning it is easy to see that for a given number of active devices a frequency will always be reached at which the last downstream device will fail to overcome its inherent loss. This follows from the frequency dependent gate line attenuation. As a result the 0 dB gain

frequency for a given distributed amplifier is dictated not by the line cutoff frequency but rather by the device parasitic resistances and hence device f_{max}.

Transmission line attenuation is a very critical factor and it must be minimized in order to achieve reasonable performance for a microwave distributed amplifier. This results in designs with drain line characteristic impedances far less than device R_{ds} and gate line characteristic admittances far greater than the loading conductance. Individual devices hence operate remote from the MAG condition, and distributed amplifier gain will be less than the MAG of its building block devices.

A more detailed analysis leading to design tradeoffs follows in Section II.

II. Distributed Amplifier Analysis and Design

2.1 Gain and Optimum Number of Devices

A schematic representation of the FET distributed amplifier is shown in Fig. 2.1. The gate and drain impedances of the FETs are absorbed into lossy artificial transmission lines formed by using lumped inductors as shown. The resultant transmission lines are referred to as the gate and drain lines. The lines are coupled by the transconductances of the FETs.

An RF signal applied at the input end of the gate line travels down the line to the terminated end where it is absorbed. As the signal travels down the gate line, each transistor is excited by the travelling voltage wave and transfers the signal to the drain line through its transconductance. If the phase velocities on the gate and drain lines are identical, then the signals on the drain line add in the forward direction as they arrive at the output. The waves travelling in the reverse direction are not in phase and any uncancelled signal is absorbed by the drain line termination.

A simplified equivalent circuit of a MESFET arrived at from typical S-parameter measurements at microwave frequencies[1] is shown in Fig. 2.2. R_i is the effective input resistance between the gate and source terminals and C_{gs} is the gate-to-channel capacitance. R_{ds} and C_{ds} are the drain to source resistance and capacitance, respectively. C_{dg} is the drain-to-gate capacitance and g_m the transconductance. In our analysis the device will be considered unilateral and C_{dg} will be neglected.

The equivalent gate and drain transmission lines are shown in Figs. 2.3(a) and 2.3(b). They are essentially loaded constant-k lines wherein the parasitic resistances of the FETs are considered the dominant loss factors.

1. R. W. Strid and R. K. Gleason, "A DC-12 GHz Monolithic GaAs FET Distributed Amplifier," IEEE Trans. Microwave Theory Tech., Vol. MTT-30, pp. 969-975, July 1982.

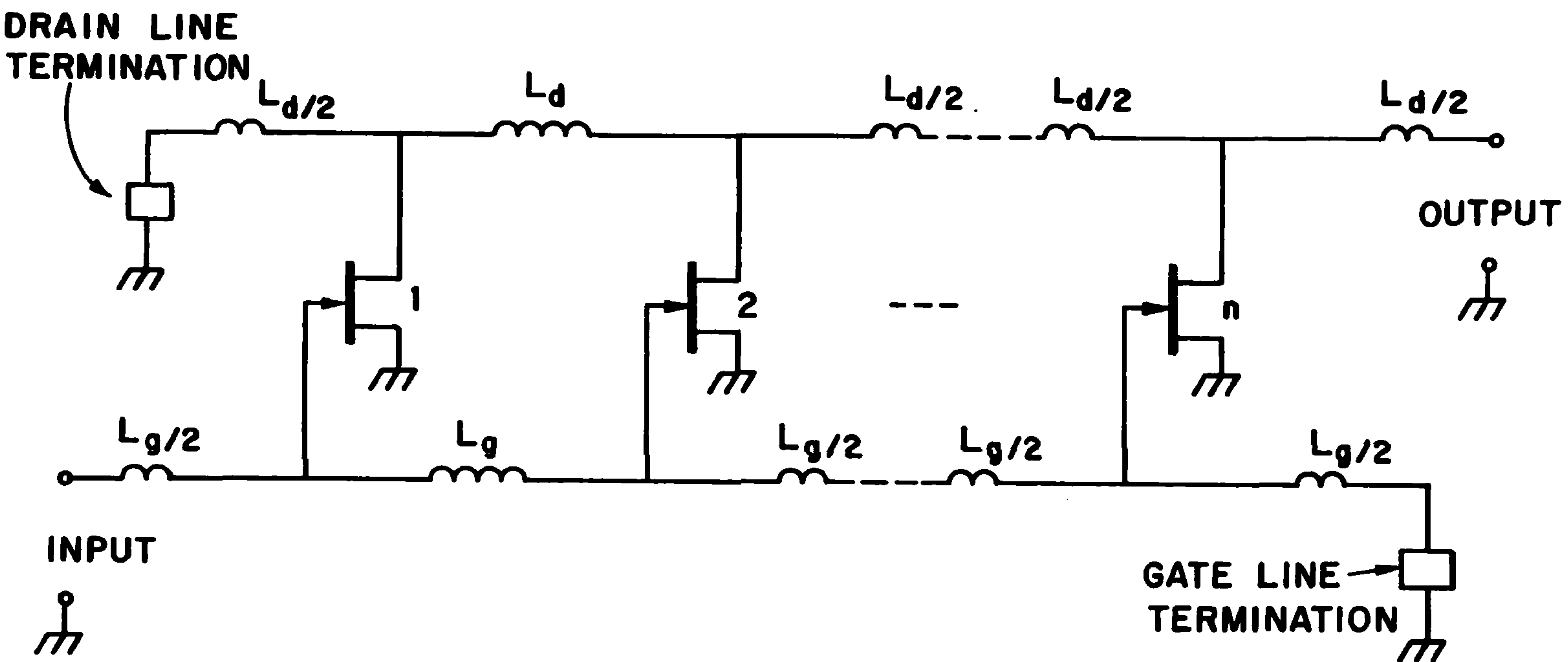

Figure 2.1. Schematic of FET Distributed Amplifier

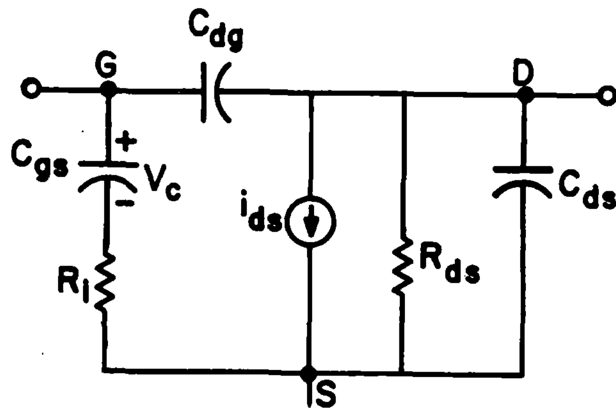

Figure 2.2. Simplified Equivalent Circuit of a MESFET

The attenuation due to metal resistance of microstrip inductors will be considered in Sec. 2.6. The lines are assumed to be terminated in their image impedances at both ends. The current delivered to the load is given by

$$I_o = \frac{1}{2} g_m e^{-\theta_d/2} \left[\sum_{k=1}^{n} V_{ck} e^{-(n-k)\theta_d}\right] \tag{2.1}$$

where V_{ck} is the voltage across C_{gs} of the kth transistor and $\theta_d = A_d + j\Phi_d$ is the propagation function on the drain line. A_d and Φ_d are the attenuation and phase shift per section on the drain line. n is the number of transistors in the amplifier.

V_{ck} can be expressed in terms of the voltage at the gate terminal of the kth FET as

$$V_{ck} = \frac{V_{Gk} e^{-j\tan^{-1}(\omega/\omega_g)}}{[1+(\frac{\omega}{\omega_g})^2]^{1/2}} \tag{2.2a}$$

$$V_{Gk} = \frac{V_i \, e^{-\frac{(2k-1)}{2}\theta_g}}{[1-(\frac{\omega}{\omega_c})^2]} \tag{2.2b}$$

where V_{Gk} is the voltage at the gate terminal of the kth transistor (Appendix A), V_i is the voltage at the input terminal of the amplifier and, $\theta_g = A_g + j\Phi_g$ is the propagation function on the gate line. A_g and Φ_g are the attenuation and phase shift per section on the gate line, $\omega_g = 1/R_i C_{gs}$ is the gate circuit radian cutoff frequency and $\omega_c = 2\pi f_c$ is the radian cutoff frequency of the lines. For constant-k type transmission lines, the phase velocity is a well known function of the cutoff frequency, f_c, of the line. By requiring gate and drain lines to have the same cutoff frequency, the phase velocities are constrained to be equal. Therefore we have, $\Phi_g = \Phi_d = \Phi$ (Appendix B). From (2.1), (2.2a) and (2.2b), I_0 can be expressed as

$$I_o = \frac{g_m V_i \sinh[\frac{n}{2}(A_g - A_d)] e^{-\frac{n}{2}(A_d + A_g)} e^{-jn\Phi - j\tan^{-1}(\omega/\omega_g)}}{2[1+(\frac{\omega}{\omega_g})^2]^{1/2}[1-(\frac{\omega}{\omega_c})^2] \sinh[\frac{1}{2}(A_g - A_d)]} \tag{2.3}$$

The power delivered to the load and input power to the amplifier are respectively given by

$$P_o = \frac{|I_o|^2}{2} Re[Z_{ID}] \approx \frac{|I_o|^2}{2} \sqrt{L_d/C_d[1-(\omega/\omega_c)^2]}$$

and

$$P_i = \frac{|V_i|^2}{2} Re[1/Z_{IG}] \approx \frac{|V_i|^2}{2} / \sqrt{L_g/C_g[1-(\omega/\omega_c)^2]}$$

where Z_{ID} and Z_{IG} are the image impedances of the drain and gate lines (Appendix C).

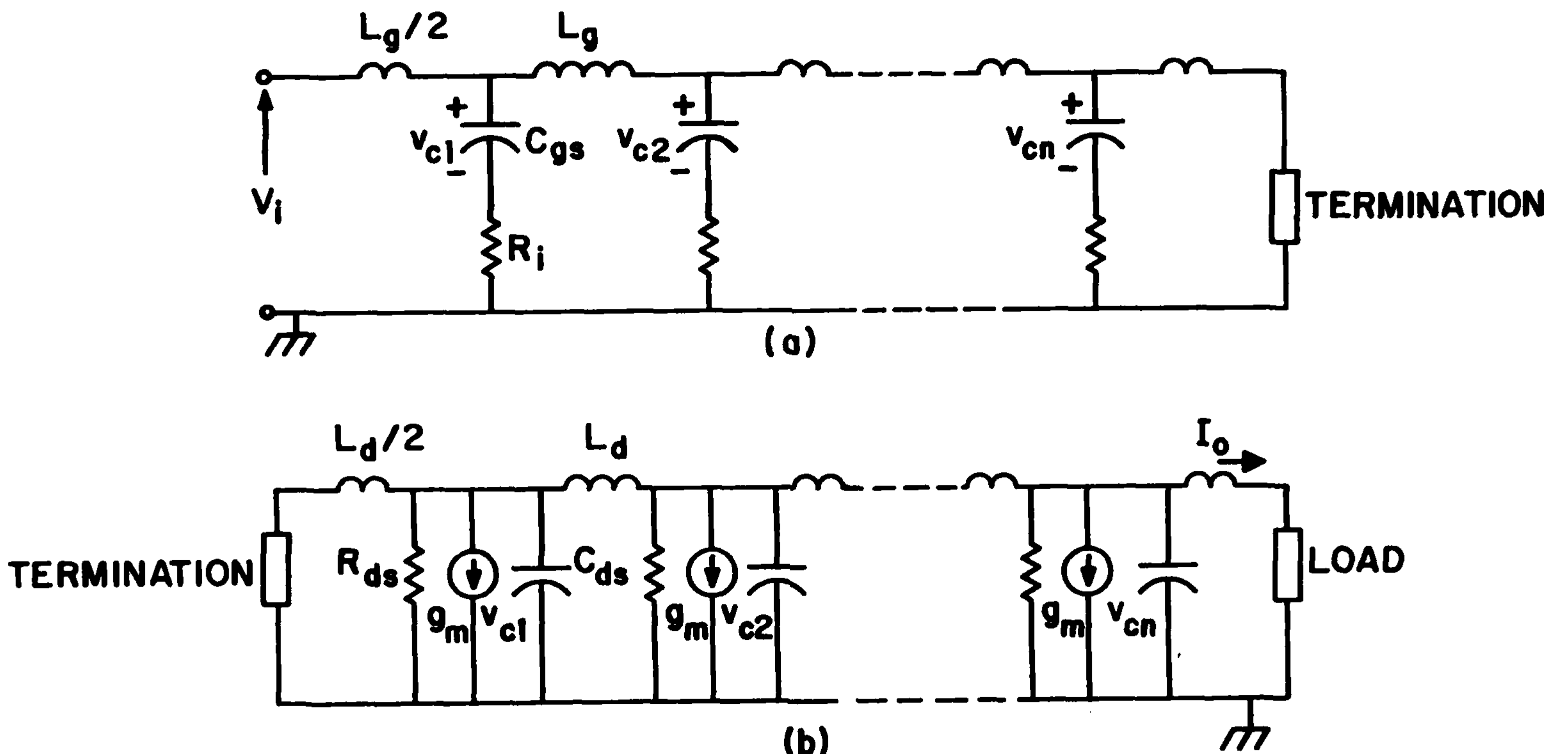

Figure 2.3. (a) Gate Transmission Line
(b) Drain Transmission Line

Therefore the power gain of the amplifier is

$$G = \frac{g_m^2 R_{01} R_{02} \sinh^2 [\frac{n}{2} (A_g - A_d)] e^{-n(A_d + A_g)}}{4[1+(\frac{\omega}{\omega_g})^2][1-(\omega/\omega_c)^2]\sinh^2[\frac{1}{2} (A_g - A_d)]} \tag{2.4}$$

Where $R_{01}(= \sqrt{L_g/C_g})$ and $R_{02}(= \sqrt{L_d/C_d})$ are the characteristic resistances of the gate and drain lines respectively.

Consider an ideal impedance transformer at port 2 which transforms Z_{ID} to Z_{IG} (input impedance of the succeeding amplifier in a tandem connection of identical distributed amplifiers) as shown in Fig. 2.4.

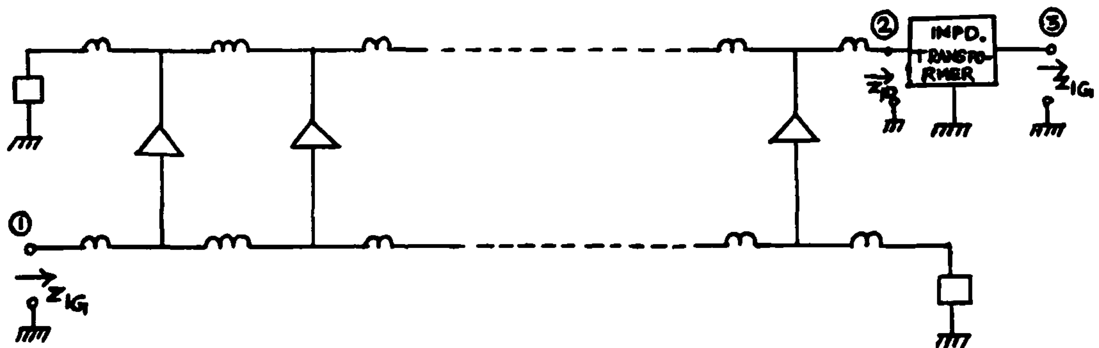

Figure 2.4. Distributed Amplifier and Impedance Transformer at Output Port

Then the magnitude of the voltage gain between ports 3 and 1 can be obtained from equation (2.4) as

$$A = \frac{g_m (R_{01} R_{02})^{1/2} \sinh[\frac{n}{2} (A_g - A_d)] e^{-\frac{n}{2}(A_d + A_g)}}{2[1+(\frac{\omega}{\omega_g})^2]^{1/2} [1-(\frac{\omega}{\omega_c})^2]^{1/2} \sinh[\frac{1}{2} (A_g - A_d)]} \tag{2.5}$$

From equation (2.5) we can show that the number of devices which maximizes gain at a given frequency is[2]

2. J. B. Beyer, et al., "Wideband Monolithic Microwave Amplifier Study," ONR Report No. NR 243-033-02, July 1982.

$$N_{opt} = \frac{\ln(A_d/A_g)}{A_d - A_g} \tag{2.6}$$

A similar relation was found by Podgorski and Wei[3] for the optimum gate width of a travelling-wave transistor. Therefore it is clear that in the presence of attenuation, the gain of a distributed amplifier cannot be increased indefinitely by adding devices. This property of the distributed amplifier can be easily explained. As the signal travels down the gate line each transistor receives less energy than the previous one due to attenuation on the gate line. Similarly, the signal excited in the drain line by a transistor is attenuated by the subsequent line sections between it and the output port. Therefore, additional transistors not only decrease the excitation of the last device but also increase the overall attenuation on the drain line. The gain of the amplifier increases with additional devices until the optimum number of devices at the given frequency is reached. Any device added beyond the optimum number is not driven sufficiently to excite a signal in the drain line which will overcome the attenuation in the extra section of the drain line, which the signal from preceeding devices will now suffer. Consequently the gain of the amplifier begins to decrease with further addition of devices.

The gain equation (2.5) can be expressed as

$$A = \frac{g_m (R_{01} R_{02})^{1/2} \sinh[\frac{n}{2}(A_g - A_d)] e^{-\frac{n}{2}(A_d + A_g)}}{2[1 + X_k^2 (\frac{\omega_c}{\omega_g})^2]^{1/2} [1 - X_k^2]^{1/2} \sinh[(A_g - A_d)/2]} \tag{2.7}$$

where $X_k = \omega/\omega_c$ is the normalized frequency.

3. A. S. Podgorski and L. Y. Wei, "Theory of Travelling-Wave Transistors," IEEE Trans. Electron Devices, Vol. ED-29, pp. 1845-1853, December 1982.

At this point analytical expressions for A_g and A_d are required. They are derived in the following section.

2.2 Attenuation on Gate and Drain Lines

For a constant-k transmission line the propagation function can be determined from the following relation[4]

$$\cosh(\theta) = 1 + \frac{Z_1}{2Z_2} \tag{2.8}$$

where θ (= $A + j\phi$) is the propagation function, A and ϕ are the attenuation and phase shift per section of the line and Z_1 and Z_2 are the impedances in the series and shunt arms of a section of constant-k line as shown in Fig. 2.5.

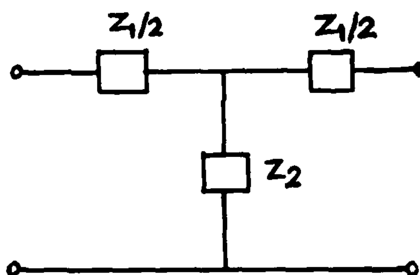

Figure 2.5. A section of constant-k line

Equation (2.8) can be expressed as

$$\cosh A \cos \phi = \mathrm{Re}[1 + \frac{Z_1}{2Z_2}] \tag{2.9a}$$

$$\sinh A \sin \phi = \mathrm{Im}[1 + \frac{Z_1}{2Z_2}] \tag{2.9b}$$

4. O. J. Zobel, "Transmission Characteristics of Electric Wave-Filters," BSTJ, Vol. 3, pp. 567-620, 1923.

By eliminating ϕ from euqations (2.9a) and (2.9b) we obtain the following equation

$$\sinh^2 A = \tanh^2 A[\mathrm{Re}(1 + \frac{Z_1}{2Z_2})]^2 + [I_m(1 + \frac{Z_1}{2Z_2})]^2 \qquad (2.10)$$

when $A \leq 0.4$, $\sinh^2 A \approx \tanh^2 A \approx A^2$. Under this condition we can derive the following equation for A from equation (2.10)

$$A \approx \frac{\mathrm{Im}[1 + \frac{Z_1}{2Z_2}]}{[1 - [\mathrm{Re}(1 + \frac{Z_1}{2Z_2})]^2]^{1/2}} \qquad (2.11)$$

Equation (2.11) is the general form of the attenuation per section of constant-k line. When evaluated for the specific networks shown in Figures (2.6a) and (2.6b) we obtain the following closed form expressions for attenuation on gate and drain lines.

$$A_g = \frac{(\omega_c/\omega_g)X_k^2}{\sqrt{1 - [1 - (\frac{\omega_c}{\omega_g})^2]X_k^2}} \qquad (2.12)$$

$$A_d = \frac{(\omega_d/\omega_c)}{\sqrt{1 - X_k^2}} \qquad (2.13)$$

where

$$\omega_g = \frac{1}{R_i C_{gs}}$$

$$\omega_d = \frac{1}{R_{ds} C_{ds}}$$

$$\omega_c = \frac{2}{\sqrt{L_g C_{gs}}} = \frac{2}{\sqrt{L_d C_{ds}}}$$

and

$$X_k = \omega/\omega_c.$$

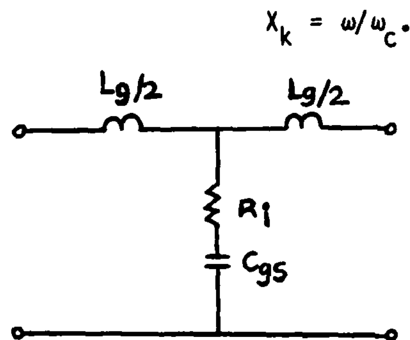

Fig. 2.6a. A section of gate line

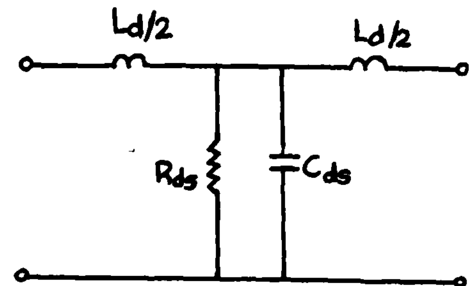

Fig. 2.6b. A section of drain line

The attenuation on gate and drain lines versus frequency with ω_c/ω_g and ω_d/ω_c as parameters are shown in Figs. (2.7a) and (2.7b) respectively. It is evident from the figures that the gate line attenuation is more sensitive to frequency than drain line attenuation. Further, unlike attenuation in the gate line the drain line attenuation does not vanish in the low frequency limit. Therefore the frequency response of the amplifier can be expected to be predominantly controlled by the attenuation on the gate line and the dc gain by the attenuation on the drain line as will be shown in the following section.

It is clear from equations (2.12) and (2.13) that attenuation on the gate and drain lines can be decreased by making ω_c/ω_g and ω_d/ω_c small. Therefore, for a given ω_c, one has to choose a device having high ω_g and low ω_d. For a given device ω_g can be increased by connecting a capacitor in series with gate terminal of the FET.[5] Similarly ω_d can be decreased by padding the drain to source capacitance by an external capacitance at the drain terminal of the FET.

5. I. S. Chang, - Paper in preparation.

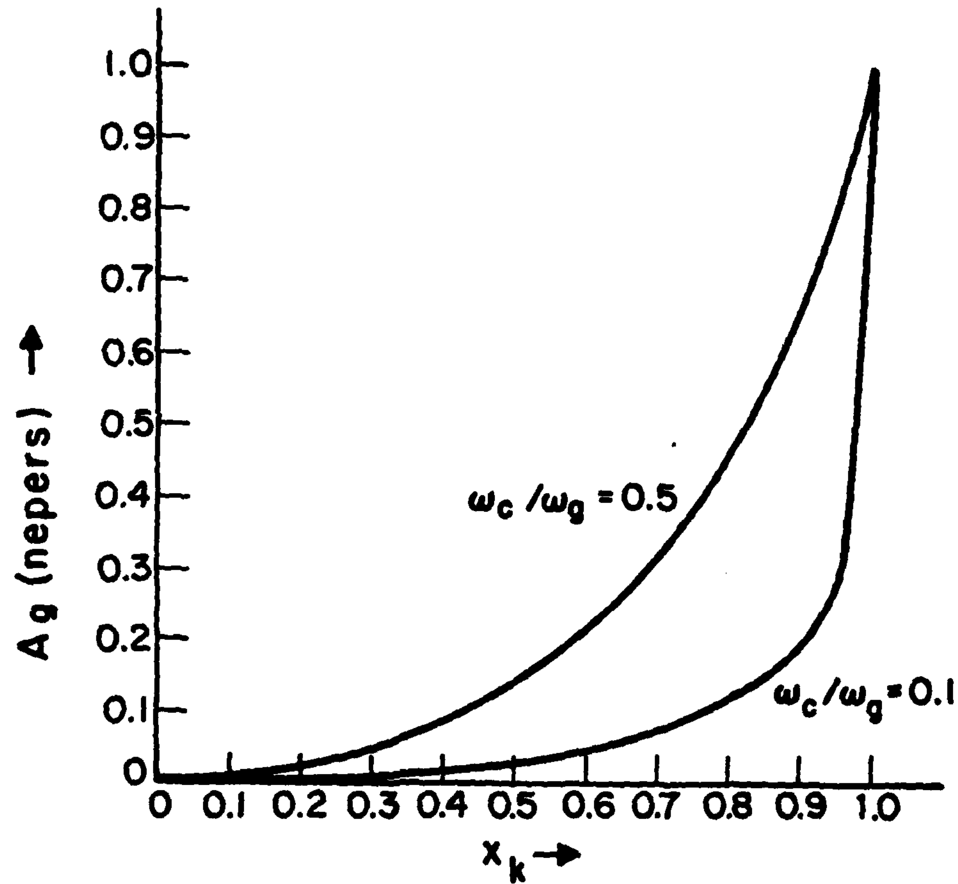

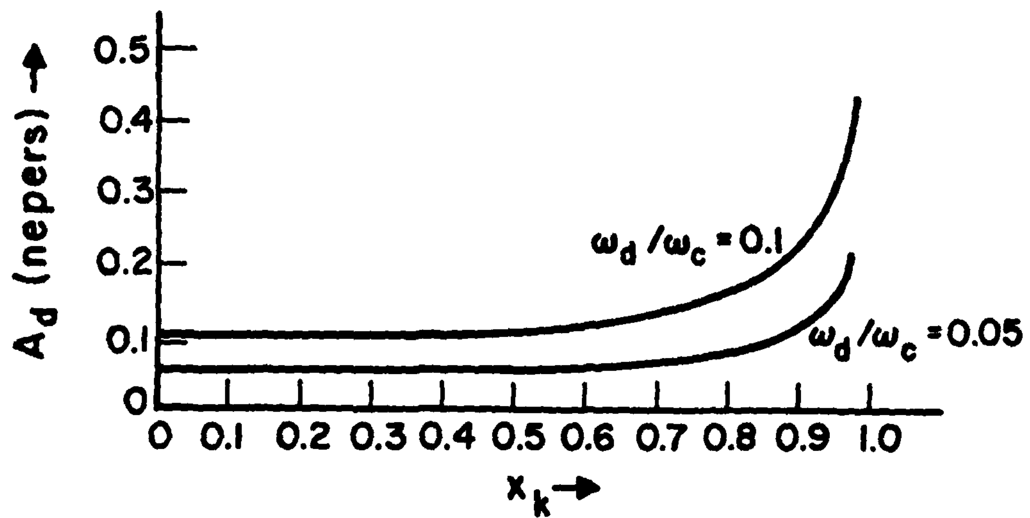

Figure 2.7. (a) Attenuation on Gate Line Versus Normalized Frequency
(b) Attenuation on Drain Line Versus Normalized Frequency

2.3. Normalized Frequency Response and Constant-Fractional Bandwidth Curves

Equations (2.12) and (2.13) can be rewritten as

$$A_g = \frac{A_{og} X_k^2}{\sqrt{1 - g X_k^2}} \tag{2.14}$$

$$A_d = \frac{A_{od}}{\sqrt{1 - X_K^2}} \tag{2.15}$$

where

$$A_{og} = \frac{\omega_c}{\omega_g}$$

$$A_{od} = \frac{\omega_d}{\omega_c}$$

and

$$g = 1 - \left(\frac{\omega_c}{\omega_g}\right)^2$$

Using (2.14) and (2.15) we can rewrite the gain equation (2.7) as

$$A = \frac{g_m (R_{01} R_{02})^{1/2}}{2} \; \frac{\exp[-n(A_{og} X_k^2/\sqrt{1-gX_k^2} + A_{od}/\sqrt{1-X_k^2})/2]}{\sqrt{1-X_k^2}\;\sqrt{1 + X_K^2(\omega_c/\omega_g)^2}}$$

$$\times \frac{\sinh[n(A_{og} X_k^2/\sqrt{1-X_k^2 g} - A_{od}/\sqrt{1-X_k^2})/2]}{\sinh[(A_{og} X_k^2/\sqrt{1-X_k^2 g} - A_{od}/\sqrt{1-X_k^2})/2]} \tag{2.16}$$

Following Horton's[6] idea, we define

$$a = n\,A_{og}/2 = \frac{n\omega_c}{2\omega_g}, \quad b = n\,A_{od}/2 = \frac{n\omega_d}{2\omega_c}, \quad g = 1 - (2a/n)^2 \tag{2.17a,b,c}$$

6. W. H. Horton, et al., "Distributed Amplifiers: Practical Considerations and Experimental Results," Proc. IRE, Vol. 38, pp. 748-753, July 1950.

and rewrite equation (2.16) using (2.17a) and (2.17b). The result is

$$A = \frac{g_m(R_{01}R_{02})^{1/2}}{2} \frac{\exp[-(aX_k^2/\sqrt{1-gX_k^2} + b/\sqrt{1-X_k^2})]}{\sqrt{1-X_k^2}\sqrt{1 + X_k^2(\frac{2a}{n})^2}}$$

$$\times \frac{\sinh[aX_k^2/\sqrt{1-gX_k^2} - b/\sqrt{1-X_k^2}]}{\sinh[(a/n)X_k^2/\sqrt{1-gX_k^2} - (b/n)/\sqrt{1-X_k^2}]} \tag{2.17d}$$

From equation (2.17d) the gain of the amplifier in the low frequency limit can be shown to be

$$A_0 = \frac{g_m(R_{01}R_{02})^{1/2}\sinh(b)e^{-b}}{2\sinh(b/n)} \tag{2.18a}$$

A_0 is referred here as the d.c. gain. The equation (2.17d) when normalized to the d.c. gain (2.18a) yields the following normalized gain equation for the amplifier

$$A_N = \frac{A}{A_0} = \frac{\sinh(b/n)e^b}{\sinh(b)} \times \frac{\exp[-(aX_k^2/\sqrt{1-gX_k^2} + b/\sqrt{1-X_k^2})]}{\sqrt{1-X_k^2}\sqrt{1 + X_k^2(\frac{2a}{n})^2}}$$

$$\frac{\times \sinh[aX_k^2/\sqrt{1-gX_k^2} - b/\sqrt{1-X_k^2}]}{\sinh[(a/n)X_k^2/\sqrt{1-gX_k^2} - (b/n)/\sqrt{1-X_k^2}]} \tag{2.18b}$$

It is evident from equation (2.18b) that the normalized frequency response of the amplifier is a function of the parameters a and b. The a and b parameters are related to gate and drain line attenuations, respectively. The dc gain of the amplifier is controlled by the attenuation on the drain line as seen in (2.18a).

From equation (2.18b) one can determine the normalized frequency response of the amplifier for assumed values of a and b as shown in Fig. 2.8. The normalized response does not change appreciably with n. The range of a and b values which yields the same frequency response can be determined from equation (2.18b) by iteration. By a proper choice of a and b parameters the amplifier can be designed to give a nearly flat response up to a frequency close to the cutoff frequency of the lines. This is the distinct advantage of the distributed amplifier using discrete transistors as compared to a travelling-wave transistor proposed by Podgorski and Wei[3] whose gain monotonically decreases due to transmission line attenuation. In the case of a distributed amplifier using discrete transistors, the rise in voltage at the gate terminals compensates to some extent the effect of gate line attenuation as the cutoff frequency is approached [equation (2.2b)]. This can be seen if one views the lumped constant gate line as cascaded π-sections. The transistor gate-source terminals are connected across the π-section terminals. It is well known that the image impedance of a π-section and hence the gate-source voltage, rises as the cutoff frequency is approached. We will demonstrate how this effect can be used to obtain nearly flat low-pass response out to frequencies approaching the cutoff of the lines.

In order to enable cascading of distributed amplifier stages, the individual amplifiers must be designed to give a nearly flat gain response up to the desired maximum frequency. This calls for an appropriate choice of a and b parameter values. An ideal frequency response is the one which is flat up to the cutoff frequency of the lines. However, depending on the values of a and b, the frequency response starts deviating from the ideal response at a frequency below the cutoff frequency of the lines. In order to select the

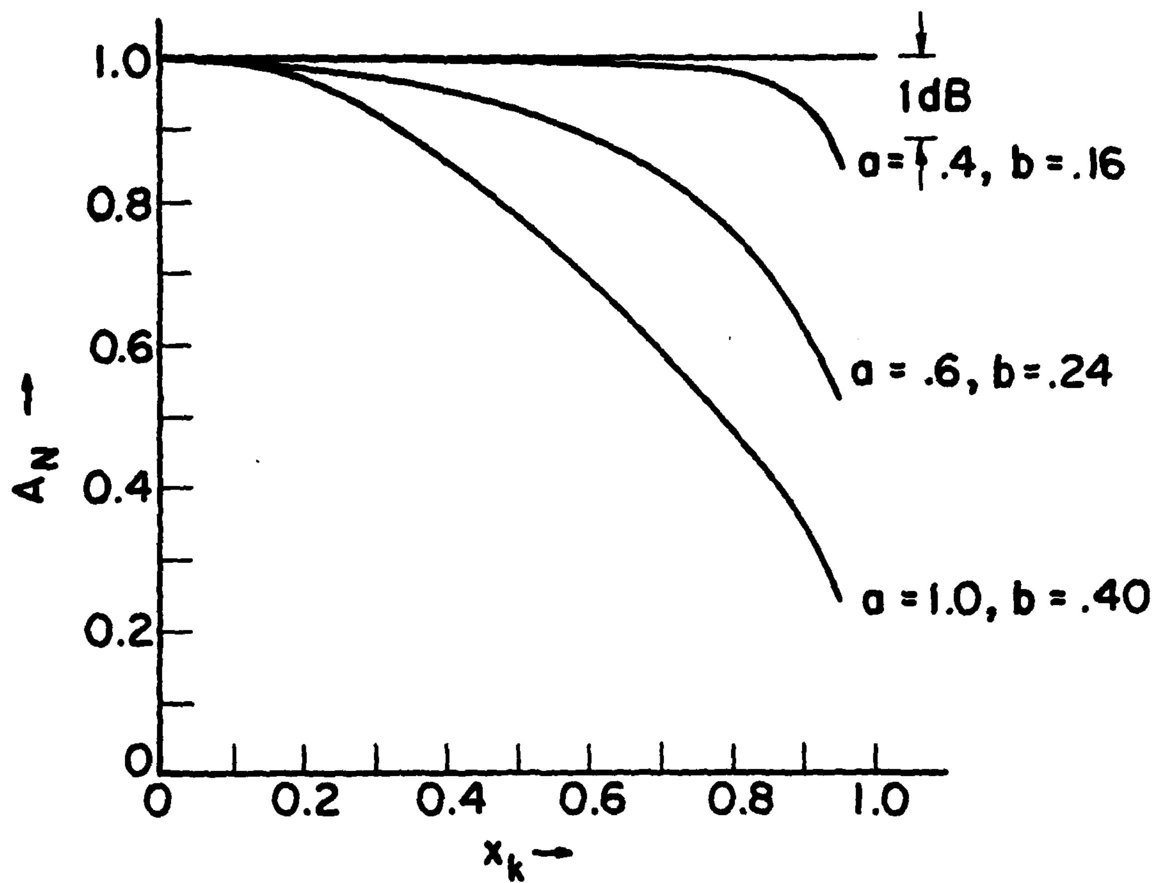

Figure 2.8. Normalized Frequency Response of MESFET Distributed Amplifiers

required frequency response and corresponding a and b values it is necessary to characterize these responses by their degrees of flatness. We define the degree of flatness as the fractional bandwidth $X = f_{1dB}/f_c$, where f_{1dB} is the frequency at which the gain of the amplifier falls below the dc gain by 1dB as shown in Fig. 2.8.

The values of parameters a and b which give the same fractional bandwidth can be determined from equation (2.18b) and are plotted on the a-b plane as shown in Fig. 2.9. These curves give the designer the values of a and b to choose from which yield the same fractional bandwidth. It is clear from Fig. 2.9 that the flatness of response is quite sensitive to the parameter 'a' which controls the attenuation on the gate line.

2.4 Gain-Bandwidth Product

Extending the analysis of Horton, et al.[6] to include the attenuation on the output line we can derive the gain-bandwidth relation starting from equation (2.18a). When $b \leq 0.4$ $\sinh(b) \approx b$ and $\sinh(b/n) \approx b/n$. Therefore equation (2.18a) can be written as

$$A_0 = \frac{n g_m (R_{01} R_{02})^{1/2} e^{-b}}{2} \qquad (2.19)$$

R_{01} and R_{02} can be expressed in terms of the cutoff frequency of the lines as follows:

$$R_{01} = \sqrt{\frac{L_g}{C_g}} = \frac{1}{\pi f_c C_{gs}} \qquad (2.20a)$$

and

$$R_{02} = \sqrt{\frac{L_d}{C_d}} = \frac{1}{\pi f_c C_{ds}} \qquad (2.20b)$$

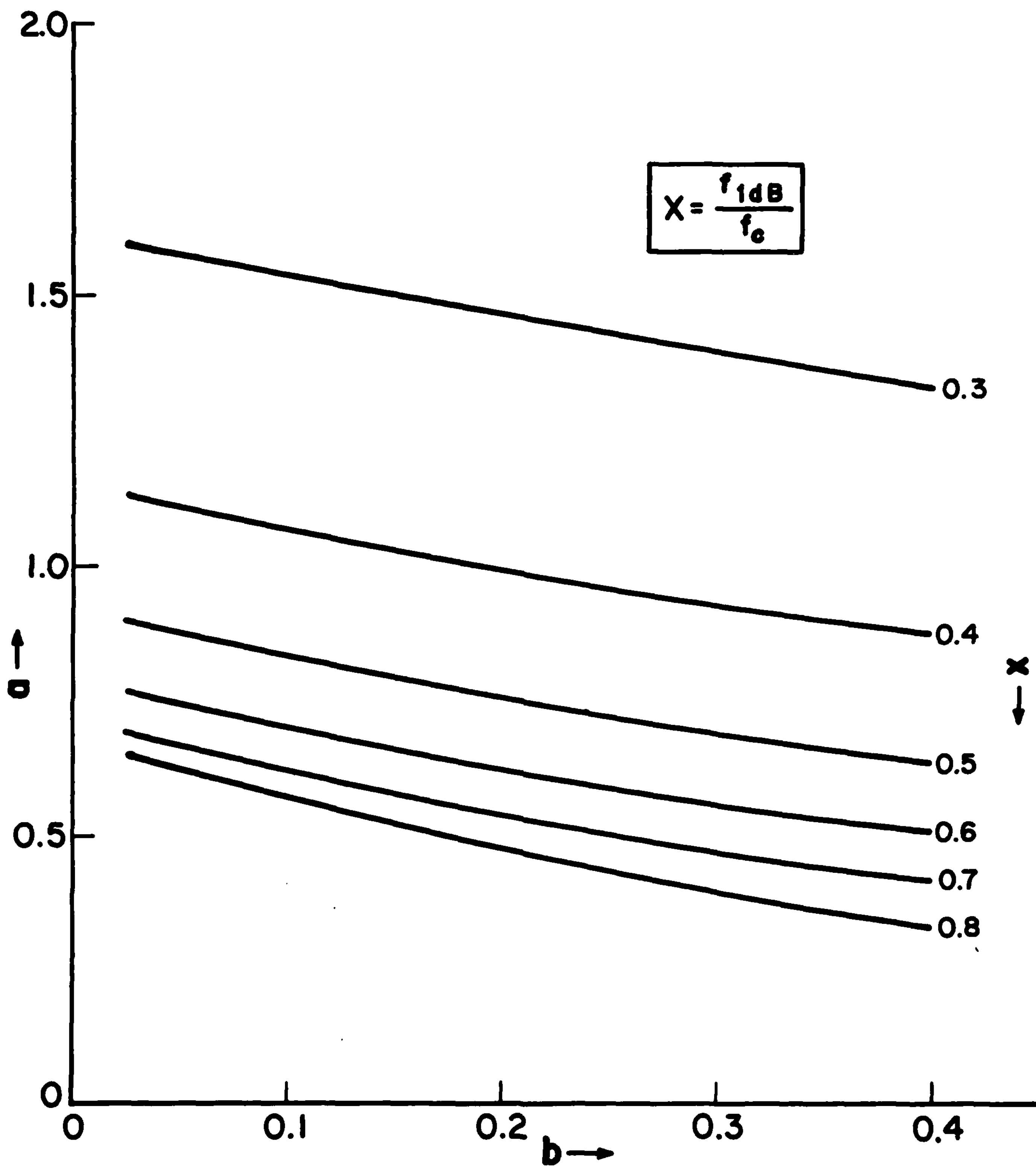

Figure 2.9. Constant-Fractional Bandwidth Curves

Using (2.20a) and (2.20b) equation (2.19) can be expressed as

$$A_0 = \frac{g_m n e^{-b}}{2\pi\sqrt{C_{gs}C_{ds}}\, f_c} \tag{2.21}$$

Using equations (2.17a) and (2.17b) equation (2.21) can be reduced to

$$\frac{A_0 f_c}{4\, f_{max}} = (ab)^{1/2} e^{-b} \tag{2.22}$$

where f_{max} is the frequency at which the maximum available gain (MAG) of the FET becomes unity.[7] It is also referred to as the maximum frequency of oscillation of the FET. f_{max} is given by

$$f_{max} \approx \frac{g_m}{4\pi C_{gs}} \sqrt{\frac{R_{ds}}{R_i}} \tag{2.23}$$

Equation (2.22) can be written as

$$A_0\, f_{1dB} = 4\, K\, X\, f_{max} \tag{2.24}$$

where $K = (ab)^{1/2} e^{-b}$ and $f_{1dB} = X\, f_c$. Fig. 2.10 shows K = const curves on the a-b plane. Equation (2.24) gives the gain-bandwidth product for a MESFET distributed amplifier. It is dependent on the values of a and b as well as the f_{max} of the FET.

The factor KX in equation (2.24) can be viewed as the gain-bandwidth product of the amplifier normalized to $4f_{max}$. The value of KX can be found from Figures 2.9 and 2.10. The maximum value can be shown to be about 0.2. Fig. 2.11 shows the normalized maximum gain-bandwidth product curve on the a-b

7. P. Wolf, "Microwave Properties of Schottky-Barrier Field-Effect Transistor," IBM J. Res. Develop., Vol. 4, pp. 125-141, March 1970.

plane. By choosing the parameter values a and b to lie on this curve one can design a distributed amplifier having maximum gain-bandwidth product. Also if n and ω_c are specified one can obtain from this curve the range of ω_d and ω_g values (device specifications) which yields maximum gain-bandwidth product.

It follows that the maximum gain-bandwidth product is given by

$$A_0 f_{1dB} \approx 0.8 f_{max} \tag{2.25}$$

It can be seen that the maximum gain-bandwidth product of the distributed amplifier is constrained by the f_{max} of the device. From equation (2.25) one can show that the frequency at which the gain of the distributed amplifier becomes unity cannot exceed 0.7 f_{max}. We have also confirmed this by the computer-aided analysis of several distributed amplifiers. Therefore it is clear that in MESFET distributed amplifiers the maximum operating frequency is constrained by the device f_{max} and not by the f_c of the lines.

2.5 Amplifier Design

Up to this point we have shown how the frequency response of the amplifier depends on a range of values of the parameters a and b, and we will now show how the choices of cutoff frequency and impedances of the lines, and particular active device and their number constrain the values of a and b and hence the frequency response. We now present a systematic design approach which will enable one to examine the possible trade-offs between the design variables and arrive at a suitable design.

The following relations can be derived from equations (2.17a) and (2.17b).

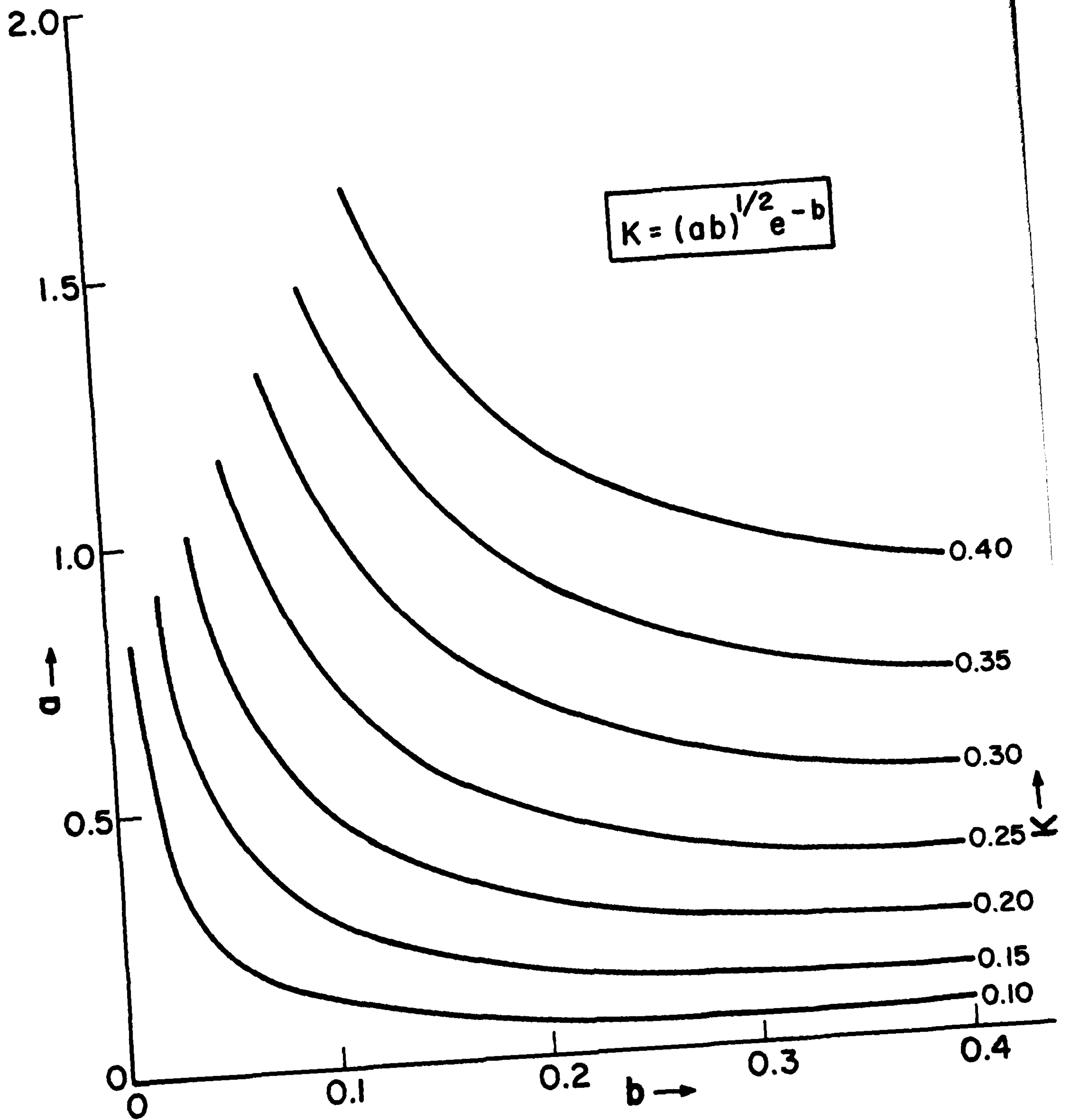

Figure 2.10. K = const Curves

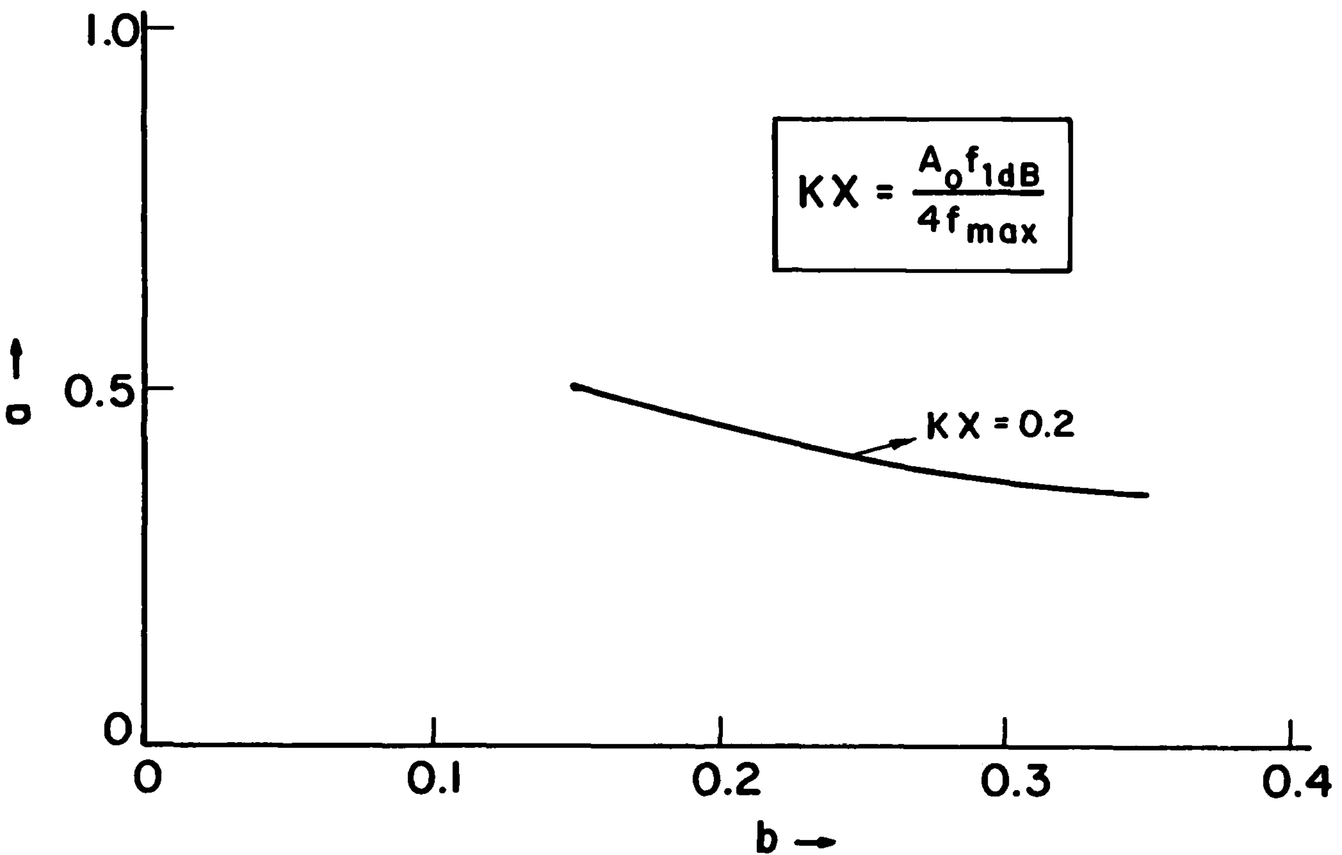

Figure 2.11. Normalized Maximum Gain-Bandwidth Product-Curve

$$ab = \frac{n^2 \omega_d}{4\omega_g} \tag{2.26}$$

$$a/b = \frac{\omega_c^2}{\omega_g \omega_d} \tag{2.27}$$

Equation (2.26) defines the value of the product ab in terms of the number of devices and the device characteristic frequencies (ω_g and ω_d). This equation defines a family of hyperbolas on the a-b plane as shown in Fig. 2.12. Equation (2.27) defines a family of lines on the a-b plane as shown in Fig. 2.12. Each line corresponds to a cutoff frequency (fc) and characteristic resistances (R_{01} and R_{02}) of the lines because they are related as follows,

$$R_{01} = \frac{1}{\pi f_c C_{gs}} \; ; \quad R_{02} = \frac{1}{\pi f_c C_{ds}}$$

$$f_c = \frac{1}{\pi\sqrt{L_g C_{gs}}} = \frac{1}{\pi\sqrt{L_d C_{ds}}}$$

The point of intersection of a hyperbola defined by equation (2.26) and a line defined by equation (2.27) determines an operating point on the a-b plane. The value of X (fractional bandwidth) and K corresponding to this operating point can be obtained from Figures 2.9 and 2.10 respectively since the coordinates (a,b) of the point are known. Then the dc gain (A_0) and bandwidth (f_{1dB}) can be obtained from the following relations.

$$f_{1dB} = X \, f_c \tag{2.28}$$

$$A_0 = \frac{4K \, X \, f_{max}}{f_{1dB}} \tag{2.29}$$

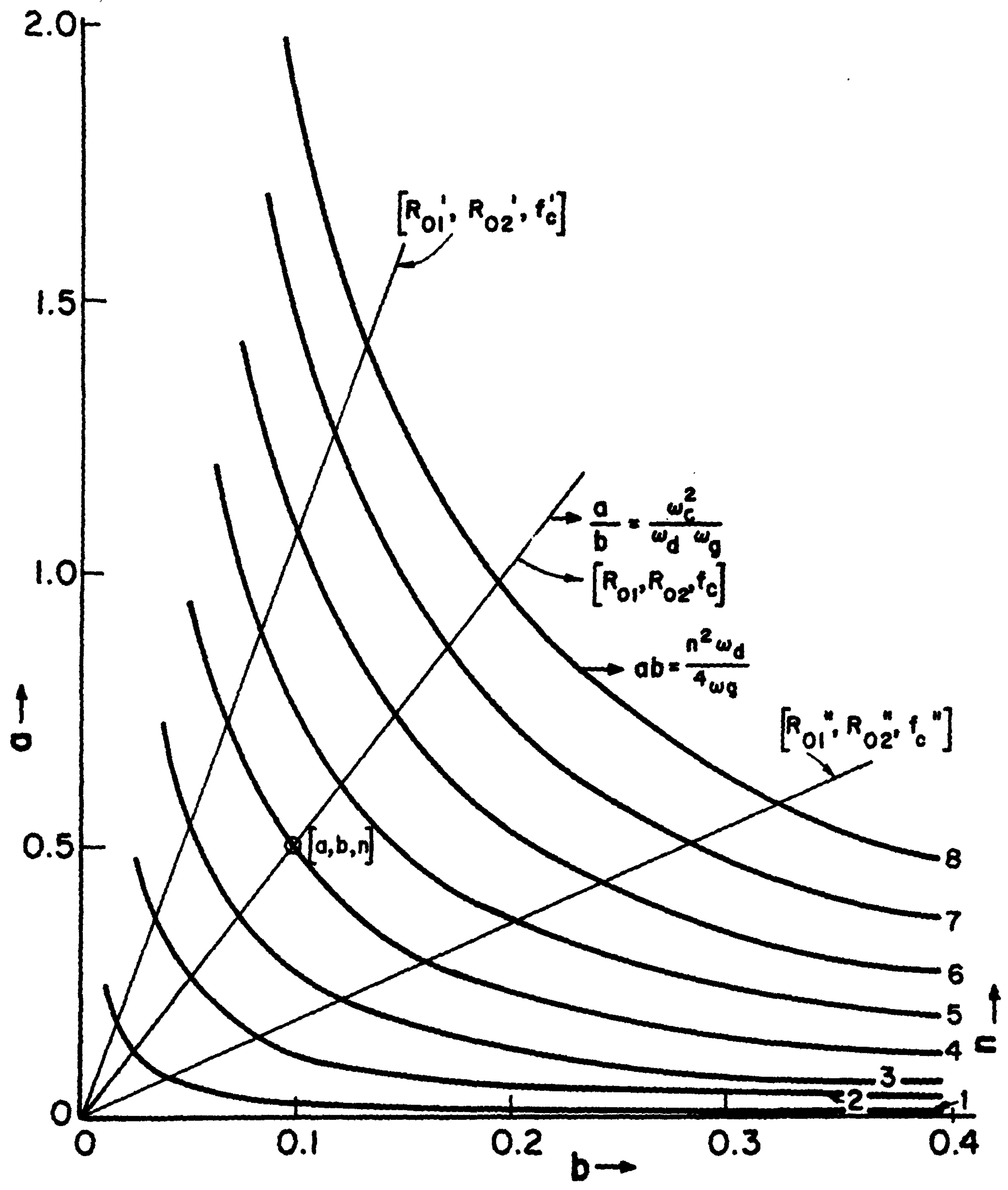

Figure 2.12. ab = const Curves and a/b = const Lines

The frequency response of the amplifier can be obtained from equation (2.18b). The amplifier is now completely defined in terms of the device, the number of devices, the cutoff frequency and the impedances of the lines and the frequency response. Superposition of Figures 2.9, 2.10 and 2.12 will enable one to examine the trade-offs between the design variables. We will now illustrate the design approach presented above by two examples.

Design Example 1

Let us consider the design of a distributed amplifier using typical 300 μm MESFETs which have the following characteristic frequencies.

$$f_g = \omega_g/2\pi = 84.2 \text{ GHz}$$

$$f_d = \omega_d/2\pi = 4.8 \text{ GHz}$$

$$f_{max} = 77.2 \text{ GHz}$$

Let $R_{01} = R_{02}$. Therefore we have $C_{gs} = C_{ds} + C_p$, since the cutoff frequencies of the lines are also constrained to be equal. C_p is an external capacitance added to the device output capacitance C_{ds}. For the MESFET considered here $C_{gs} = 0.27$ pF, $C_{ds} = 0.11$ pF and $R_{ds} = 300\ \Omega$. Therefore we obtain the following equations.

$$f'_d = 1/2\pi R_{ds}(C_{ds}+C_p) = 1.96 \text{ GHz} \tag{2.30}$$

$$ab = \frac{n^2\omega'_d}{4\omega_g} = (5.8\times10^{-3})n^2 \tag{2.31}$$

$$a/b = \frac{\omega_c^2}{\omega'_d\omega_g} = (6.06\times10^{-21})f_c^2 \tag{2.32}$$

The set of design curves consisting of curves defined by equation (2.31), the lines defined by (2.32), fractional bandwidth curves (Fig. 2.9) and K = const curves (Fig. 2.10) are plotted on the a-b plane as shown in Fig. 2.13.

For an amplifier having $R_{01} = R_{02} = 50\Omega$, $f_c = 23.6$ GHz and $n = 4$ we obtain the following values for a, b, X, and K from Fig. 2.13.

$$a = .56$$

$$b = .17$$

$$X = .7$$

$$K = .25$$

Therefore the bandwidth of the amplifier is

$$f_{1dB} = X\, f_c = 16.52 \text{ GHz}$$

and the dc gain is

$$A_0 = \frac{4\, KX\, f_{max}}{f_{1dB}} = 3.26 \ (10.3 \text{ dB})$$

The frequency response of this amplifier predicted by equation (2.18b) and the response obtained by using the standard microwave circuit analysis program are shown in Fig. 2.14. They are in good agreement. The image terminations are realized by using the standard m-derived half section filters at both ends of the lines (see section 2.7).

A careful study of Fig. 2.13 reveals that for a given cutoff frequency (and hence the impedance of the lines) the gain of the amplifier can be increased by adding devices at the expense of bandwidth. On the other hand, if the number of devices is decreased one can obtain a larger bandwidth by sacrificing gain. If the number of devices is fixed a decrease in cutoff frequency (and hence an increase in the impedance of the lines) results in an increase in gain and reduction in bandwidth.

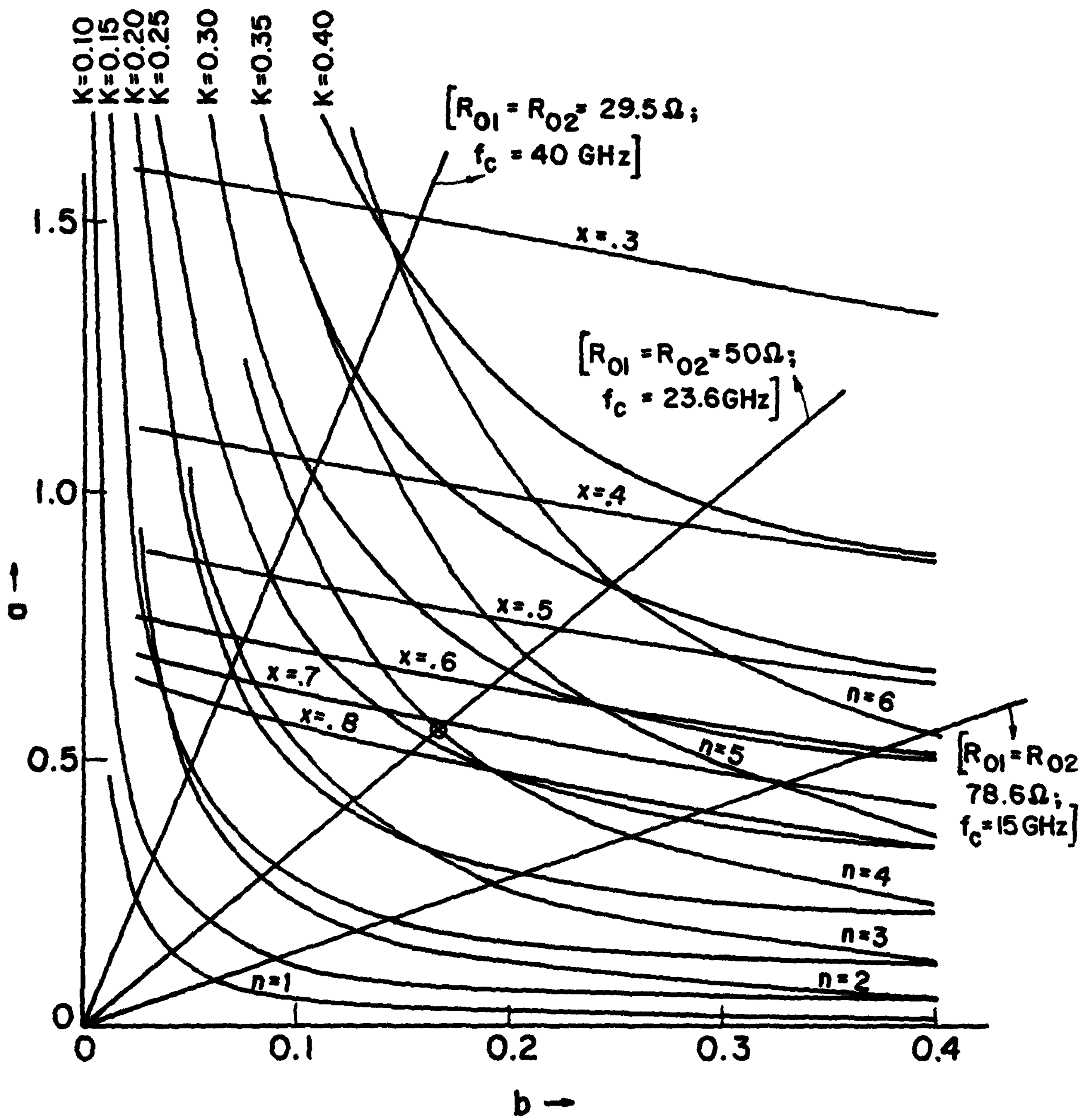

Figure 2.13. Design Curves for the Distributed Amplifier using Typical 300 μm MESFETs

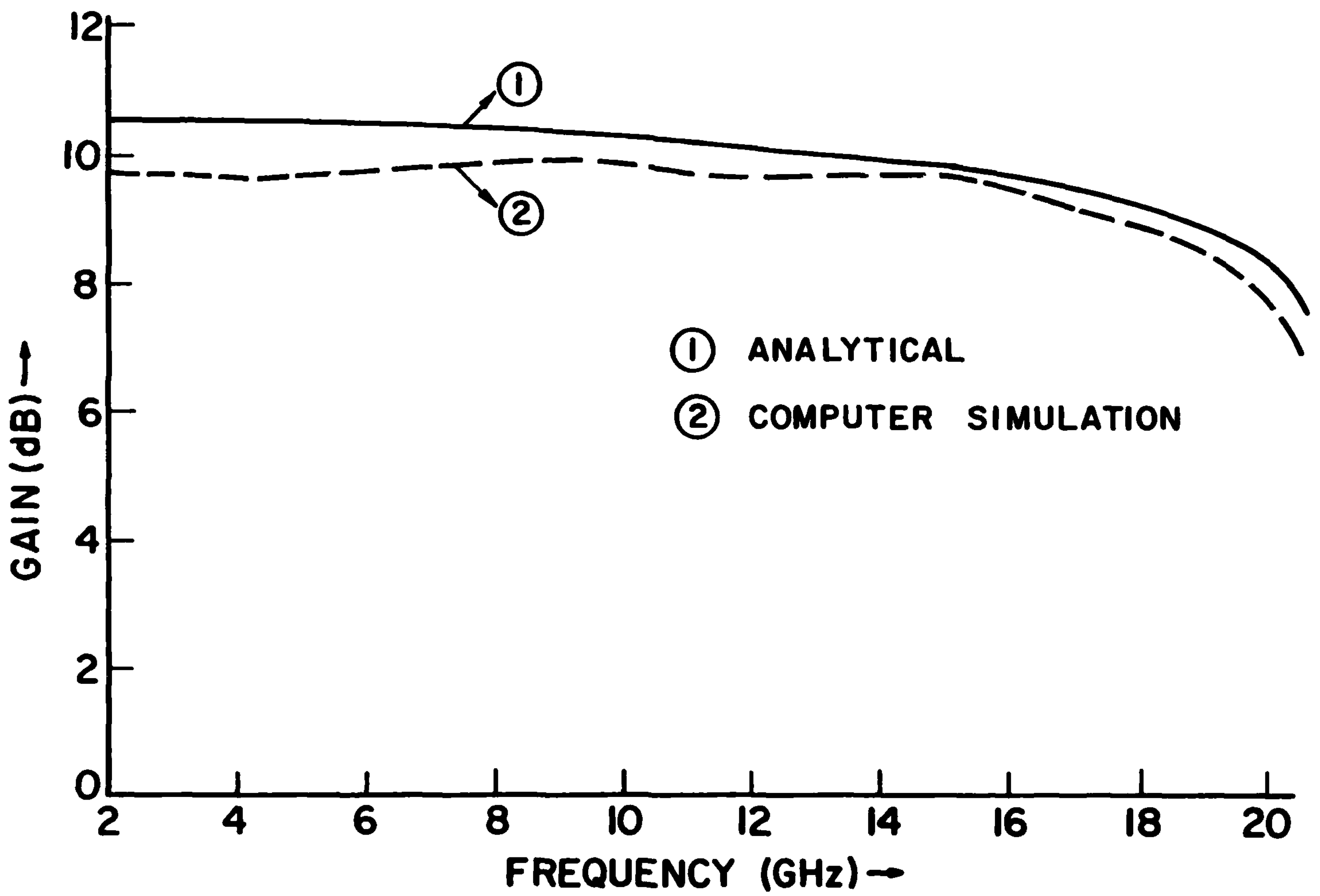

Figure 2.14. Frequency Response of the Four-Section Distributed Amplifier using Typical 300 μm MESFETs

Design Example 2

Let us consider a 60 μm gate width MESFET having the following characteristic frequencies

$$f_g = \omega_g/2\pi = 257.66 \text{ GHz}$$

$$f_d = \omega_d/2\pi = 11.46 \text{ GHz}$$

$$f_{max} = 136.14 \text{ GHz.}$$

Let $R_{01} = R_{02}$. Therefore, as in the previous example $C_{gs} = C_{ds} + C_p = C_d'$. For the FET considered here $C_{gs} = 0.07$ pF and $R_{ds} = 555.55\ \Omega$. Therefore we have

$$f_d' = \omega_d'/2\pi = \frac{1}{2\pi R_{ds} C_d'} = 4.03 \text{ GHz} \quad (2.33)$$

Therefore

$$ab = \frac{n^2 \omega_d'}{4\omega_g} = (3.915 \times 10^{-3}) n^2 \quad (2.34)$$

$$a/b = \frac{\omega_c^2}{\omega_d' \omega_g} = (9.63 \times 10^{-22}) f_c^2 \quad (2.35)$$

The design curves for this device are plotted in Fig. 2.15. For $R_{01} = R_{02} =$ 50 Ω, we have $f_c = 89.66$ GHz. For n = 5, we get the following values of a, b, K, and X from the design curves.

$$a = 0.87$$

$$b = 0.1125$$

$$K = 0.280$$

$$X = 0.47$$

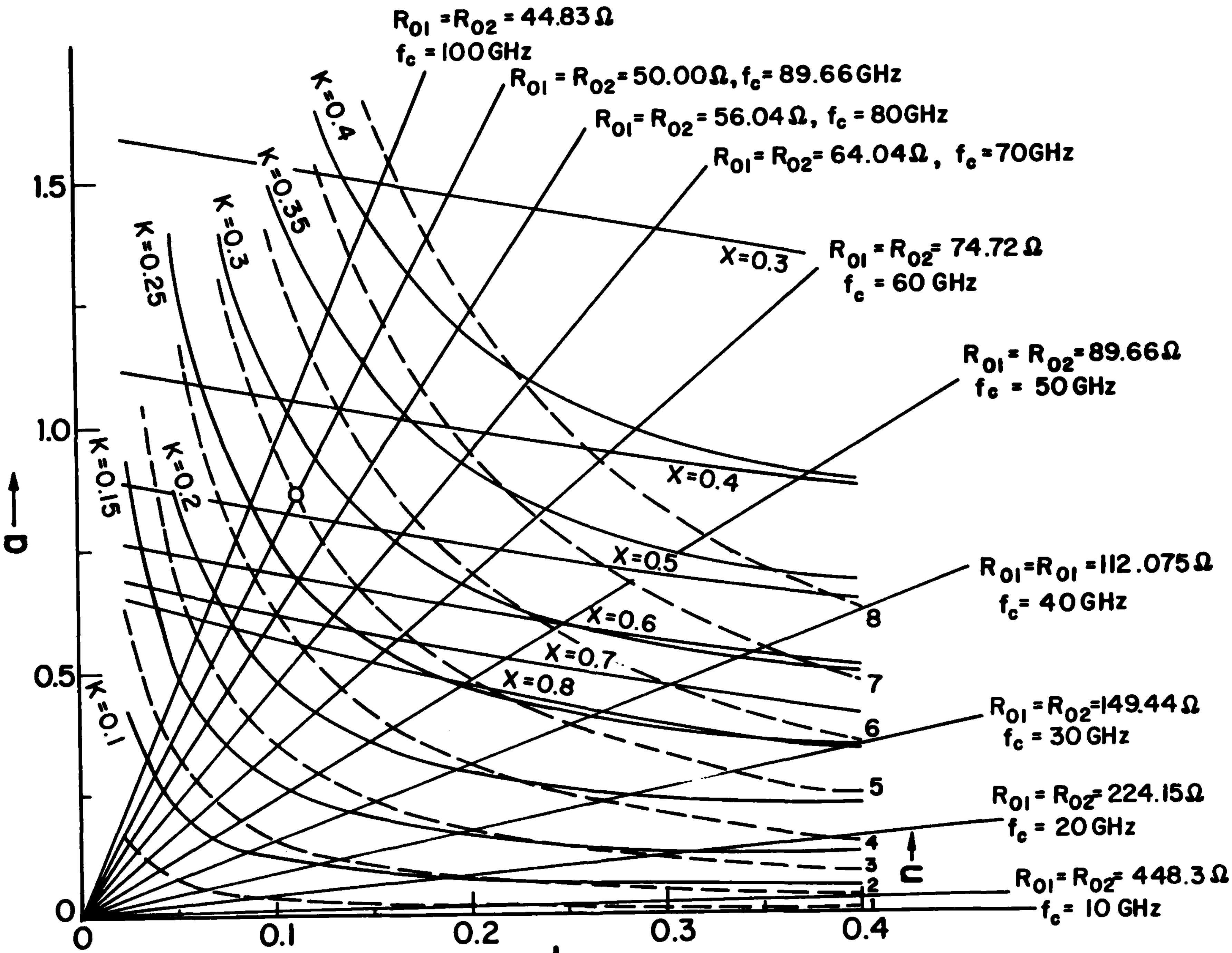

Figure 2.15. Design curves for Five-Section Distributed Amplifier using 60 μm MESFETs.

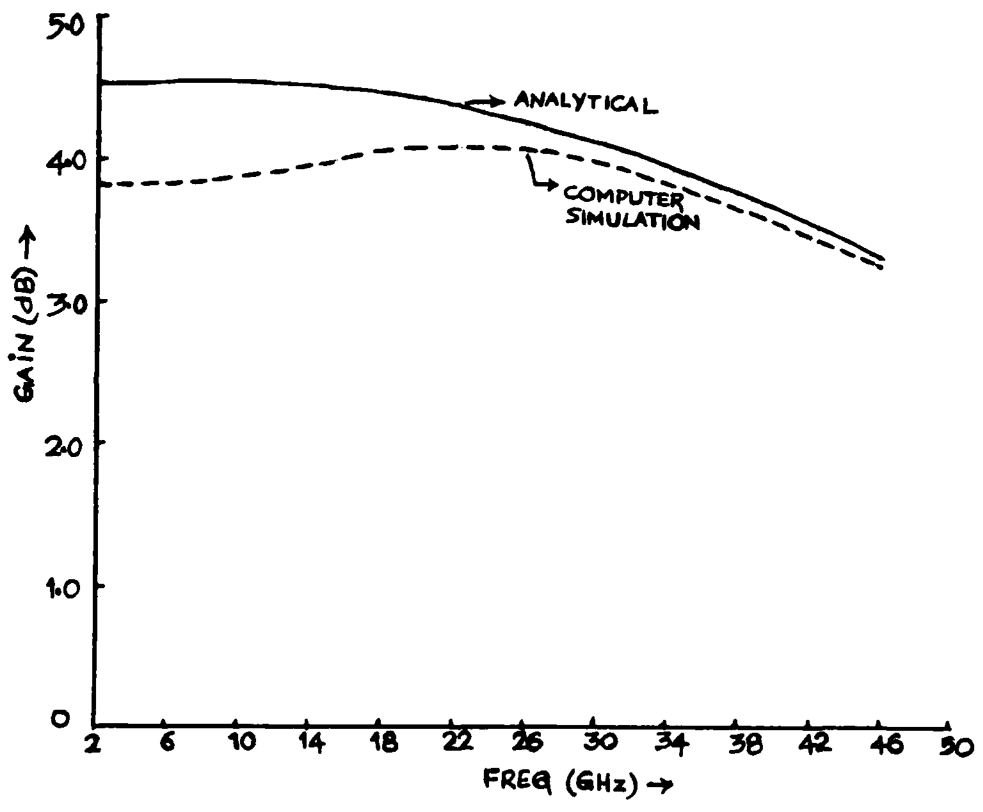

Figure 2.16. Frequency Response of the Five-Section Distributed Amplifier Using 60 μm MESFETs

Therefore, $f_{1dB} = Xf_c = 42.14$ GHz

$$A_0 = \frac{4\ KX\ f_{max}}{f_{1dB}}$$

$$= 1.7\ (4.61\ dB).$$

The frequency response of the amplifier obtained from equation (2.18b) is compared with the results of computer simulation in Fig. 2.16. The agreement between the two is good. The image terminations were realized by m-derived half-section filters as in the previous example.

2.6 Synthesis of Inductors using Microstrip Transmission Lines

Up to now, we have assumed the distributed amplifiers to be constructed from lumped inductors. In the case of MMIC's, lumped inductors are not generally possible, although amplifiers using printed inductors have been demonstrated.[1] Typically, a short piece of microstrip transmission line is used.

Figure 2.17 shows a typical layout for an MMIC distributed amplifier with short microstrip interconnections being employed as inductors. It is quite clear that geometric considerations place a lower limit on the length of inductors.

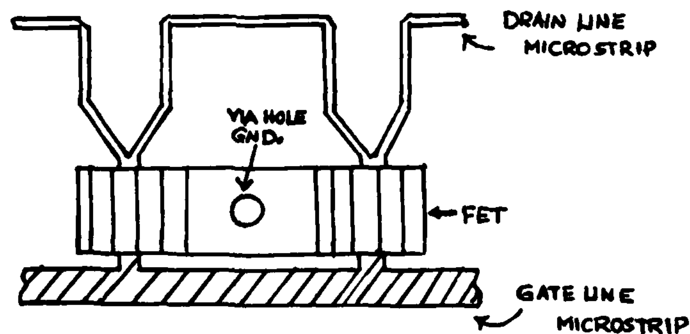

Figure 2.17. Typical Layout for an MMIC Distributed Amplifier

Ideally, this synthetic inductor should be frequency independent. If a microstrip transmission line of length, d, is modelled as a π-section, the Y-matrix is

$$[Y] = \begin{bmatrix} Y_0 \coth\gamma d & \frac{-Y_0}{\sinh\gamma d} \\ \frac{-Y_0}{\sinh\gamma d} & Y_0 \coth\gamma d \end{bmatrix} \quad (2.36)$$

where $Y_0 = Z_0^{-1}$, Z_0 being the characteristic impedance of the microstrip line, γ = the complex propagation function, and d = line length. In the lossless case, $\gamma = \beta$, and the circuit can be represented as in Fig. 2.18a.

The series element, $-j\, Y_0 \csc \beta d$, represents an inductive susceptance. If the transmission line is electrically short (i.e. $\beta d \ll 1$), then it can be easily shown that the equivalent inductance (see Fig. 2.18b) is

$$L_s = \frac{Z_0 d}{v_p} \quad (2.37)$$

where v_p is the phase velocity of the line. For $d < \lambda/7$, the error is less than 15%.

Next, the shunt element, $jY_0 \tan \frac{\beta d}{2}$ must be evaluated. This term is a capacitive susceptance when the line is electrically short. For the same restrictions as we employed previously, the equivalent capacitance (see Fig. 2.18b) is

$$C_s = \frac{d}{Z_0 v_p} \,. \quad (2.38)$$

It is important to note that this end capacity will not, in general, be negligible compared to C_{gs}. The new gate line circuit is shown in Fig. 2.19. The presence of the junction capacitance, C_{jg}, requires a new expression for A_g. Also, we will assume the microstrip has a finite resistance in the metal, and we will attribute R_{Lg}, to these metal losses.

The shunt, dielectric losses have been neglected as they tend to be ovnrshadowed by the other losses. Frequency dependence in R_{Lg} has also been neglected.

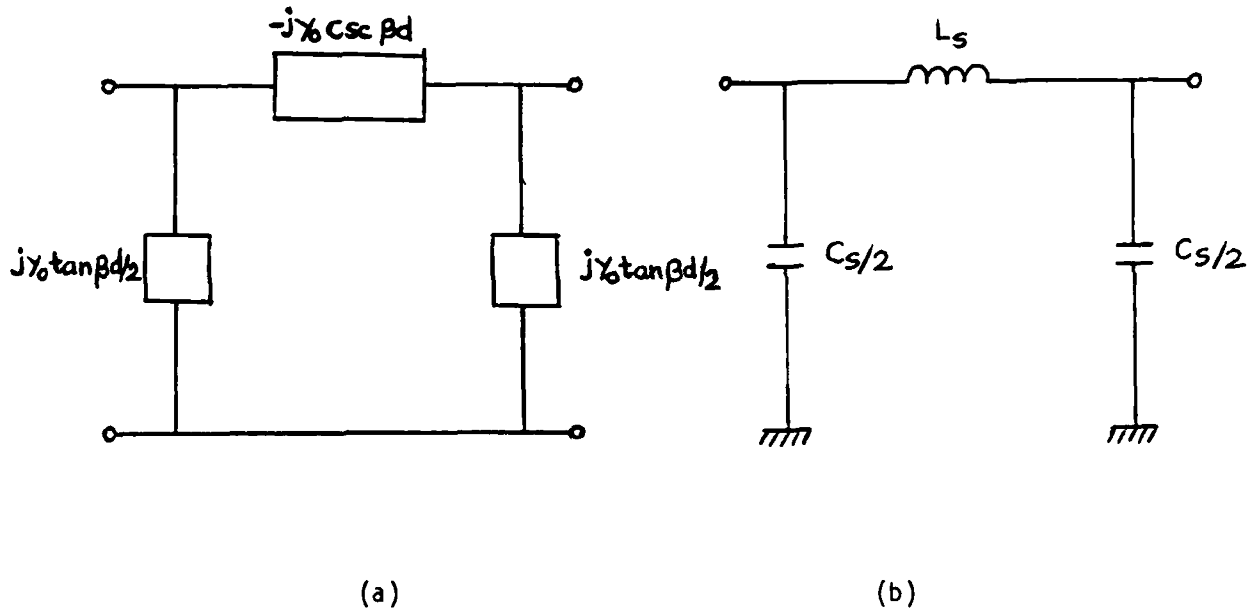

(a) (b)

Figure 2.18. Transmission lire model.

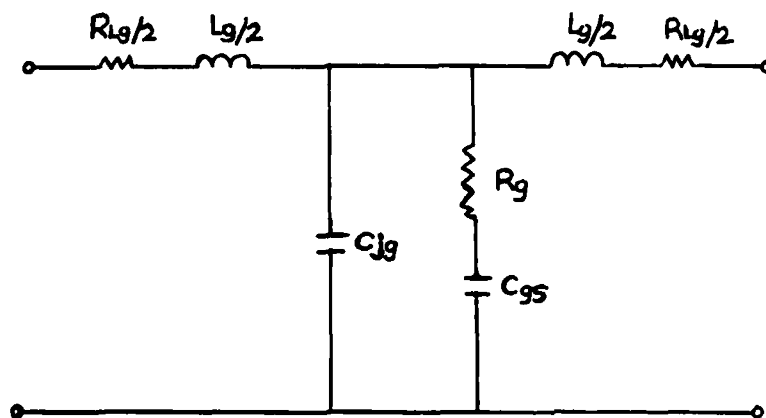

Figure 2.19. Constant-k T-section gate line model when microstrip inductors are used.

Equation 2.11 is our general form attenuation equation, and can be applied here. After some considerable algebraic manipulation,

$$A_g = [\omega R_{Lg}(C_{gs} + C_{jg}) + \omega^3 R_g C_{gs}^2 (R_{Lg} R_g C_{jg} + L_g)]$$

$$\times \{-\omega^4 L_g^2 (C_{gs} + C_{jg})^2 - \omega^4 R_g^2 C_{gs}^4 (R_{Lg} - \omega^2 L_g R_g C_{jg})^2$$

$$+ 2\omega^4 L_g R_g C_{gs}^2 (C_{gs} + C_{jg})(R_L - \omega^2 L_g R_g C_{jg})$$

$$+ 4\omega^2 L_g (C_{gs} + C_{jg}) - 4\omega^2 R_g C_{gs}^2 (R_{Lg} - \omega^2 L_g R_g C_{jg})$$

$$+ 4\omega^4 R_g^2 C_{gs}^2 L_g (C_{gs} + C_{jg}) - 4\omega^4 R_g^3 C_{gs}^4 (R_{Lg} - \omega^2 L_g R_g C_{jg})\}^{-1/2} \qquad (2.39)$$

We now define the following terms:

$$R_g = pR_0 \qquad (2.40a)$$

$$R_{Lg} = qR_g = pq\, R_0 \qquad (2.40b)$$

$$R_0 = \sqrt{\frac{L_g}{C_{gs} + C_{jg}}} \qquad (2.40c)$$

$$\omega_g = \frac{1}{R_g C_{gs}} \qquad (2.40d)$$

$$\omega_c = \frac{2}{\sqrt{L_g (C_{gs} + C_{jg})}} \qquad (2.40e)$$

$$\omega_{cg} = \frac{2}{\sqrt{L_g C_{gs}}} \qquad (2.40f)$$

$$\omega_{Lg} = \frac{2}{\sqrt{L_g C_{jg}}} \qquad (2.40g)$$

$$a = \frac{1}{1 - q \dfrac{\omega_c^2}{4\omega_g^2}} \qquad (2.40h)$$

$$G = 1 + \frac{q}{2} + \frac{\omega_c^2}{\omega_{Lg}^2} - \frac{q^2}{16}\frac{\omega_c^2}{\omega_g^2} - \frac{q}{16}\frac{\omega_c^2}{\omega_g^2} \tag{2.40i}$$

$$F = \frac{q}{2}\frac{\omega_c^2}{\omega_{Lg}^2} + \frac{\omega_c^2}{4\omega_{Lg}^2} - \frac{\omega_g^2}{2\omega_{Lg}^2} \tag{2.40j}$$

$$A_{1g} = \frac{pq}{2\sqrt{a}} \tag{2.40k}$$

$$A_{0g} = \frac{\omega_c^3}{\omega_g \omega_{cg}^2}\left(pq\frac{\omega_c^2}{\omega_{Lg}^2} + 1\right)\frac{1}{\sqrt{a}} \tag{2.40l}$$

Using these definitions it is possible to write Eq. 2.39 as

$$A_g = \frac{A_{1g} + A_{0g}X_k^2}{\sqrt{1 - X_k^2\left(\frac{1}{a} - \frac{G}{a}\frac{\omega_c^2}{\omega_g^2}\right) + X_k^4\frac{\omega_c^4}{\omega_g^4}\frac{F}{a} - X_k^6\frac{\omega_c^8}{a\,\omega_g^4\omega_{Lg}^4}}} \tag{2.41}$$

For typical designs, $\omega_c < \omega_g$ *and* $\omega_c < \omega_{Lg}$*. It is then quite reasonable to* neglect all terms of frequency dependence greater than X_k^2. Comparing Eq. 2.41 to Eqs. 2.14 and 2.15 it can be seen that, for

$$\frac{1}{a} - \frac{G}{a}\frac{\omega_c^2}{\omega_g^2} \approx 1 \tag{2.42}$$

the equation (2.41) is nearly identical to the sum of Eqs. 2.14 and 2.15. The term A_{1g} is "moved" to eq. 2.15, as this part of A_g acts in a manner identical to A_{0d} in Eq. 2.15, and has the same frequency dependence.

If we take a similar approach to the drain line, the new drain line attenuation expression is

$$A_d = \frac{A_{1d} + A_{0d}}{\sqrt{1-X_k^2}} \tag{2.43}$$

where $$A_{1d} = \frac{q\omega_c}{4\omega_d} \tag{2.43a}$$

$$A_{0d} = \frac{\omega_d}{\omega_c} \tag{2.43b}$$

$$X_k = \omega/\omega_c \tag{2.43c}$$

$$\omega_c = \frac{2}{\sqrt{L_c(C_{ds} + C_{jd})}} \tag{2.44a}$$

$$\omega_d = \frac{1}{R_{ds}C_{ds}} \tag{2.44b}$$

$$q = \frac{R_{Ld}}{R_{ds}} \tag{2.44c}$$

and the new schematic is shown in Fig. 2.20.

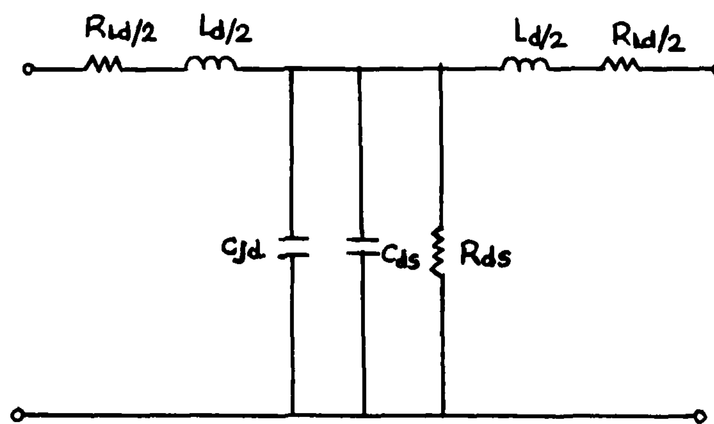

Figure 2.20. Constant-k T-Section Drain Line Model when Microstrip Inductors are Used.

Under these circumstances, the coefficients, a and b, defined in Eqs. 2.17a and 2.17b, must be redefined. Hence

$$a = A_{0g}/2 \tag{2.45a}$$

$$b = (A_{0d} + A_{1d} + A_{1g})/2 \tag{2.45b}$$

become the design coefficients when series inductor loss and end-capacitance of the inductor are non-negligible.

If one wishes to reduce the value of the junction capacitor, C_j, a higher impedance microstrip line is required. This means, for the same inductance, a narrower and slightly shorter physical line size. For drain inductors, this would also mean higher current densities. Typically, a current density of 10^5 A/cm^2 is used as the maximum current density which gold can carry before conductor degradation due to electromigration occurs. It may be necessary to increase conductor width (and, hence, junction capcity) to satisfy this constraint.

Effectively, the inductor design has been bound by three parameters: length, impedance, or width, and current density. If the length constraint is removed, Eqs. 2.37 and 2.38 are no longer valid and must be replaced by

$$L_s = \frac{Z_0}{\omega} \sin\left(\frac{\omega d}{v_p}\right) \qquad (d < \lambda/4) \tag{2.46}$$

$$C_s = \frac{2}{Z_0\omega} \tan\left(\frac{\omega d}{2v_p}\right) \qquad (d < \lambda/4) \tag{2.47}$$

which indicate that the series inductance decreases with increasing frequency, while the shunt capacity increases with increasing frequency. As C_s is shunted by some device capacity, the effect of a changing C_s is moderated and the LC product tends to decrease as frequency increases. Thus, the poles in

A_g and A_d tend to move upward with frequency. The result is a decrease in the attenuation when compared to a line constructed from a fixed inductor of the apparent value at low frequencies ($d < \lambda/7$).

Design using frequency dependent elements has the obvious disadvantage of not being easily accessible analytically. The ability to choose microstrip impedance and length independently of any constraint precludes the possibility of a general case analysis. Only specific case examples are possible. A computer searching numerically for an optimum response to specific cases is the best approach.

2.7 Image Parameter Terminations and Sources

In the course of developing the gain equations, the assumption of image matching at all ports and between all cells was implicit. But real sources and real loads are not image sources and image terminations. The importance of this point is not emphasized in the literature, and requires clarification.

For a lossless T-section constant-k filter, the input impedance is

$$Z_I = R_0\sqrt{1-(f/f_c)^2}. \tag{2.48}$$

Assuming R_0 is the impedance (real) of the system to which this line is connected, at 80% of f_c, $\Gamma = 0.25$; at 90% of f_c, $\Gamma = 0.39$. These represent modest mismatch errors, but transmission loss is not the only criteria to consider. The termination of the gate line can have a significant effect on the high frequency response of an amplifier.

Figure 2.21 shows an example of the significance of correctly terminating the gate line. The line has a 20 GHz cutoff frequency. At 18 GHz, the voltage available at the gate of the last transistor is nearly 2 dB less with a real load than with the correct image load. The significance of this is not

immediately obvious in light of the -3 dB drop already experienced by this, the last, transistor in the image terminated line. But the line terminated in a real load is down 3 dB at 15 GHz, not 18 GHz as is the image matched line. Thus, the bandwidth has been increased 20% by using the correct (image) termination.

Generation of image parameter loads and sources from real loads and sources is relatively simple. It is well known in image parameter filter theory that the m-derived half-section filter serves as a convenient matching circuit from real to image loads. In particular, as Fig. 2.22 shows, the match to a real load is very good up to 90% of f_c for m = 0.6. When compared to a current microwave cascade type of amplifier where bandwidths of 1.5 octaves are very good, this circuit offers a tremendously broadband match.

It should be noted that this matching circuit is necessary in the gate termiantion only when amplifier -3 dB bandwidth is 0.7 f_c or above. Below 0.6 f_c, the mismatch error is not sufficient to require any matching networks.

When one considers input/output matching, the rules change very little. For a typical line (gate or drain), the impedance is quite constant up to about 0.7 f_c. Return loss is often much better than 10 dB with no matching sections. Above 0.7 f_c, return losses decrease to < 10 dB, which suggest the use of matching networks. The improvement in match with an m-derived half-section in the gate line is not significant above 0.8 f_c due to the large inductive component of gate input impedance near f_c. The drain line has less inductive reactance near f_c, and the match provided by an m-derived 1/2-section is usually very good up to 0.9 f_c. Amplifiers which operate above 0.8 f_c may benefit from judicious use of computer optimization of the matching network.

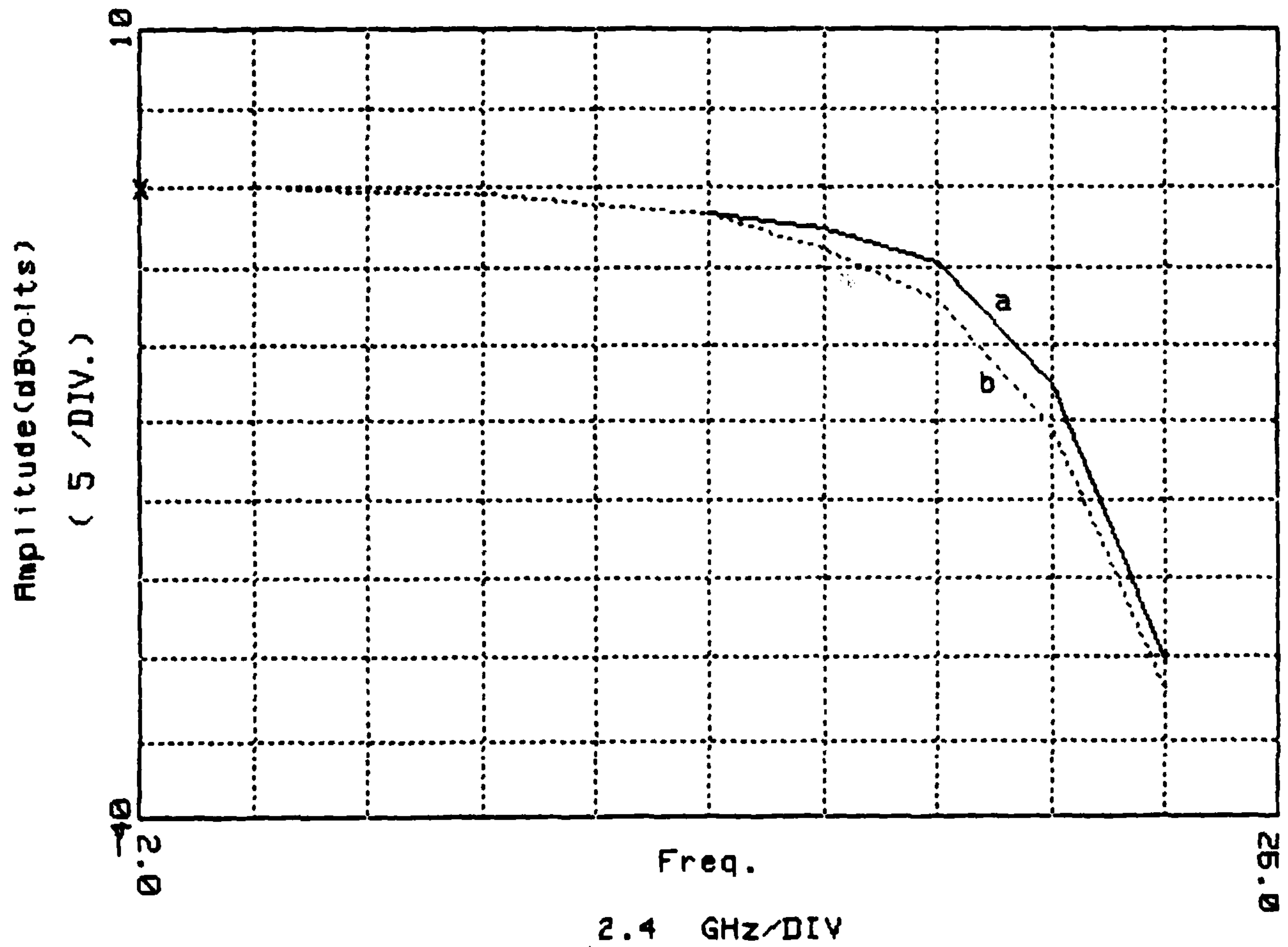

a) Matched Response b) Unmatched Response

Figure 2.21. Plot of gate voltage for last transistor in the line when image and real loads are used.

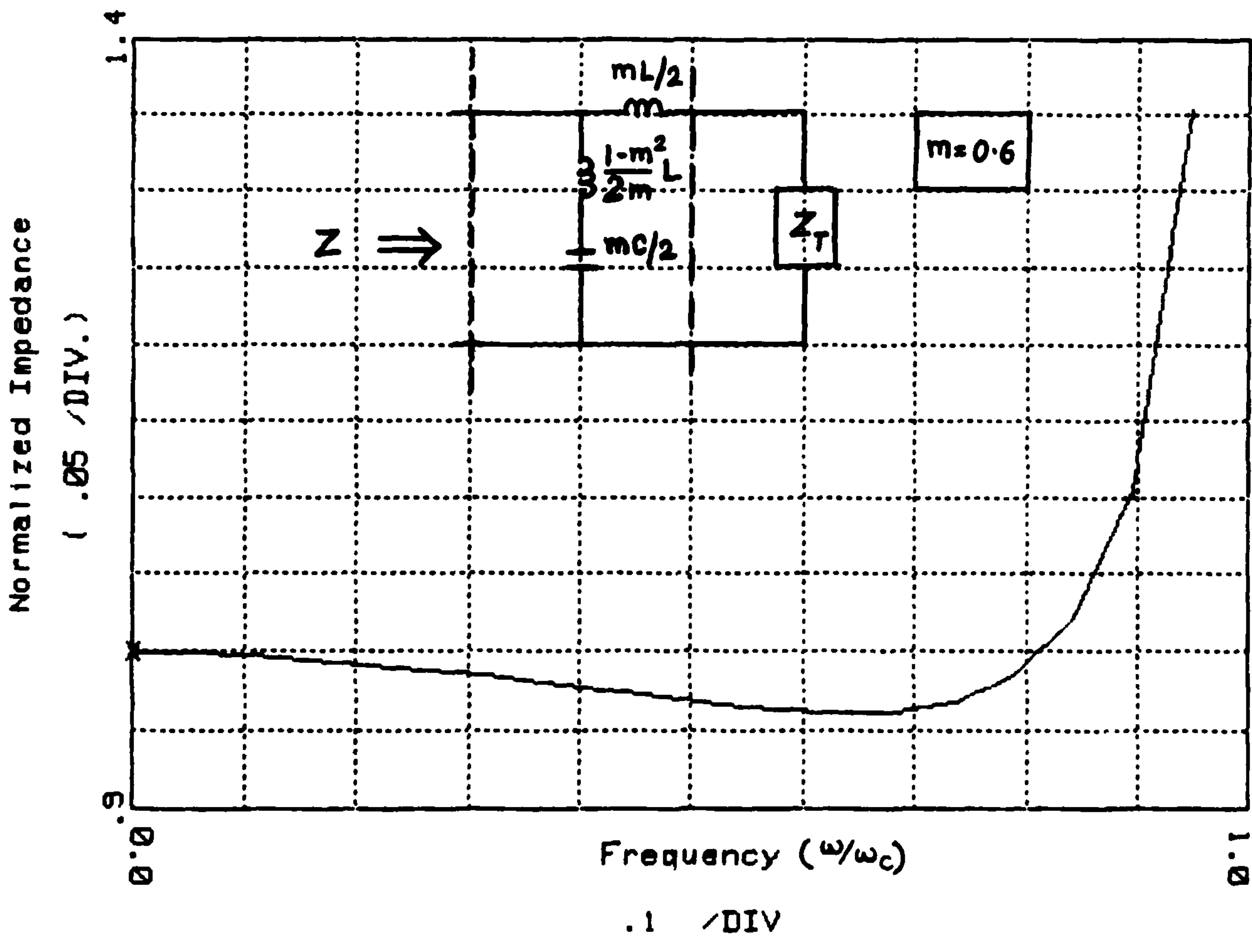

Figure 2.22. Half T-Section Impedance

Now we will illustrate by an example the effect of incorrectly terminating a distributed amplifier and the improvement in the performance with image terminations.

Consider the amplifier shown in Fig. 2.23.

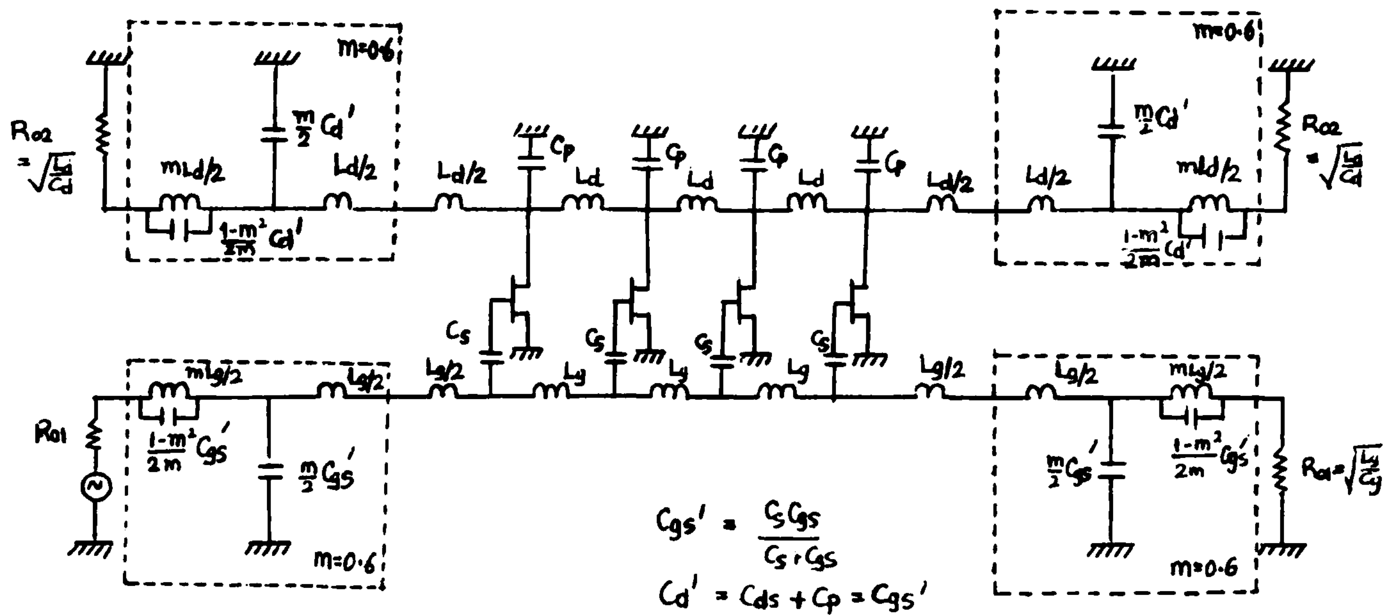

Figure 2.23. 4-section distributed amplifier.

The networks inside the dashed-line boxes convert the source and load resistances R_{01} and R_{02} into appropriate image impedances. In the example $R_{01} = R_{02} = 50\ \Omega$. Figure 2.24 shows the frequency response of the amplifier under the following terminal conditions.

1. Resistive termination
2. Image termination synthesized using Smith chart[5]
3. m-derived half-section termination designed according m-derived filter theory
4. Conjugate match at input and output ports obtained mathematically.

It is evident from Figure 2.24 that image terminations improve the frequency response of the amplifier particularly near the upper end of the band.

In Figure 2.25 the input and output reflection coefficients of the amplifier versus frequency are plotted. The improvement in match with image terminations is clearly seen.

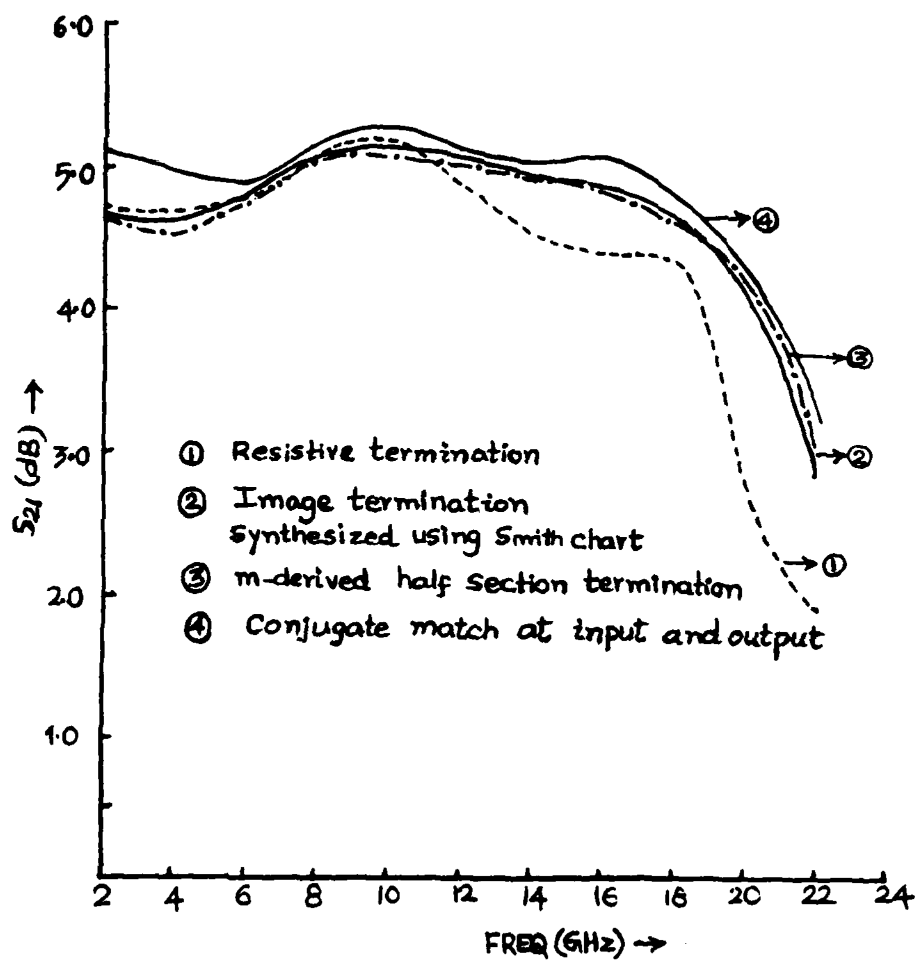

Figure 2.24. Frequency Response of 4-Section Distributed Amplifer

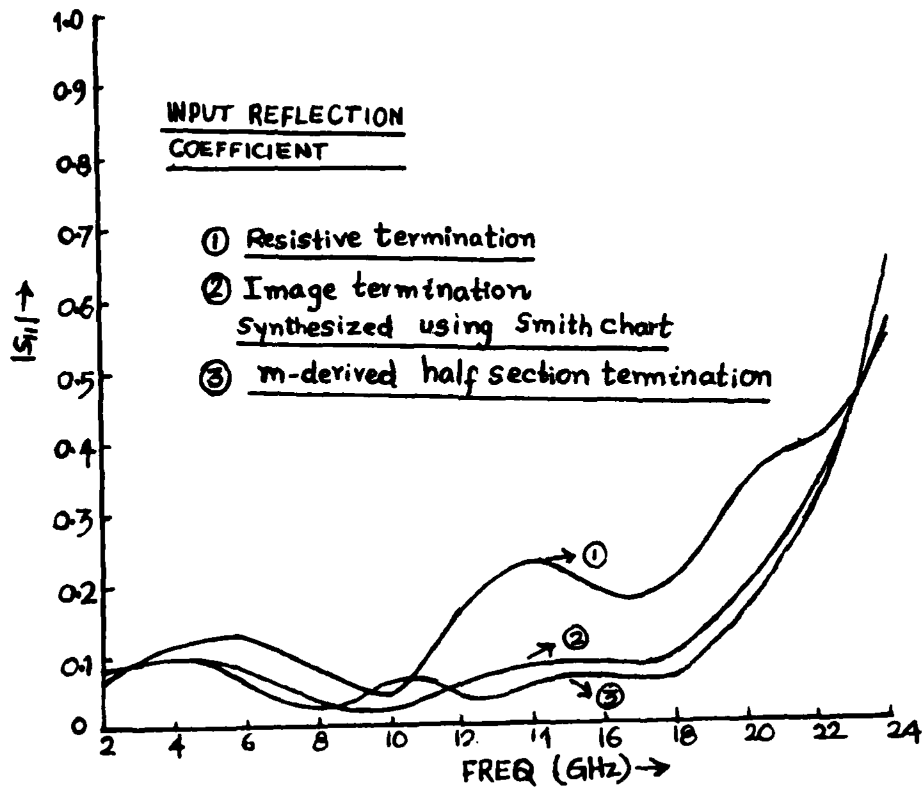

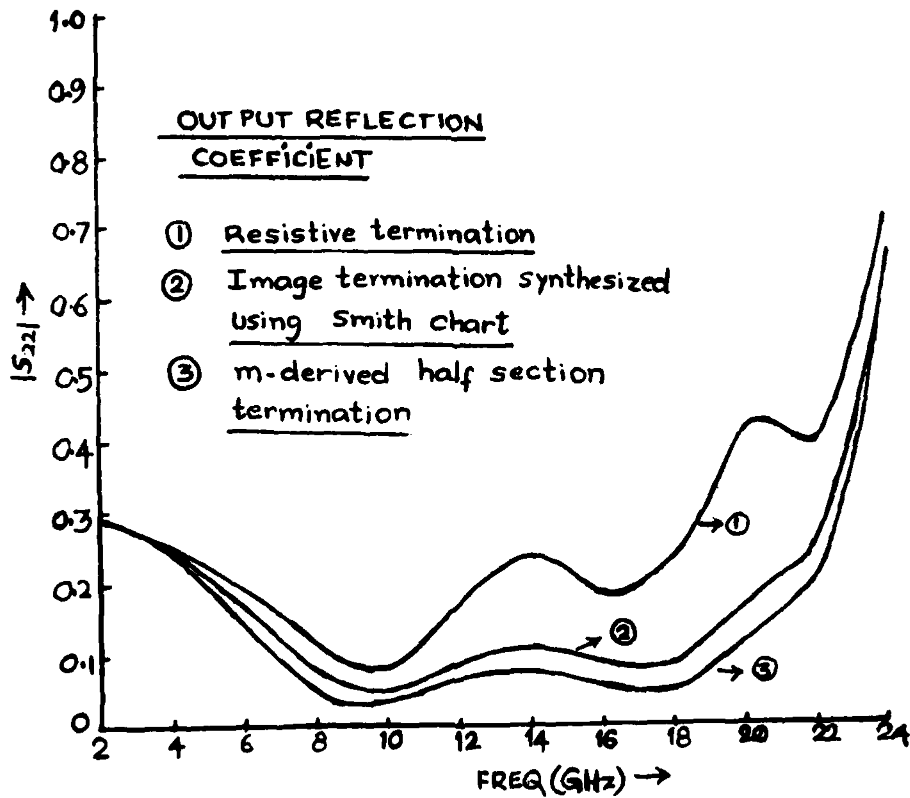

Figure 2.25. Input and Output Reflection Coefficients of 4-Section Distributed Amplifier

2.8 Conclusion

The analysis of MESFET distributed amplifier has been carried out. The gate and drain line attenuations caused by the device parasitic resistances have been found to be the critical factors controlling the frequency response of the amplifier.

The systematic design approach presented enables one to examine the trade-offs between the design variables such as the device, the number of devices and cutoff frequency and impedances of the lines and arrive at a design which gives the desired gain and bandwidth. In addition the constraints which yield maximum gain-bandwidth product have been identified. The analytically predicted frequency response is in good agreement with the response predicted by the standard microwave circuit analysis program.

The synthesis of microstrip-line inductors and image sources and terminations has also been presented.

III. Distributed Paraphase Amplifier

3.1 Introduction

During this report period we have begun work on wideband phase shifter design. The phase shifter concept as originally proposed (Sec. 3.2) requires a wideband paraphase amplifier. Our initial attempts at designing a paraphase distributed amplifier consisting of a distributed common gate amplifier and a distributed common source amplifier each fed from a common input line show some promise.

This report shows the results of a computer simulation as well as the equations of unbalance, phase deviation, and reflection coefficient. The results show a 1 dB bandwidth from 5 to 20 GHz with a gain unbalance of less than 1 dB and a phase deviation of less than 10° from the desired 180°. The reader is referred to Appendix D for algebraic details used in particular derivations.

3.2 Phase Shifter Principle

The concept on which the active phase-shifter using a gain-controlled paraphase amplifier works is presented schematically in Fig. 3.1.

The 360° phase shifter is achieved by summing 4 vectors $A\underline{/0}°$, $B\underline{/90}°$, $C\underline{/180}°$, $D\underline{/270}°$ with predetermined amplitude. These 4 quadrature vectors were realized by one 90° hybrid and two gain-controlled distributed paraphase amplifiers. Then by using an in-phase four-way power combiner (active or passive), the four controlled vectors are combined to yield 360° of continuous phase shift.

3.3 Distributed Paraphase Amplifier Design Consideration

The wideband distributed paraphase amplifier is based on the concept of

the distributed amplifier. It consists of two distributed FET amplifiers, one is a distributed common-source amplifier. The other is a distributed common-

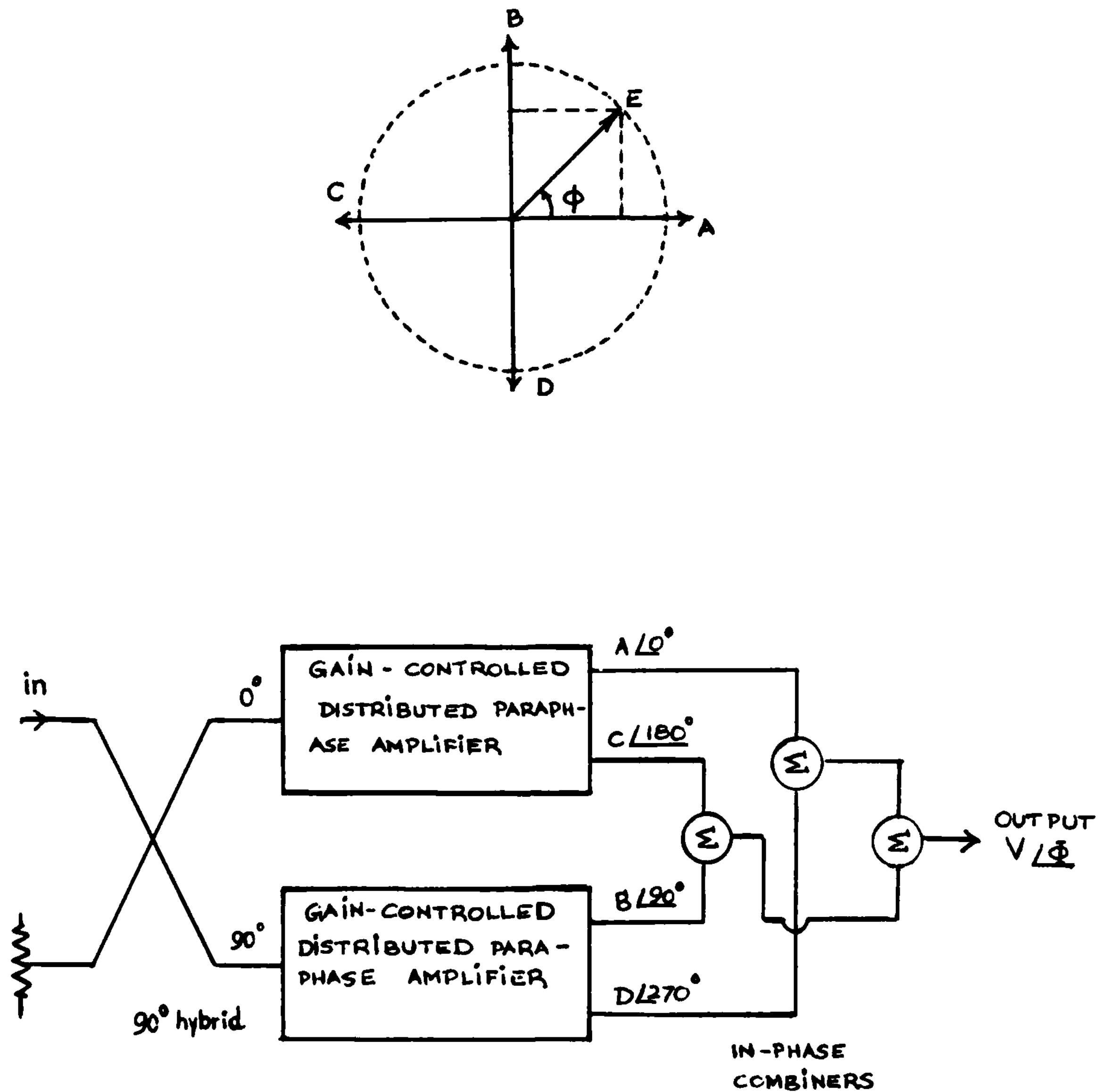

Figure 3.1. Schematic of a 360° FET phase shifter.

gate amplifier. These two amplifiers share a common input transmission line (shown in Fig. 3.2). If the phase velocities of the signals on the three transmission lines are identical the output signals on the two drain lines will add respectively and will have 180° of phase shift resulting from the two different amplifier configurations.

The first step in designing a paraphase amplifier is to determine the parameters of the transmission lines, that is L's, which are section of microstrip line short with respect to the wavelength, and C's, which include the parasitic capacitances of the transistors. In addition, the main design goal is to get good balance and accurate 180° difference for the two output signals.

According to the fundamentals of circuit theory the following equations of input and output admittance of an FET are derived.

(a) Input admmittance

for common-gate amplifier

$$Y_{ig} = R_g \omega^2 C_g^2 + g_m + \frac{1}{R_d}(1 - A_V) + j\omega[C_g + C_d(1 - A_V)] \quad (3.1)$$

$$g_{ig} = R_g \omega^2 C_g^2 + g_m + \frac{1}{R_d}(1 - A_V) \quad (3.2)$$

$$C_{ig} = C_g + C_d(1 - A_V) \quad (3.3)$$

where R_g - Gate-to-source resistance

C_g - Gate-to-source capacitance

R_d - Drain-to-source resistance

C_d - Drain-to-source capacitance

g_m - Device transconductance

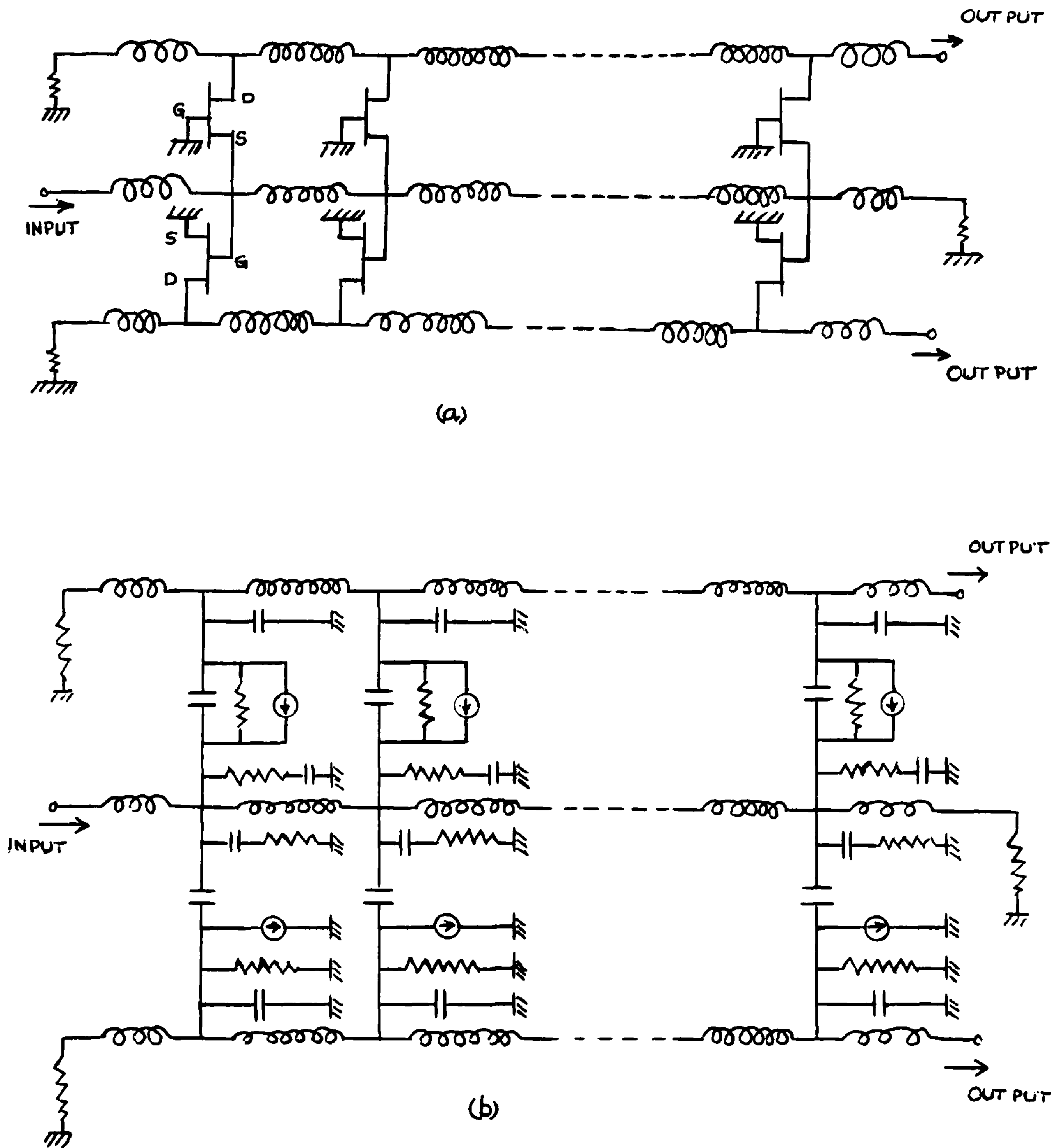

Fig. 3.2. (a) Schematic of a distributed paraphase amplifier.
(b) Equivalent circuit of a distributed paraphase amplifier.

$\omega = 2\pi f$ f - Operating frequency

A_v - Amplifier D.C. voltage gain

$$A_v \approx \frac{g_m}{Y_D + Y_L} \tag{3.4}$$

where Y_L - terminal admittance of drain line

$Y_D = 1/R_d$

For common-source amplifier

$$Y_{is} = R_g \omega^2 C_g^2 + j\omega[C_g + C_{dg}(1 + A_V)] \tag{3.5}$$

$$g_{is} = R_g \omega^2 C_g^2 \tag{3.6}$$

$$C_{is} = C_g + C_{dg}(1 + A_V) \tag{3.7}$$

(b) Output admittance

For common-gate amplifier

$$Y_{0g} = \frac{1}{R_d}\left(1 - \frac{1}{A_V}\right) + j\omega\left[C_{dg} + C_d\left(1 - \frac{1}{A_V}\right)\right] \tag{3.8}$$

$$g_{0g} = \frac{1}{R_d}\left(1 - \frac{1}{A_V}\right) \tag{3.9}$$

$$C_{0g} = C_{dg} + C_d\left(1 - \frac{1}{A_V}\right) \tag{3.10}$$

For common-source amplifier

$$Y_{0s} = \frac{1}{R_d} + j\omega[C_d + C_{dg}(1 + \frac{1}{A_V})] \qquad (3.11)$$

$$g_{0s} = \frac{1}{R_d} \qquad (3.12)$$

$$C_{0s} = C_d + C_{dg}(1 + \frac{1}{A_V}) \qquad (3.13)$$

(c) Transmission Line Characteristic Impedance

We initially determine the characteristic impedance of the input line from $R_0 = \sqrt{L/C}$ but since C is now larger than it is in a single common source amplifier and the practical values of L are restricted, we choose the value of R_0 to be 20 Ω for the input line of the paraphase amplifier.

For the drain line we may use a higher impedance in order not to sacrifice gain. We also use an in-phase combiner whose load and generator resistances are not equal.[1] This combiner performs impedance matching as well as combining.

3.4 Computer simulation of distributed paraphase amplifier

Figure 3.3, 3.4 are the voltage gain (S_{21}), output unbalance and phase difference of the distributed paraphase amplifier by computer simulation using the HP OPNODE circuit design program. Fig. 3.3 is obtained using typical 150 μm FETs. In this case the 20 Ω characteristic impedance

1. J. J. Taub and G. P. Kurpis, "A more general N-way hybrid power divider," IEEE Trans. on MTT, MTT-17, No. 7, July 1969, pp. 406-408.

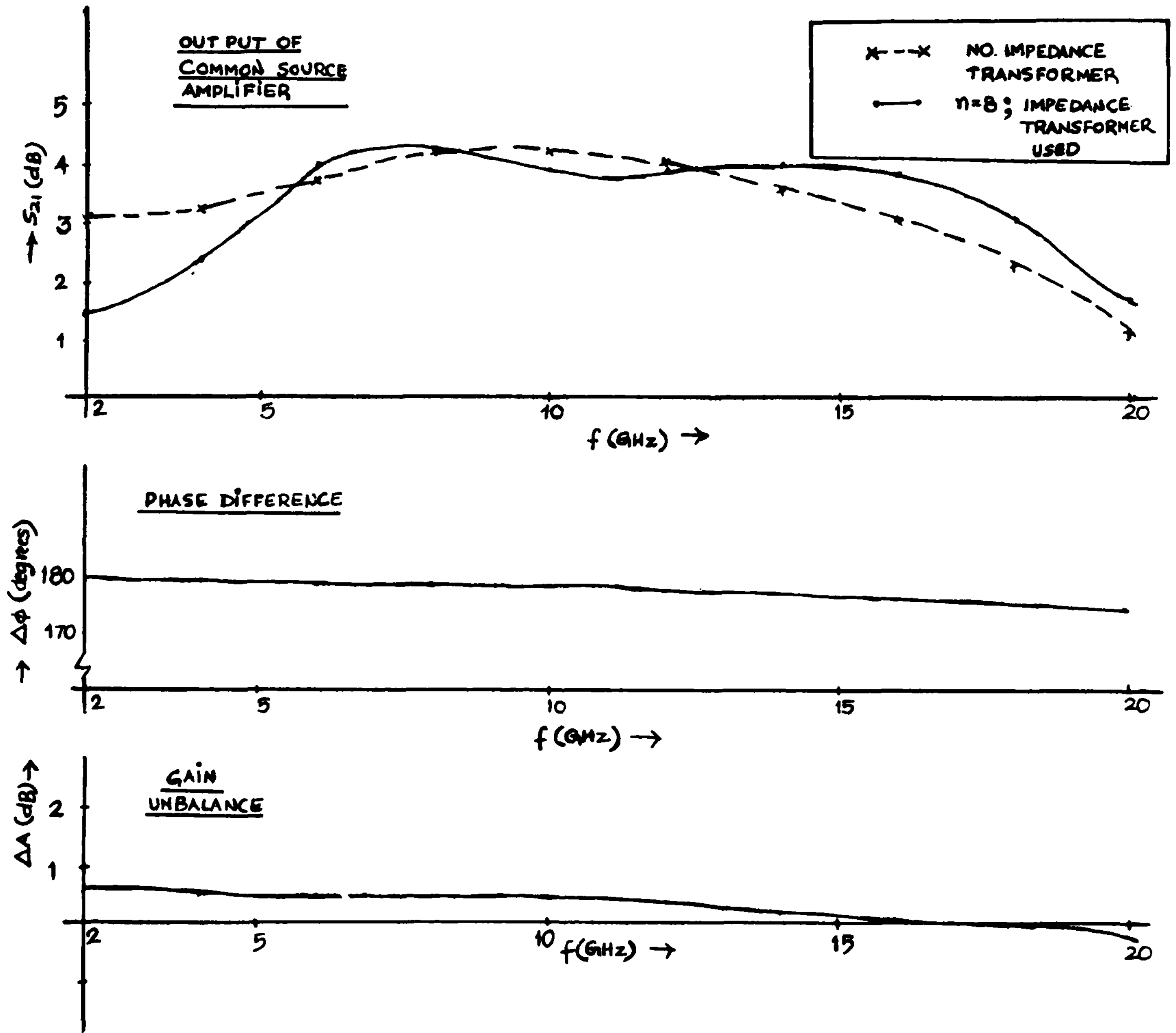

Figure 3.3. Voltage gain, output unbalance and phase difference of the distributed paraphase amplifier using 150 μm FETs.

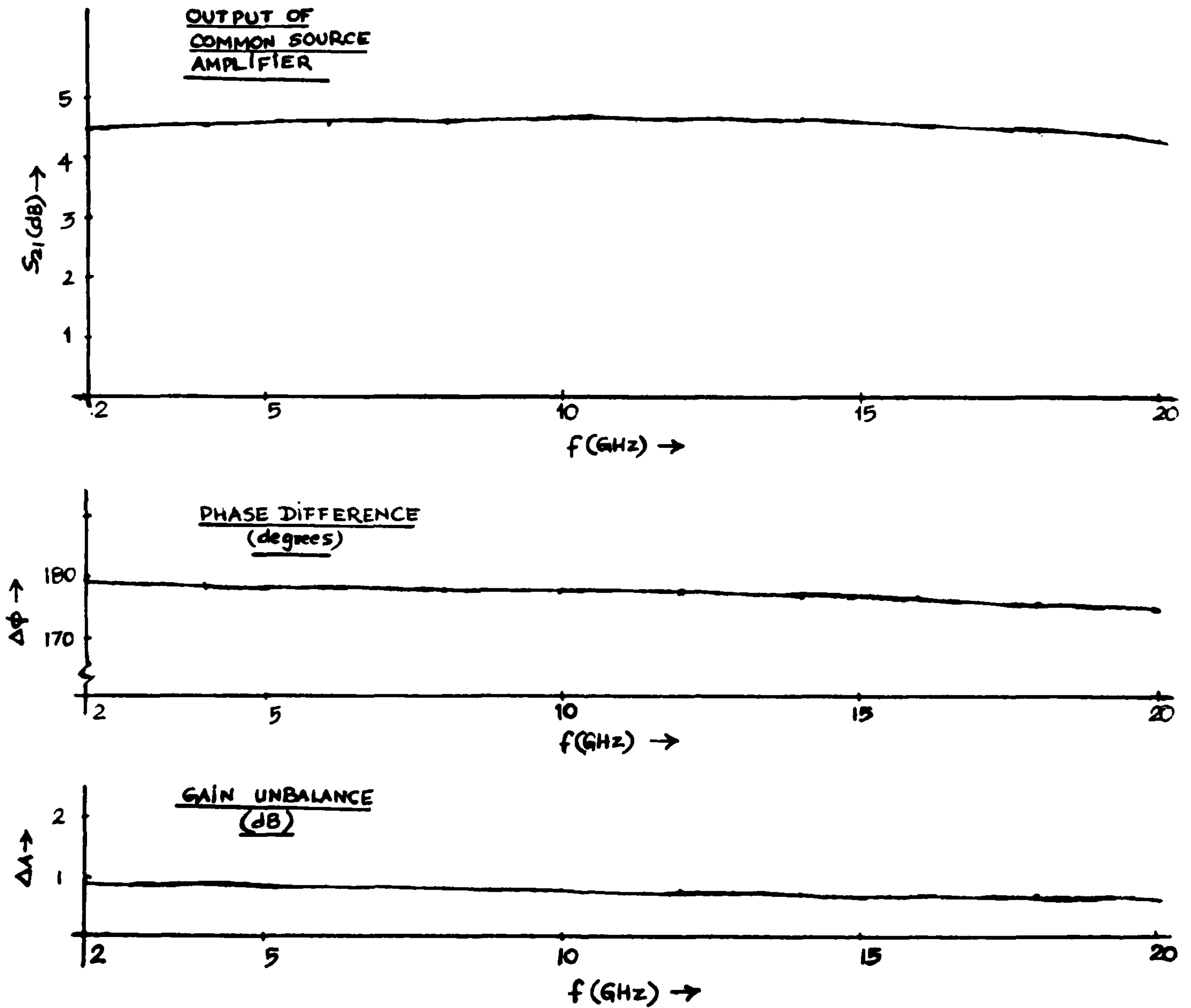

Fig. 3.4. Voltage gain, output unbalance and phase difference of the distributed paraphase amplifier using 60 μm FETs.

input line is used, and hence an impedance transformer[2] is inserted between preamplifier and paraphase amplifier. Fig. 3.3 also shows that a preamplifier with a 20 Ω drain line is used to eliminate the transformer and obtain wide bandwith.

Fig. 3.4 is for a 60 μm FET. It has low input capacitance and no impedance transformer is needed.

3.5 Analysis

The unbalance, ΔA, and phase deviation, δφ, of the paraphase amplifier are expressed as follows (Appendix D)

$$\Delta A\ (\text{db}) \approx 20\log\frac{1 + 1/g_m R_d}{1 + Z_{D\pi}/2R_d} + 20\log\frac{\cosh\left(\frac{n}{2}\frac{A_d}{A_v}\right)}{\cosh\left(\frac{A_d}{2A_v}\right)} + 10\log\left(e^{n\frac{A_d}{A_v}}\right) \qquad (3.14)$$

$$\delta_\phi = \arctan\frac{\omega C_d}{\frac{1}{R_d} + g_m} - \arctan\frac{\omega C_d}{\frac{1}{R_d} + \frac{2}{Z_{D\pi}}} \qquad (3.15)$$

Figure 3.5 shows the comparison between results from eqs. (3.14), (3.15) and results from computer simulation for a 60 μm FET.

2. G. L. Matthaei, "Tables of Chebyshev impedance transforming networks of low-pass filter form," Proc. of the IEEE, Aug. 1964, pp. 939-963.

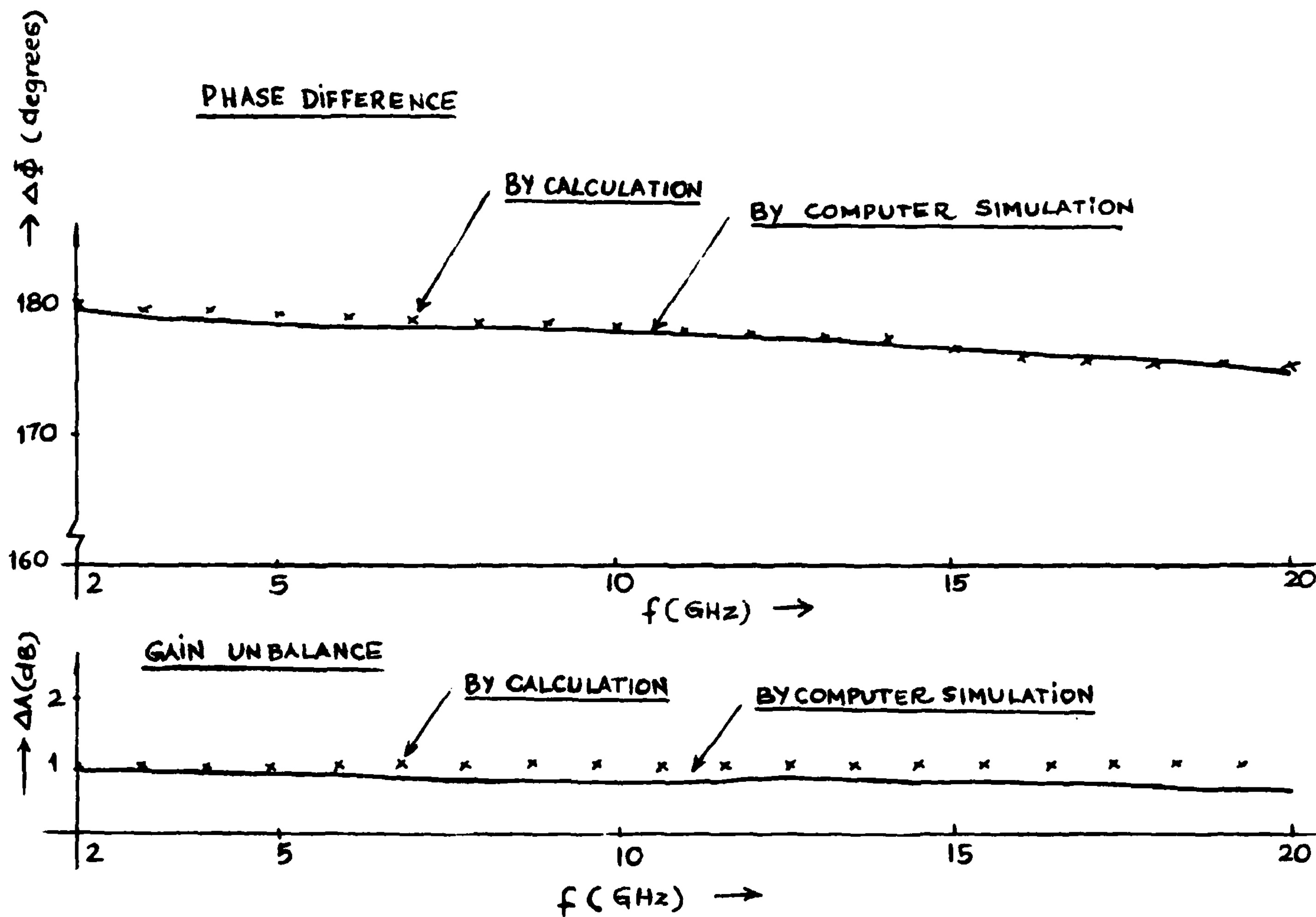

Figure 3.5. The unbalance and phase difference from both calculation and computer simulation.

The reflection coefficient of distributed paraphase amplifier is obtained as follows

$$\Gamma = \frac{(R_1 - R_2)\coth(nA) + Z_0 - R_1R_2/Z_0}{(R_1 + R_2)\coth(nA) + Z_0 + R_1R_2/Z_0} \qquad (3.16)$$

where R_1 - the terminal resistance of input line

R_2 - the equivalent generator resistance

$$Z_0 = \sqrt{\frac{L}{C}} \sqrt{1 - (\frac{\omega}{\omega_c})^2 - \frac{1 - j\frac{\omega}{\omega_g}}{1 + (\frac{\omega}{\omega_g})^2}} \qquad (3.17)$$

$$A = 1 - 2\,(\frac{\omega}{\omega_c})^2 + j2\omega\omega_g/\omega_c^2 \qquad (3.18)$$

$$\omega_g = g_i/C_g$$

$$g_i = g_{is} + g_{ig}$$

Figure 3.6 shows the reflection coefficients from both the calculation using eq. (3.16) and computer simulation.

Because the common gate amplifier heavily loads the input transmission line its characteristic impedance deviates considerably from $\sqrt{L/C}$, especially at low frequencies. As a result we have also considered use of a distortionless line for the input line. For such a case we add resistance in series with L such that R/L = G/C. (See Fig. 3.7).

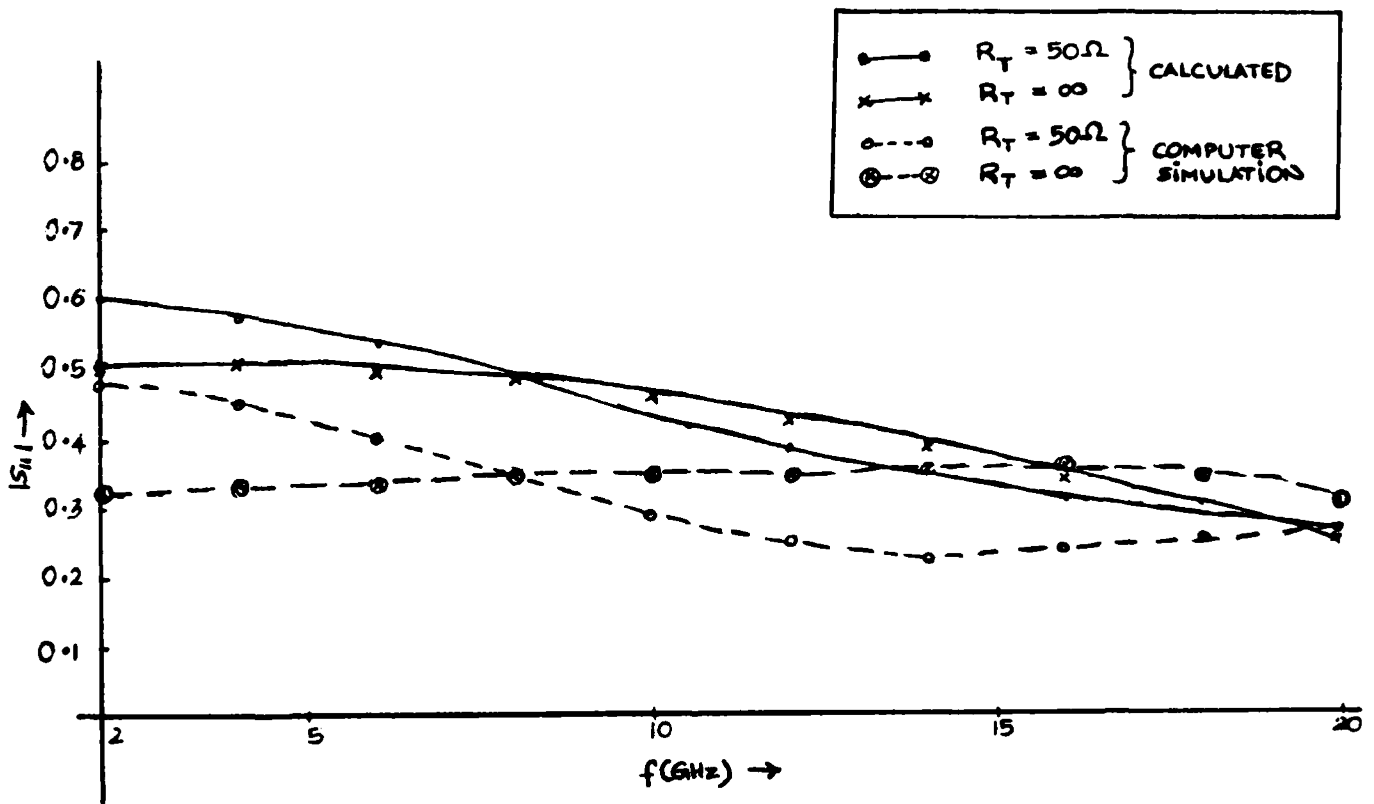

Figure 3.6. The effects of the terminal resistance on the reflection coefficient of paraphase amplifier.

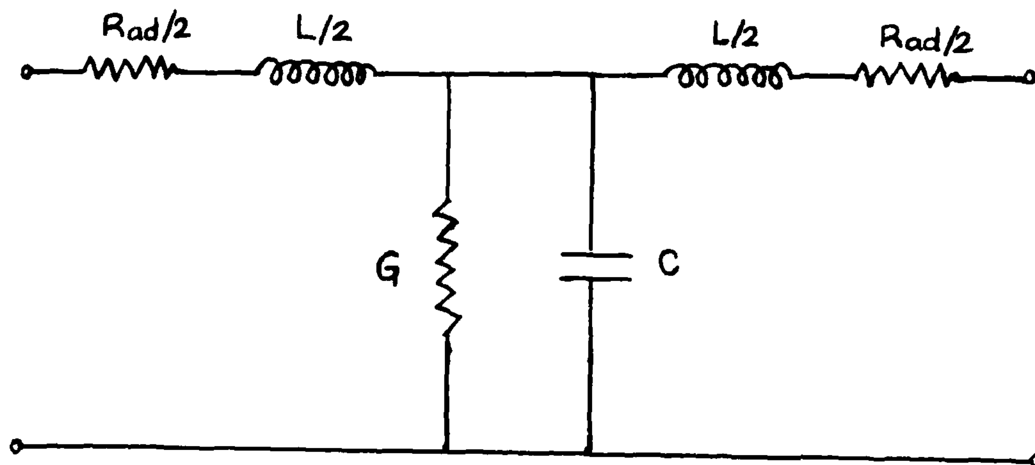

Figure 3.7. A section of distortionless input line.

The characteristic impedance of input line will now be

$$Z_0 = \sqrt{\frac{L}{C}} \sqrt{1 + \frac{(\omega_g + j\omega_c)^2}{\omega_c^2}} \tag{3.21}$$

If the terminal resistance of input line is equal to $\sqrt{L/C}$ the reflection coefficient of input line will be less than .1 (see Figure 3.8). Good matching is obtained, and the gain response is flattened whereas the output unbalance and phase deviation are the same as that without R_{ad}. However, the gain of paraphase amplifier is about 2 dB less than that without R_{ad}.

If we still use the LC transmission line and increase the terminal resistance of the input line (let it be larger than $\sqrt{L/C}$, for example, two or three times), the flattened reflection coefficient response and flattened gain response will be obtained. In addition the gain of the paraphase amplifier is higher than that when the terminal resistance is equal to $\sqrt{L/C}$ (see Figure 3.9), whereas the output unbalance and phase deviation are the same as that with a terminal resistance equal to $\sqrt{L/C}$.

3.6. Design curves for the distributed paraphase amplifier

The design procedure given in section 2.5 can be extended for the distributed paraphase amplifier as follows.

The voltage gain of the common-source amplifier in the distributed paraphase amplifier is given by (Eq. 2.5)

$$A_S = \frac{g_m (R_{01}R_{02})^{1/2} \sinh[\frac{n}{2}(A_g - A_d)]\, e^{-\frac{n}{2}(A_d + A_g)}}{2[1 + (\frac{\omega}{\omega_g})^2]^{1/2}[1 - (\frac{\omega}{\omega_c})^2]^{1/2} \sinh[\frac{1}{2}(A_g - A_d)]} \tag{3.22}$$

However, for this case

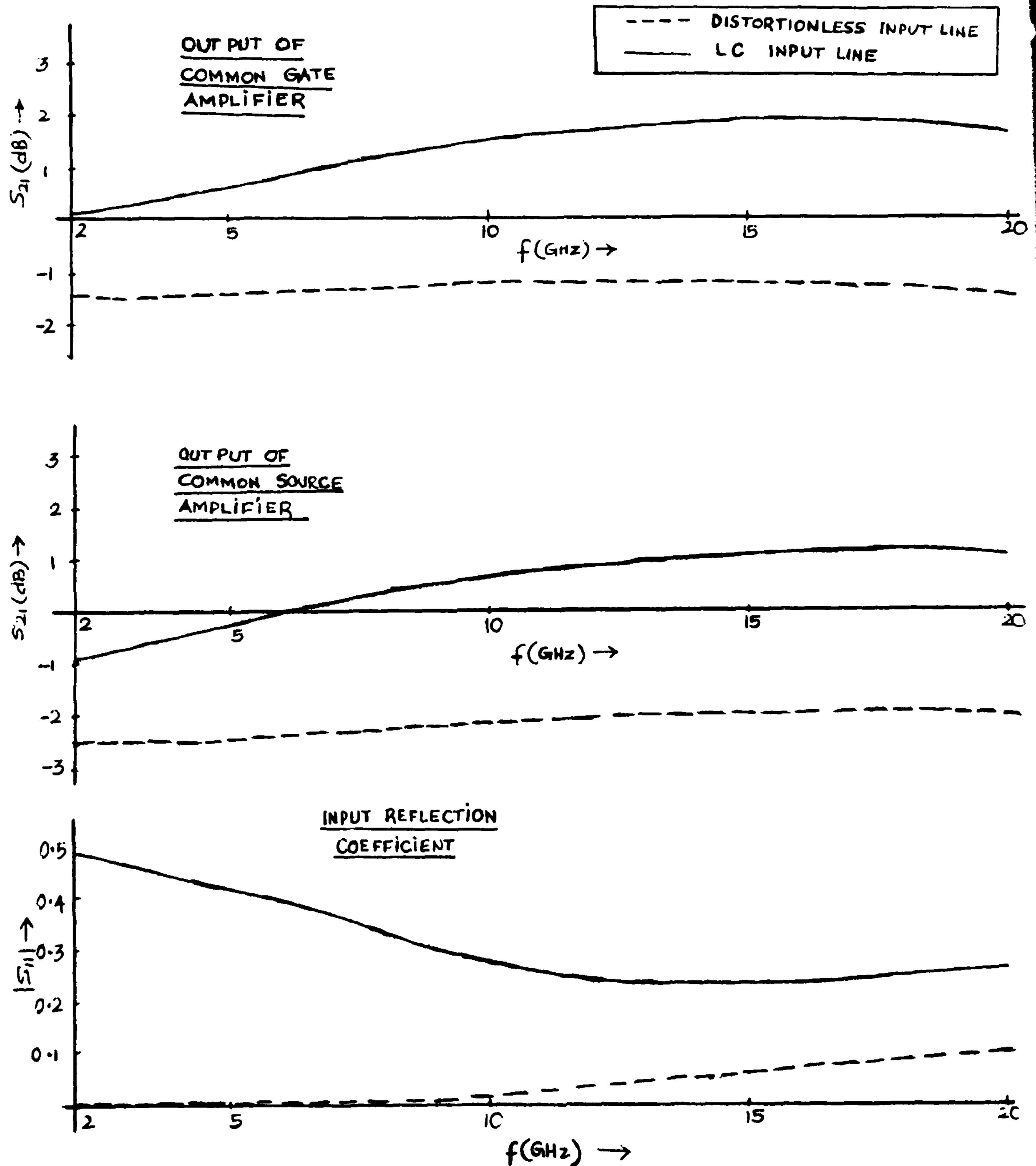

Figure 3.8. Voltage gain, output unbalance and phase difference of the distributed paraphase amplifier using the distortionless input line.

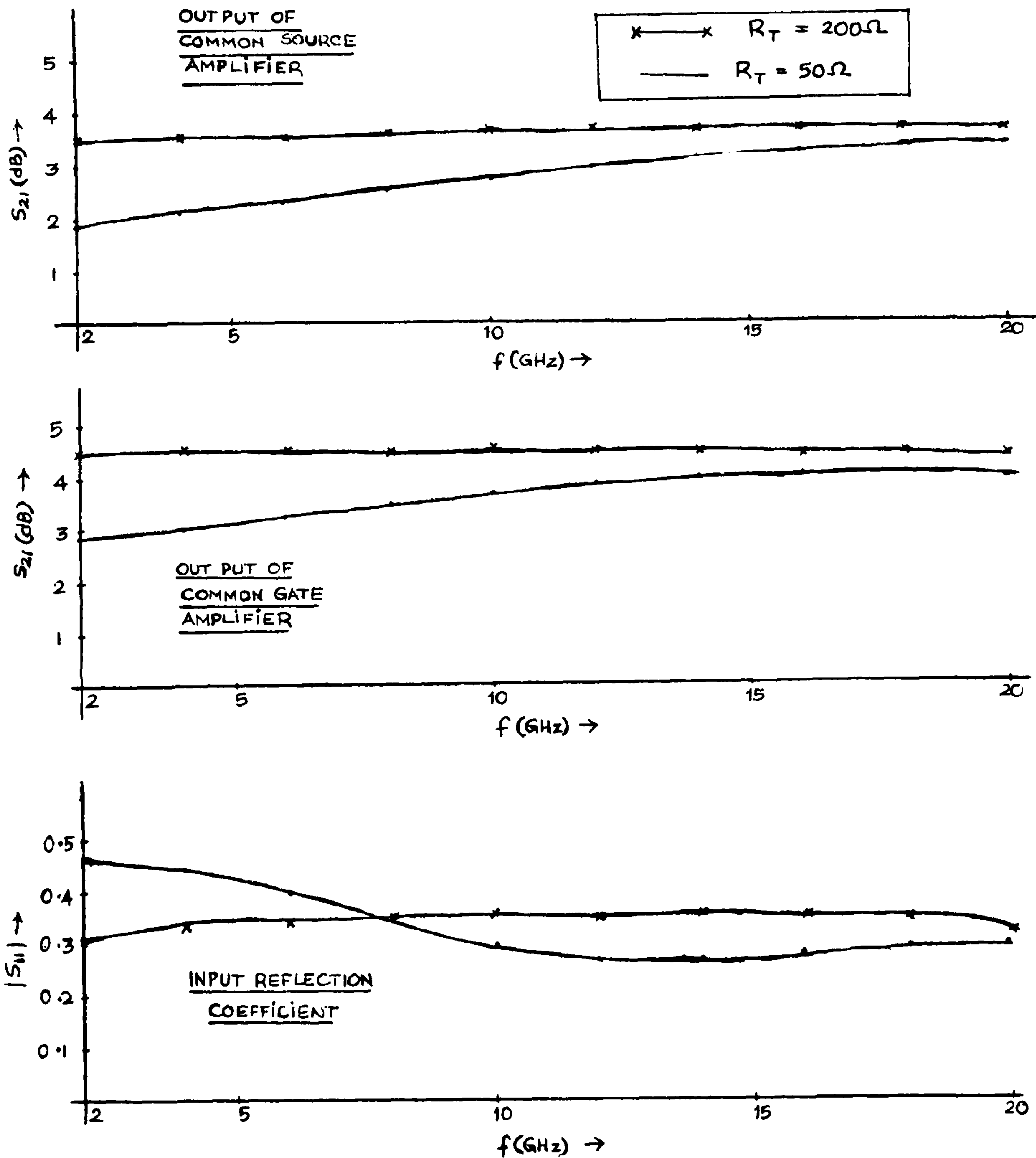

Figure 3.9. The effects of the terminal resistance.

$$A_g = \frac{\frac{\omega_c}{\omega_g}\left(\frac{\omega}{\omega_c}\right)^2}{\sqrt{1-\left(\frac{\omega}{\omega_g}\right)^2}} \qquad (3.23a)$$

and

$$A_d = \frac{\frac{\omega_d}{\omega_c}}{\sqrt{1-\left(\frac{\omega}{\omega_c}\right)^2}} \qquad (3.23b)$$

From Eqs. 2.13 and 2.17a,b respectively

$$X_k = \omega/\omega_c \qquad (3.24a)$$

$$a = \frac{n}{2}\ \frac{\omega_c}{\omega_g} \qquad (3.24b)$$

$$b = \frac{n}{2}\ \frac{\omega_d}{\omega_c} \qquad (3.24c)$$

Using the above, the D.C. gain of the common-source amplifier in the distributed paraphase amplifier can be shown to be

$$A_{s0} \approx \frac{n}{2}\, g_m (R_{01}R_{02})^{1/2} e^{-b} \qquad (3.25)$$

Then the normalized gain equation for the amplifier is obtained as follows

$$A_N = \frac{A_s}{A_{s0}} = \frac{1}{(1-X_k^2)^{1/2}\left[1+\left(\frac{2a}{n}X_k\right)^2\right]^{1/2}} \times \frac{e^b}{n} \times \frac{\sinh\left(\frac{b-aX_k^2}{\sqrt{1-X_k^2}}\right)}{\sinh\left(\frac{b-aX_k^2}{n\sqrt{1-X_k^2}}\right)}\, e^{-\frac{b+aX_k^2}{\sqrt{1-X_k^2}}} \qquad (3.26)$$

The fractional bandwidth, $X = f_{1db}/f_c$, can be determined as a function of a and b and plotted on the a-b plane as shown in Fig. 3.10.

In addition, the following relations can be derived from equations (3.24b and 3.24c).

$$ab = \frac{n^2 \omega_d}{4\omega_g}$$

and (3.27)

$$a/b = \frac{\omega_c^2}{\omega_d \omega_g}$$

If we define

$$P = \frac{\omega_d}{\omega_g} \qquad (3.28)$$

and

$$M = \frac{\omega_c}{\omega_g} \qquad (3.29)$$

then

$$ab = \frac{n^2}{4} P \qquad (3.30)$$

$$a/b = \frac{M^2}{P} \qquad (3.31)$$

Equations (3.30) and (3.31) can be plotted on the a-b plane for a specified P as shown in Fig. 3.11. The family of curves shown consititute the design curves for the distributed paraphase amplifier.

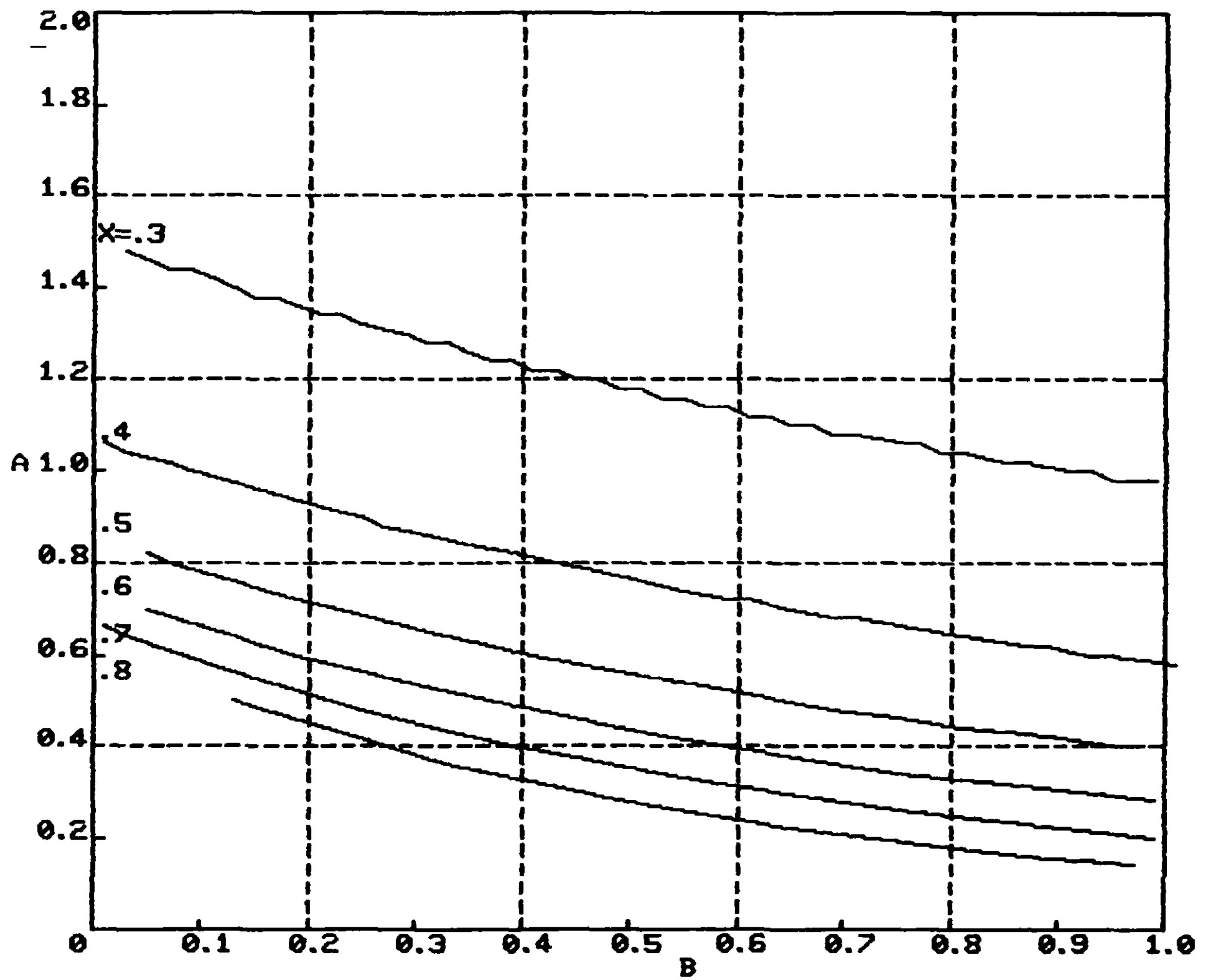

Fig. 3.10. Constant-fractional bandwidth curves of the distributed paraphase amplifier.

Further, the parameters P and M can be written as

$$P = \frac{\omega_d}{\omega_g} = \frac{\frac{1}{R_{ds}C_{ds}}}{\frac{1}{R_iC_{gs}}}$$

$$= \frac{\frac{1}{R_{ds}C_{ds}} \sqrt{L_dC_{ds}}}{\frac{1}{R_iC_{gs}} \sqrt{2L_gC_{gs}}}^{*}$$

$$= \frac{1}{2} \frac{R_{02}R_i}{R_{01}R_{ds}} \tag{3.32}$$

$$M = \frac{\omega_c}{\omega_g} = \frac{\frac{2}{\sqrt{2L_gC_{gs}}}}{\frac{1}{R_iC_{gs}}}$$

$$= \frac{R_i}{R_{01}} \tag{3.33}$$

Equations (3.32) and (3.33) reveal that P is the product of the ratio R_{02}/R_{01} and R_i/R_{ds}. When $R_{01} = R_{02}$, we have

$$P = \frac{1}{2} \frac{R_i}{R_{ds}} \tag{3.34}$$

---

*For a paraphase amplifier we have $\omega_c = \frac{2}{\sqrt{2L_gC_{gs}}}$ since the two transistors are connected in parallel on the input transmission line.

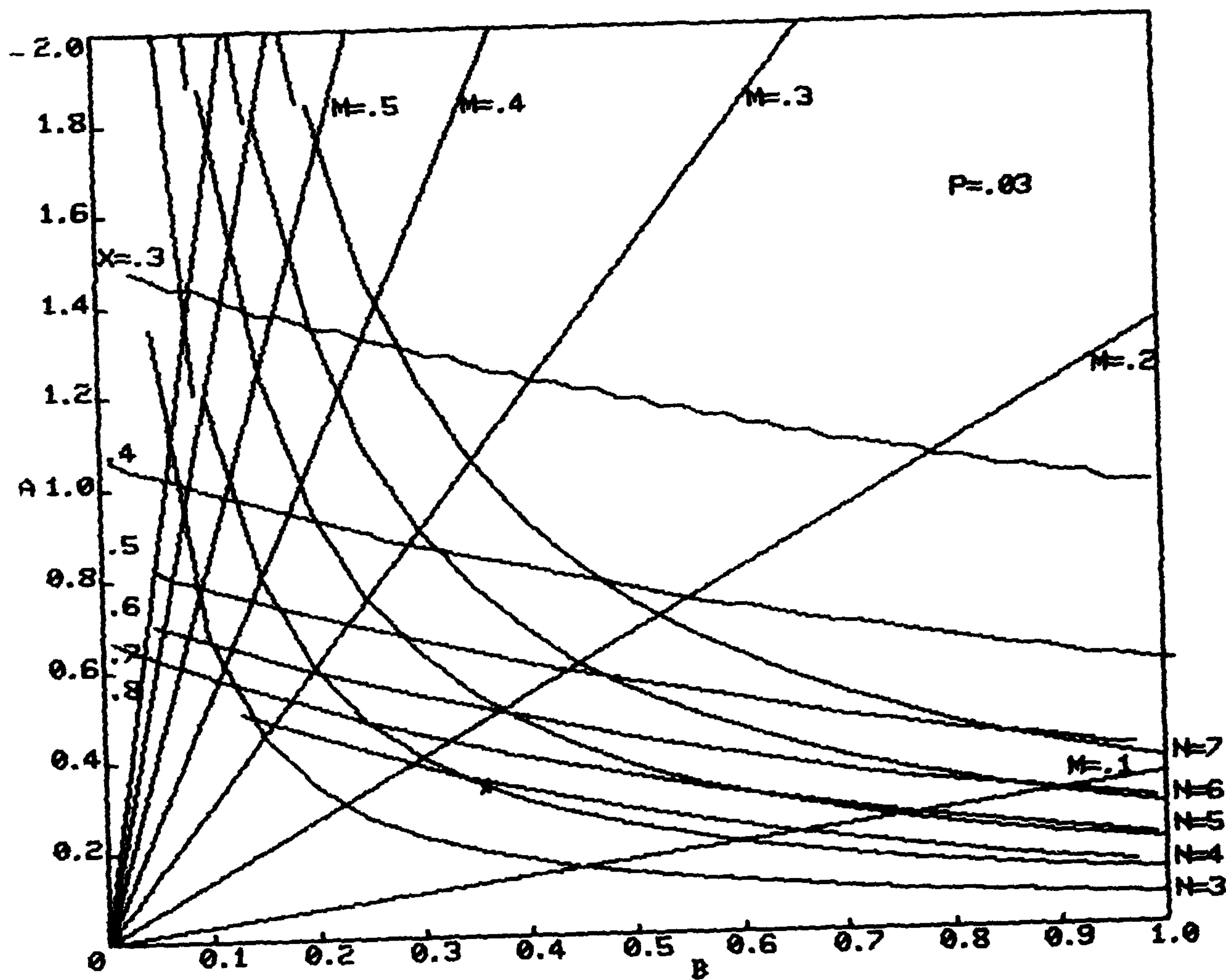

Fig. 3.11. Design curves for the distributed paraphase amplifier (for a specified P).

Then the parameter P is dependent only on the ratio of the transistor input and output resistances. The quantity M is the ratio of the gate-source resistance of the transistor and the characteristic resistance of the input line.

One can obtain a set of design curves corresponding to different values of P, which are useful for designing with various MESFETs.

Design Example

Let us consider the design of a distributed paraphase amplifier using typical 60 μm gate width MESFETs having

$$R_i = 8.7\ \Omega$$

$$R_{ds} = 556\ \Omega$$

$$C_{gs} = .071\ \text{pF}$$

Let $R_{01} = 50\ \Omega$ and $R_{02} = 200\ \Omega$. Therefore we have

$$P = \frac{1}{2}\,\frac{R_{02}}{R_{01}}\,\frac{R_i}{R_{ds}} \simeq .03$$

and

$$M = \frac{R_i}{R_{01}} = .174$$

We obtain the following values from the design curves in Fig. 3.11.

$$N = 4$$

$$X = \frac{f_{1db}}{f_c} = .82$$

Since

$$f_c = \frac{1}{2\pi C_{gs} R_{01}} = 44.2 \text{ GHz}$$

the 1 db bandwidth of the paraphase amplifier will be

$$f_{1db} = Xf_c = 36.2 \text{ GHz.}$$

The frequency response of the distributed paraphase amplifier shown in Fig. 3.12 is obtained by a general-purpose circuit simulation program - "SPICE". It shows that the 1 db bandwidth is 38.5 GHz. The agreement between the bandwidth predicted by the design curves and the computer simulation is satisfactory.

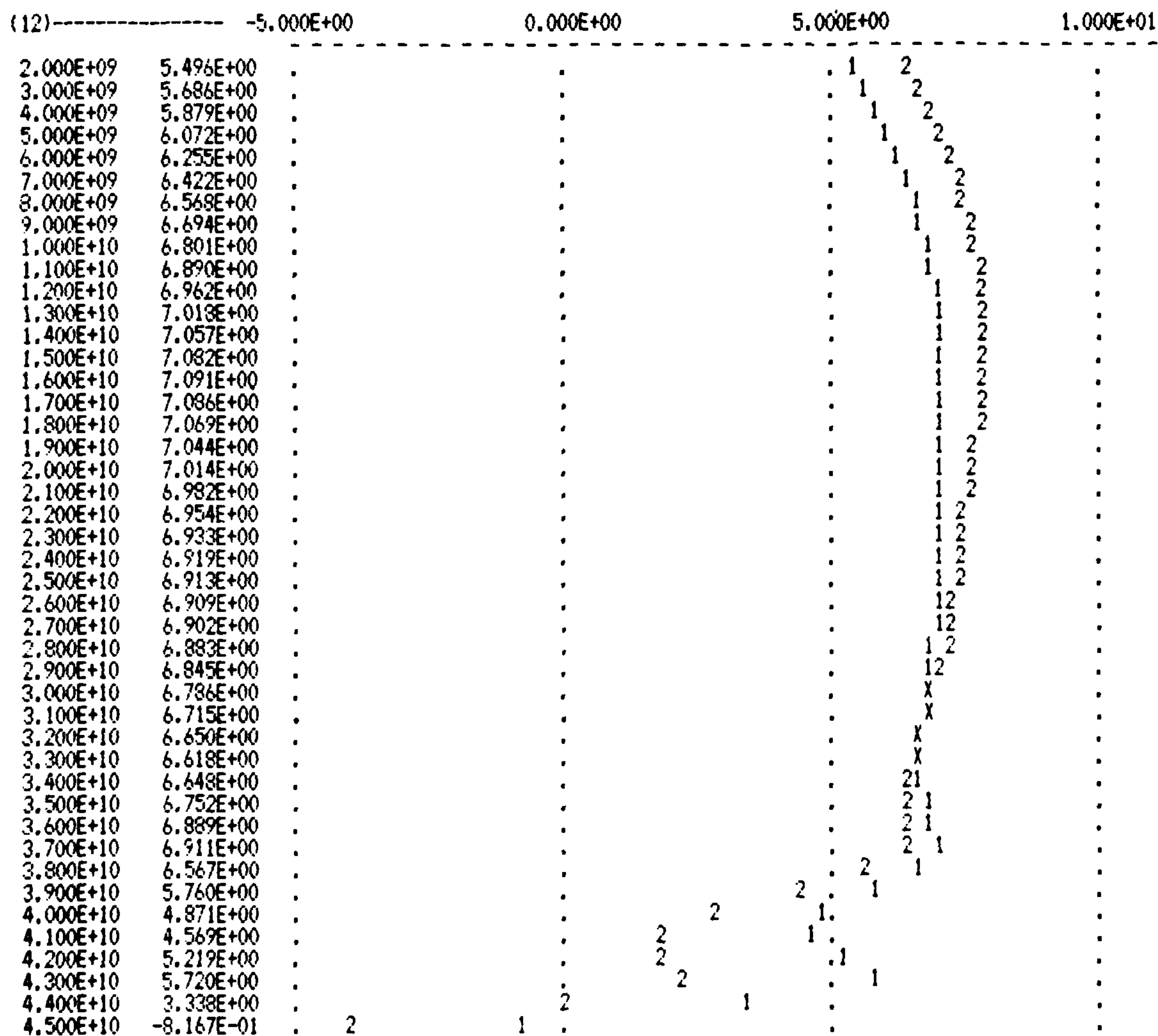

Fig. 3.12. Frequency response of the four section distributed paraphase amplifier using typical 60 μm MESFETs (R_{01} = 50 Ω, R_{02} = 200 Ω).

1. VDB(18) - voltage gain of common-source amplifier in db.

2. VDB(17) - voltage gain of common-gate amplifier in db.

3.7. Conclusion

A wide bandwidth distributed paraphase amplifier using FET's has been designed. The extra broadband gain (about 3 dB to 4 dB) with good flatness was shown by computer simulation. The output unbalance ΔA is less than 1 dB and phase deviation δ_ϕ is less than 10° from 2 to 20 GHz.

The equations of unbalance, phase deviation and reflection coefficient were derived. A set of design curves have been presented which enable one to determine the number of devices required and the achievable bandwidth using a preselected MESFET. The good agreement between the predicted performance and computer simulation has been shown.

IV. Summary, Conclusion and Present Efforts

The MESFET distributed amplifier has been analyzed and a systematic approach to its design has been presented. The analysis has revealed that the attenuation on gate and drain lines caused by the device input and output resistances respectively, are the critical factors which control the frequency response of the amplifier.

The normalized frequency response of the amplifier is a function of a and b parameters which are related to gate and drain line attenuations respectively. The normalized responses can be characterized by their fractional bandwidth defined as $x = f_{1\ dB}/f_c$. There is a range of a and b values which give the same fractional bandwidth. Constant-fractional bandwidth curves can be plotted on the a-b plane. These curves are independent of the device chosen, however, choice of the device restricts one to operation within a certain well defined region of the ab plane.

The equation ab = constant defines a set of hyperbolas on the a-b plane and is dependent on the device characteristic frequencies (ω_g and ω_d) and the number of devices. Similarly the equations a/b = constant defines a set of lines on the a-b plane and is dependent on the device characteristic frequencies and the cut-off frequency (hence impedance) of the lines.

One can also plot a set of curves defined by $K = (ab)^{1/2}e^{-b}$ on the a-b plane. The superposition of the above mentioned curves enables one to examine the trade-offs between the design variables such as the device, the number of devices and cutoff frequency and impedances of the lines and arrive at a design which gives the desired gain and bandwidth.

The gain-bandwidth product of the amplifier is given by

$$A_0 f_{1dB} = 4\ KX\ f_{max}$$

where K and X are functions of a and b. The maximum value of gain-bandwidth product is 0.8 f_{max}. By an appropriate choice of a and b parameters one can design a distributed amplifier having the maximum gain-bandwidth product. The maximum frequency of operation of the amplifier is constrained by the device f_{max}.

The report has also dealt with the analysis and design of MESFET distributed paraphase amplifier which is an important component of the 0-360° continuously variable broadband phase shifter. Equations for gain unbalance and phase deviation in distriubted paraphase amplifier have been derived. A set of design curves has also been presented. A distributed paraphase amplifier having a gain unbalance of less than 1 dB and phase deviation of less than 10° from 2 to 20 GHz has been designed using the standard microwave circuit analysis program.

Present work focusses on refinement of distributed amplifier design procedures as constrained by practical fabrication limitations, and to the analysis and design of a broadband continuously variable 0-360° phase shifter.

APPENDIX A

Equation for gate-to-source voltage

Consider the gate line of FET distributed amplifier shown in Fig. 1.

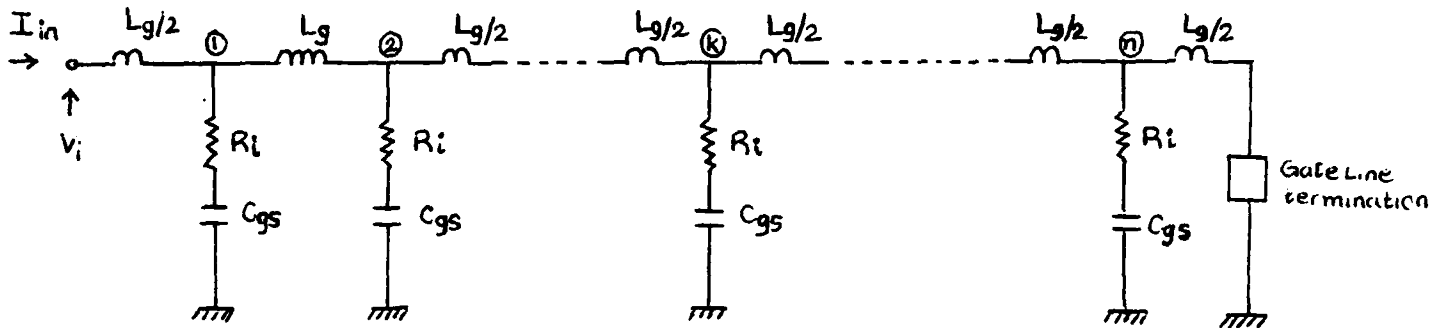

Fig. 1. Gate Line

The gate line in Fig. 1 can also be viewed as a cascade connection of constant-k π-sections as shown in Fig. 2.

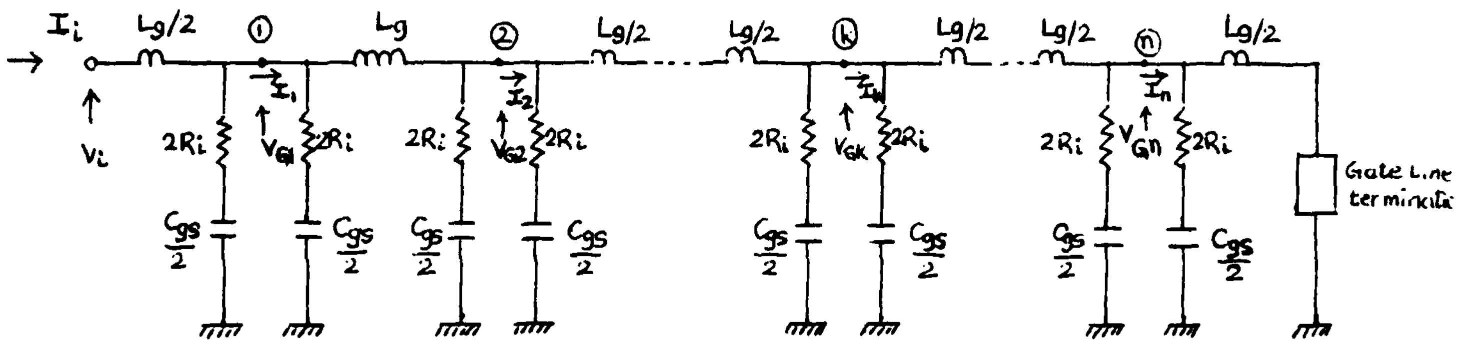

Fig. 2. Gate line as cascaded constant-k π-sections.

The current I_k at the kth transistor gate terminal can be expressed in terms of the current at the input terminal of the amplifier as

$$\frac{I_k}{I_i} = e^{-[\theta_g/2 + (k-1)\theta_g]} = e^{-\frac{(2k-1)\theta_g}{2}} \tag{1}$$

V_{Gk} = voltage at the gate terminal of kth FET

$$= I_k Z_{G\pi} \qquad (2)$$

where $Z_{G\pi}$ = π-section image impedance of the gate line $\approx \dfrac{\sqrt{L_g/C_g}}{\sqrt{1-(\omega/\omega_c)^2}}$

Therefore $$V_{Gk} = I_k \frac{\sqrt{L_g/C_g}}{\sqrt{1-(\omega/\omega_c)^2}} \qquad (3)$$

We also have

$$I_i = \frac{V_i}{Z_{GT}} \qquad (4)$$

where Z_{GT}= T-section image impedance of the gate line $\approx \sqrt{L_g/C_g[1-(\omega/\omega_c)^2]}$

Therefore $$I_i = \frac{V_i}{\sqrt{\frac{L_g}{C_g}\;[1 - (\frac{\omega}{\omega_c})^2]}} \qquad (5)$$

From (1), (3), and (5) we get

$$V_{Gk} = \frac{V_i e^{-\frac{(2k-1)\theta_g}{2}}}{[1 - (\frac{\omega}{\omega_c})^2]}$$

APPENDIX B

Equations for Phase Shift on Gate and Drain Lines

For a constant-k line, the propagation function is given by[4]

$$\cosh(\theta) = 1 + \frac{Z_1}{2Z_2} \qquad (1)$$

where θ ($= A + j\phi$) is the propagation function, A and ϕ are the attenuation and phase shift per section of constant-k line and Z_1 and Z_2 are the impedances in the series and shunt arms of a section of constant-k line as shown in Fig. 1

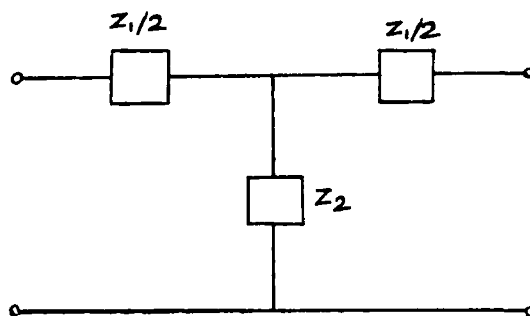

Fig.1. A section of constant-k line

Equation (1) can be written as

$$\cosh(\theta) = \cosh(A+j\phi) = \cosh A \cos\phi + j \sinh A \sin\phi = 1 + \frac{Z_1}{2Z_2} \qquad (2)$$

For $A \leq 0.4$, $\cosh A \approx 1$.

Therefore we have from equation (2)

$$\cos\phi = \mathrm{Re}\left[1 + \frac{Z_1}{2Z_2}\right] \qquad (3)$$

When equation (3) is evaluated for the gate and drain line T-sections shown in Fig. 2(a) and 2(b) we get

$$\phi_g \approx \cos^{-1} \left[1 - \frac{2\omega^2/\omega_c^2}{1+(\omega/\omega_g)^2}\right] \tag{4}$$

and

$$\phi_d \approx \cos^{-1} [1-2\omega^2/\omega_c^2] \tag{5}$$

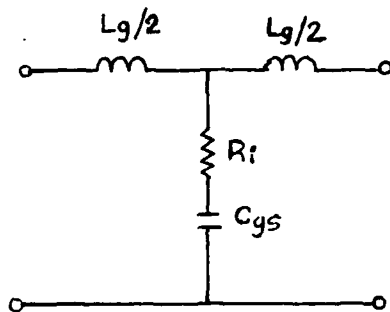

(a) A section of gate line

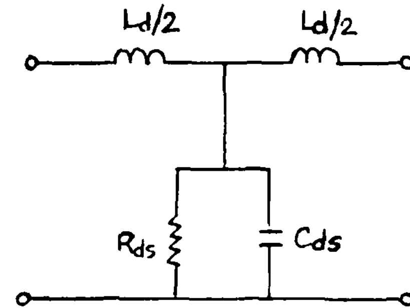

(b) A section of drain line

Fig. 2. Gate and drain line T-sections.

For typical designs $\omega_c < \omega_g$. It can be shown from equations (4) and (5) that for frequencies less than 0.7 ω_c, $\phi_g \approx \phi_d$.

APPENDIX C

Image impedances of gate and drain lines

Consider the T and π-sections of constant-k lines as shown in Fig. 1(a) and 1(b) respectively.

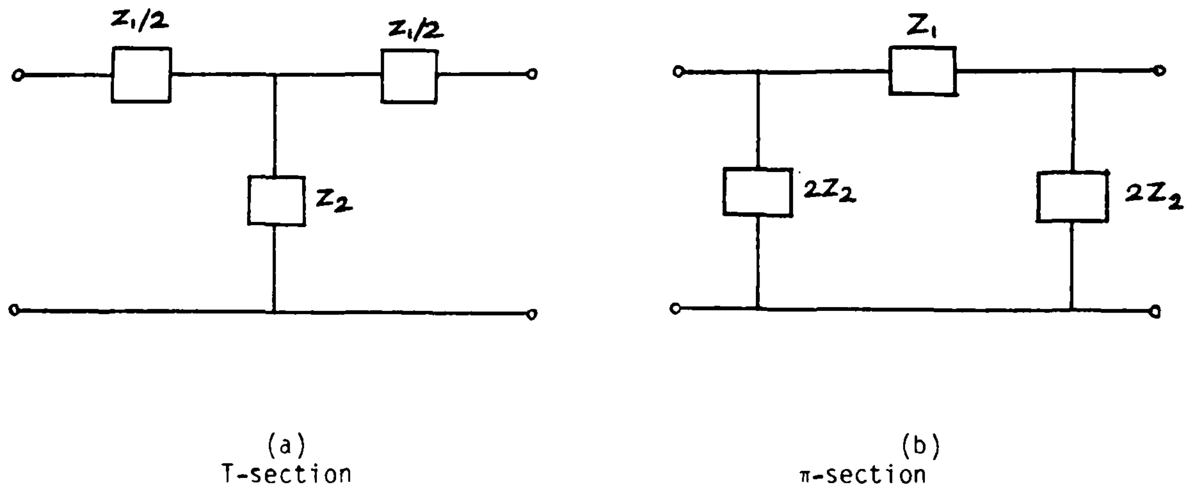

(a) T-section

(b) π-section

Fig. 1. T and π-sections of constant-k lines.

The image impedances (Z_{IT} and $Z_{I\pi}$) of the networks in Fig. 1(a) and Fig. 1(b) are given by [4]

$$Z_{IT} = \sqrt{Z_1 Z_2} \sqrt{1 + \frac{Z_1}{4Z_2}} \tag{1}$$

$$Z_{I\pi} = \sqrt{Z_1 Z_2} \Big/ \sqrt{1 + \frac{Z_1}{4Z_2}} \tag{2}$$

For the gate and drain line T-section shown in Fig. 2(a) and 2(b) one can easily derive the image impedances given below from equation (1).

$$Z_{IG} = \sqrt{\frac{L_g}{C_g}} \left[1 - \left(\frac{\omega}{\omega_c}\right)^2 + j\left(\frac{\omega}{\omega_g}\right)\right]^{1/2} \tag{3}$$

$$Z_{ID} = \sqrt{\frac{L_d}{C_d}} \left[\frac{1}{1 + \left(\frac{\omega_d}{\omega}\right)^2} - \left(\frac{\omega}{\omega_c}\right)^2 + j\,\frac{1}{\left(\frac{\omega_d}{\omega}\right) + \left(\frac{\omega}{\omega_d}\right)}\right]^{1/2} \tag{4}$$

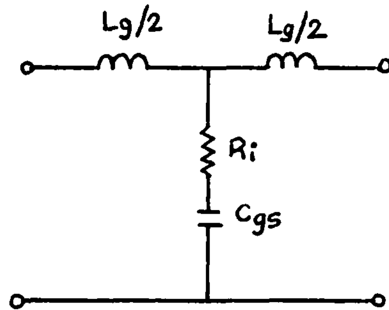

(a)
Gate Line T-Section

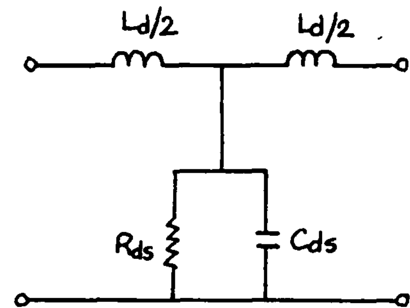

(b)
Drain Line T-Section

Fig. 2. Gate and drain line T-sections.

When (ω/ω_g) is negligibly small in comparison to $(1 - \frac{\omega^2}{\omega_c^2})$ in equation (3) we have

$$Z_{IG} \approx \sqrt{\frac{L_g}{C_g}\left[1 - \left(\frac{\omega}{\omega_c}\right)^2\right]} \tag{5}$$

For typical designs $\omega_c < \omega_g$ and equation (5) has been found to be valid for $\omega < 0.7\,\omega_c$. When $\omega \gg \omega_d$ in equation (4) we have

$$Z_{ID} \approx \sqrt{\frac{L_d}{C_d}\left[1 - \left(\frac{\omega}{\omega_c}\right)^2\right]} \tag{6}$$

APPENDIX D

1. Equations for gain unbalance and phase deviation

(1) Derivation of gain of distributed common-gate amplifier

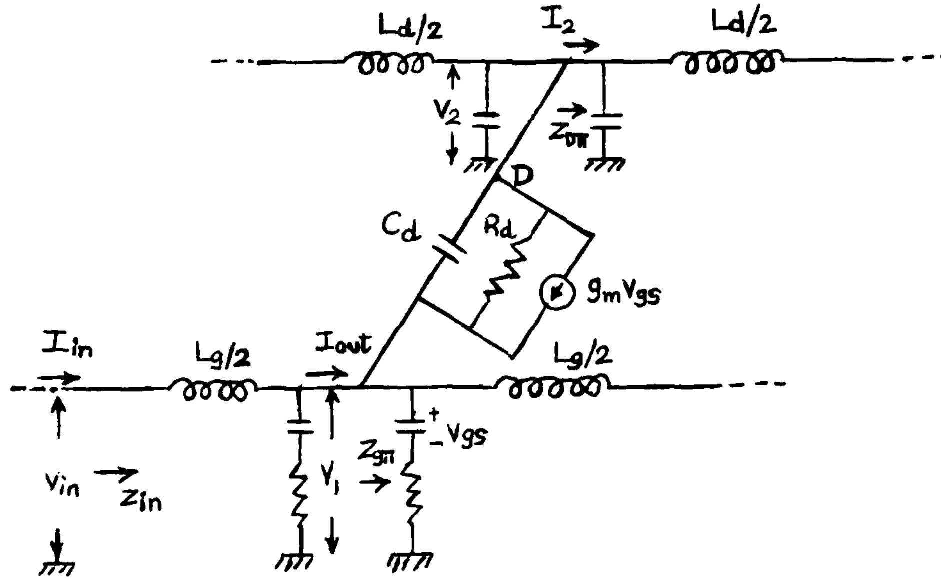

Fig. 1. Equivalent circuit of common-gate amplifier.

By summing current at node D (shown in Fig. 1) we obtain

$$g_m V_{gs} + (V_2 - V_1)\left(\frac{1}{R_d} + j\omega C_d\right) + V_2 \frac{2}{Z_{D\pi}} = 0 \qquad (1)$$

where
$$V_{gs} = -\frac{V_1}{\sqrt{1 + \left(\frac{\omega}{\omega_g}\right)^2}}$$

$$\omega_g = \frac{1}{R_g C_g}$$

$$\omega_c = 2/\sqrt{L_g C_g}$$

$$V_1 = \frac{V_{in}}{\left(1 - \left(\frac{\omega}{\omega_c}\right)^2\right)} \quad e^{-\theta_g/2}$$

θ_g - the propagation function on the input line

$Z_{D\pi}$ - the image impedance of the drain line

$$V_2\left(\frac{2}{Z_{D\pi}} + \frac{1}{R_d} + j\omega C_d\right) = V_1\left(\frac{1}{R_d} + j\omega C_d + \frac{g_m}{\sqrt{1+\left(\frac{\omega}{\omega_g}\right)^2}}\right) \tag{2}$$

$$V_2 = \frac{V_1\left(\frac{1}{R_d} + \frac{g_m}{\sqrt{1+\left(\frac{\omega}{\omega_g}\right)^2}} + j\omega C_d\right)}{\frac{2}{Z_{D\pi}} + \frac{1}{R_d} + j\omega C_d}$$

$$= \frac{V_{in} Z_{D\pi}}{1 - \left(\frac{\omega}{\omega_c}\right)^2} \cdot \frac{\frac{1}{R_d} + \frac{g_m}{\sqrt{1+\left(\frac{\omega}{\omega_g}\right)^2}} + j\omega C_d}{2 + \frac{Z_{D\pi}}{R_d} + j\omega C_d Z_{D\pi}} \tag{3}$$

$$I_2 = \frac{V_2}{Z_{D\pi}} = \frac{V_{in}}{1 - \left(\frac{\omega}{\omega_c}\right)^2} \cdot \frac{\frac{1}{R_d} + \frac{g_m}{\sqrt{1+\left(\frac{\omega}{\omega_g}\right)^2}} + j\omega C_d}{2 + \frac{Z_{D\pi}}{R_d} + j\omega C_d Z_{D\pi}} \tag{4}$$

Then the current derivered to the load is given by

$$I_o = \frac{V_{in}}{1 - \left(\frac{\omega}{\omega_c}\right)^2} \cdot \frac{\frac{1}{R_d} + \frac{g_m}{\sqrt{1+\left(\frac{\omega}{\omega_g}\right)^2}} + j\omega C_d}{2 + \frac{Z_{D\pi}}{R_d} + j\omega C_d Z_{D\pi}} \cdot \frac{\sinh\left[\frac{n}{2}(A_d' - A_g)\right] e^{-\frac{n}{2}(A_d' + A_g)}}{\sinh\left[\frac{1}{2}(A_d' - A_g)\right]} \tag{5}$$

Therefore the power gain of the common-gate amplifier is

$$G_g = \frac{R_{01}R_{02}}{1 - (\frac{\omega}{\omega_c})^2} \cdot \frac{(\frac{1}{R_d} + \frac{g_m}{\sqrt{1 + (\frac{\omega}{\omega_g})^2}})^2}{(2 + \frac{Z_{D\pi}}{R_d})^2} \cdot \frac{\sinh^2[\frac{h}{2}\,(A_d'-A_g)]e^{-n(A_d'+A_g)}}{\sinh^2[\frac{1}{2}\,(A_d'-A_g)]}$$

$$= \frac{R_{01}R_{02}g_m^2}{4[1 - (\frac{\omega}{\omega_c})^2][1 + (\frac{\omega}{\omega_g})^2]} \cdot \frac{(1 + \frac{\sqrt{1 + (\frac{\omega}{\omega_g})^2}}{g_m R_d})^2}{(1 + \frac{Z_{D\pi}}{2R_d})^2} \cdot \frac{\sinh^2[\frac{n}{2}\,(A_d'-A_g)]e^{-n(A_d'+A_g)}}{\sinh^2[\frac{1}{2}\,(A_d'-A_g)]} \qquad (6)$$

(2) Comparison with the power gain of common-source amplifier

$$G_s = \frac{R_{01}R_{02}\; g_m^2}{4[1 - (\frac{\omega}{\omega_c})^2][1 + (\frac{\omega}{\omega_g})^2]} \quad \frac{\sinh^2[\frac{h}{2}\,(A_d-A_g)]e^{-n(A_d+A_g)}}{\sinh^2\,[\frac{1}{2}\,(A_d-A_g)]} \qquad (7)$$

According to equation 2.13 the drain line attenuation is given by

$$A_d = \frac{\omega_d/\omega_c}{\sqrt{1-X_k^2}}$$

$$= \frac{g_0 R_{02}}{2\sqrt{1-X_k^2}} \qquad (8)$$

where g_0 - the output conductance of the transistor

R_{02} - the characteristic impedance of the drain line

The attenuations on the drain line for the common-gate and common-source amplifiers are not the same since the output conductances are not the same.

For the common-source amplifier

$$g_{0s} = \frac{1}{R_d} \tag{9}$$

For the common-gate amplifier

$$g_{0g} = \frac{1}{R_d}\left(1 - \frac{1}{A_v}\right)$$

$$= g_{0s}\left(1 - \frac{1}{A_v}\right) \tag{10}$$

where R_d - drain-to-source resistance

A_v - D.C. voltage gain of the amplifer

The attenuation on the drain line of common-gate amplifier is

$$A_d' = \frac{g_{0g}R_{02}}{2\sqrt{1-X_k^2}}$$

$$= \frac{g_{0s}R_{02}}{2\sqrt{1-X_k^2}}\left(1 - \frac{1}{A_v}\right)$$

$$= A_d\left(1 - \frac{1}{A_v}\right) \tag{11}$$

where A_d is the attenuation on the drain line of common-source amplifier.

The unbalance ΔA is obtained as follows

$$\Delta A(dB) = 10 \log \frac{G_g}{G_s}$$

$$= 20 \log \frac{1 + \sqrt{1 + (\frac{\omega}{\omega_g})^2} / (g_m R_d)}{1 + \frac{Z_{D\pi}}{2R_d}}$$

$$+ 20 \log \frac{\sinh\{\frac{n}{2} [A_d(1 - \frac{1}{A_v}) - A_g]\} \sinh[\frac{1}{2} (A_d - A_g)]}{\sinh\{\frac{1}{2} [A_d(1 - \frac{1}{A_v}) - A_g]\} \sinh[\frac{n}{2} (A_d - A_g)]} + 10 \log(e^{n \frac{A_d}{A_V}}) \tag{12}$$

when $\frac{n}{2} \frac{A_d}{A_v} << 1$, $\sinh(\frac{n}{2} \frac{A_d}{A_v}) \simeq 0$. Under this condition we can derive the following equation for ΔA from equation (12)

$$\Delta A \text{ (db)} \simeq 20 \log \frac{1 + \frac{1}{g_m R_d}}{1 + \frac{Z_{D\pi}}{2R_d}} + 20 \log \frac{\cosh(\frac{n}{2} \frac{A_d}{A_v})}{\cosh(\frac{1}{2} \frac{A_d}{A_v})} + 10 \log(e^{n \frac{A_d}{A_v}}) \tag{13}$$

where $Z_{D\pi} = \sqrt{\frac{L_d}{C_d}} \Big/ \sqrt{1 - (\frac{\omega}{\omega_c})^2}$

$$\omega_C = 2/\sqrt{L_d C_d}$$

The phase deviation δ_ϕ is obtained as follows

$$\delta_\phi = \arctan \frac{\omega C_d}{\frac{1}{R_d} + g_m} - \arctan \frac{\omega C_d}{\frac{1}{R_d} + \frac{2}{Z_{D\pi}}} \tag{14}$$

2. Equations for characteristic impedance

(1) *A T-section network, shown in Fig. 2, has ABCD matrix as follows.*

$$\begin{bmatrix} A & B \\ C & D \end{bmatrix} = \begin{bmatrix} \frac{Z_{11}}{Z_{12}} & \frac{\Delta}{Z_{12}} \\ \frac{1}{Z_{12}} & \frac{Z_{22}}{Z_{12}} \end{bmatrix} \quad \Delta = Z_{11}Z_{22} - Z_{12}^2 \tag{15}$$

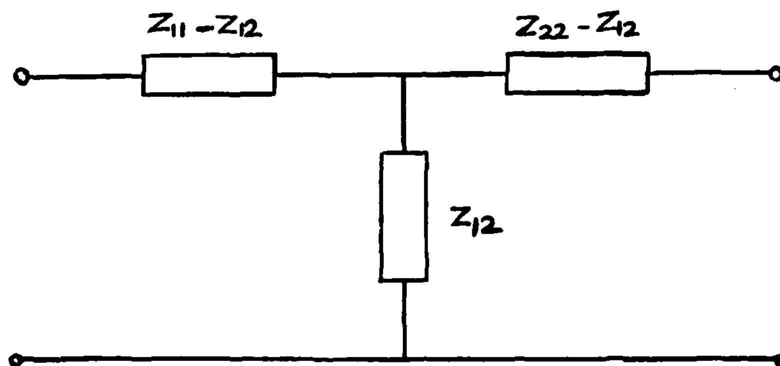

Fig. 2. A T-section network.

(2) In our case the T-section is represented by;

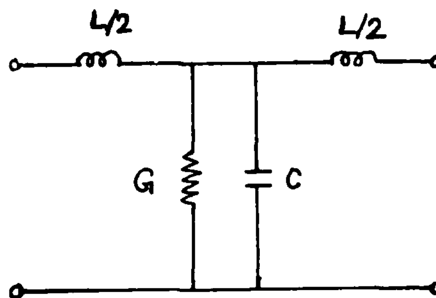

Fig. 3. A section of input line

$$Z_{11} - Z_{12} = j\omega L/2$$

$$Z_{12} = 1/(G+j\omega C)$$

$$Z_{11} = Z_{22} = j\omega L/2 + 1/(G+j\omega C)$$

So $$Z_0 = \sqrt{\frac{B}{C}} = \sqrt{Z_{11}Z_{22} - Z_{12}^2}$$

$$= \sqrt{[j\omega L/2 + 1/(G+j\omega C)]^2 - [\frac{1}{G+j\omega C}]^2}$$

$$= \sqrt{\frac{j\omega L}{G+j\omega C} - \frac{\omega^2 L^2}{4}}$$

$$= \sqrt{\frac{L}{C}} \sqrt{\frac{j\omega C}{G+j\omega C} - \frac{\omega^2 LC}{4}}$$

$$= \sqrt{\frac{L}{C}} \sqrt{1 - (\frac{\omega}{\omega_c})^2 - \frac{G}{G+j\omega C}}$$

$$= \sqrt{\frac{L}{C}} \sqrt{1 - \left(\frac{\omega}{\omega_C}\right)^2 - \frac{1 - j\frac{\omega C}{G}}{1 + \left(\frac{\omega C}{G}\right)^2}}$$

$$= \sqrt{\frac{L}{C}} \sqrt{1 - \left(\frac{\omega}{\omega_c}\right)^2 - \frac{1 - j\frac{\omega}{\omega_g}}{1 + \left(\frac{\omega}{\omega_g}\right)^2}} \tag{16}$$

where $\omega_c = \frac{2}{\sqrt{LC}}$ $\omega_g = \frac{G}{C}$

(2) For a distortionless T-section as follows

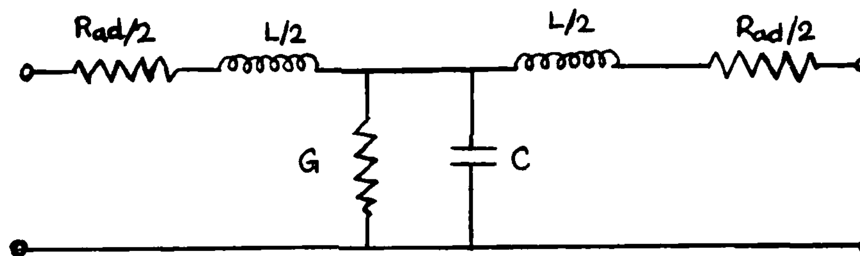

Fig. 4. A section of distortionless line

$$Z_{11} = R_{ad}/2 + j\omega L/2 + 1/(G+j\omega C)$$

$$Z_{12} = 1/(G+j\omega C)$$

$$R_{ad} = GL/C$$

$$Z_0 = \sqrt{Z_{11}Z_{22} - Z_{12}^2}$$

$$= \sqrt{\left(\frac{R_{ad}}{2} + \frac{j\omega L}{2} + \frac{1}{G+j\omega C}\right)^2 - \left(\frac{1}{G+j\omega C}\right)^2}$$

$$= \sqrt{\left(\frac{R_{ad}}{2} + \frac{j\omega L}{2}\right)^2 + 2\,\frac{\frac{R_{ad}}{2} + j\omega L/2}{G + j\omega C}}$$

$$= \sqrt{\left(\frac{R_{ad}}{2} + \frac{j\omega L}{2}\right)^2 + \frac{L}{C}}$$

$$= \sqrt{\frac{L}{C}}\ \sqrt{1 + \left(\frac{R_{ad}}{2}\sqrt{\frac{C}{L}} + j\omega\,\frac{\sqrt{LC}}{2}\right)^2}$$

$$= \sqrt{\frac{L}{C}}\ \sqrt{1 + \left(\frac{\sqrt{LC}}{2}\,\frac{G}{C} + j\,\frac{\omega\sqrt{LC}}{2}\right)^2}$$

$$= \sqrt{\frac{L}{C}}\ \sqrt{1 + \frac{(\omega_g + j\omega)^2}{\omega_c^2}} \tag{17}$$

DISTRIBUTION LIST

CONTRACT N00014-80-C-0923

Addressee	Copies
Office of Naval Research Code 414 Arlington, VA 22217	4
Naval Research Laboratory 4555 Overlook Avenue, S.W. Washington, DC 20375	
Code 6810	1
Code 6811	1
Code 6820	1
Code 6850	1
Code 6851	1
Defense Documentation Center Building 5, Cameron Station Alexandria, VA 22314	12
Dr. Y. S. Park AFWAL/DHR Building 450 Wright-Patterson AFB OH 45433	1
Dr. W. Wisseman Texas Instruments Central Research Lab M.S. 134 13500 North Central Expressway Dallas, TX 75265	1
Dr. R. Bierig Raytheon Company 131 Spring Street Waltham, MA 02173	1
Dr. H. Nathanson Westinghouse Research and Development Center Beulah Road Pittsburgh, PA 15235	1
Dr. F. Eisen Rockwell International Science Center P.O. Box 1085 Thousand Oaks, CA 91360	1
Mr. Lothar Wandinger ECOM/AMSEL/TL/IJ Fort Monmouth, NJ 07003	1
Dr. William Lindley MIT Lincoln Laboratory E118E, P.O. Box 73 Lexington, MA 02173	1
Commander U.S. Army/ERADCOM Attn: V. Gelnovatch, DELET-M Fort Monmouth, NJ 07703	1
Dr. F. Sterzer RCA Microwave Technology Center Princeton, NJ 08540	1
Commander Naval Electronics Systems Command Attn: J. P. Letellier, Code 6142 Washington, DC 20360	1
Commander Naval Air Systems Command Attn: A. Glista, Jr., AIR 330 Washington, DC 20361	1
Dr. R. Bell, K-101 Varian Associates, Inc. 611 Hansen Way Palo Alto, CA 94304	1
Dr. Robert Archer Hewlett-Packard Corporation 1501 Page Road Palo Alto, CA 94306	1
Drs. E. J. Crescenzi, Jr. and K. Niclas Watkins-Johnson Company 3333 Hillview Avenue Stanford Industrial Park Palo Alto, CA 94304	1

Enclosure (1)

Dr. W. Weisenberger 1
Communications Transistor Corp.
301 Industrial Way
San Carlos, CA 94070

Drs. F. A. Brand and 1
J. Saloom
Microwave Associates
Northwest Industrial Park
Burlington, MA 01803

Commander, AFAL 1
AFWAL/AADM
Attn: Dr. Don Rees
Wright-Patterson AFB
OH 45433

Professor Walter Ku 1
Cornell University
Phillips Hall
Ithaca, NY 14853

Mr. Horst W. A. Gerlach 1
Harry Diamond Laboratories
800 Powder Mill Road
Adelphia, MD 20783

A.G.E.D. 1
201 Varick Street
9th Floor
New York, NY 10014

Dr. Ken Weller 1
TRW Systems
MS/1414
One Space Park
Redondo Beach, CA 90278

Professor L. Eastman 1
Cornell University
Phillips Hall
Ithaca, NY 14853

Professors Hauser and 1
Littlejohn
North Carolina State University
Department of Electrical Engineering
Raleigh, NC 27607

Professors Rosenbaum and Wolfe 1
Washington University
Semiconductor Research Laboratory
St. Louis, MO 63130

Dr. W. H. Perkins 1
General Electric Company
Electronics Lab 3-115/B4
P.O. Box 4840
Syracuse, NY 13221

Dr. Bryan Hill 1
AFWAL/AADE
Wright-Patterson AFB
OH 45433

Dr. J. Schellenberg 1
Hughes Aircraft Company
Electron Dynamics Division
3100 W. Lomita Boulevard
P.O. Box 2999
Torrance, CA 90509

Mr. H. Willing 1
Radar Directorate
BMD - Advanced Technical Center
P.O. Box 1500
Huntsville, AL 35807

Dr. R. M. Malbon 1
Avantek, Inc. M.S. 1C
3175 Bowers Avenue
Santa Clara, CA 94304

Dr. S. Wanuga 1
General Electric Company
Electronics Lab 134
Electronics Park
Syracuse, NY 13221

Professor D. Navon 1
University of Massachusetts
Department of Electrical and
Computer Engineering
Amherst, MA 01003

Dr. J. Degenford 1
MS/3717
Westinghouse Advanced Technology Lab
Box 1521
Baltimore, MD 21203

Dr. C. Krumm 1
Hughes Research Laboratory
3011 Malibu Canyon Road
Malibu, CA 90265

Commandant 1
Marine Corps
Scientific Adviser (Code AX)
Washington, DC 20380

Professor J. Beyer 1
University of Wisconsin
Department of Electrical and
Computer Engineering
Madison, WI 53706

Dr. Sven Roosild 1
DARPA
1400 Wilson Blvd.
Arlington, VA 22209

Professor Hiro Yamasaki
Hughes Aircraft Company
3100 West Lomita Blvd.
P.O. Box 2999
Torrance, California 90509